UILU-ENG-74-2023

...L ENGINEERING STUDIES

STRUCTURAL RESEARCH SERIES NO. 411

WAVE PROPAGATION IN AN ELASTIC HALF SPACE DUE TO COUPLES APPLIED AT A POINT BENEATH THE SURFACE

By
T. E. FAREWELL
A. R. ROBINSON

A Joint Technical Report
of Research Programs

Sponsored by the
U.S. ARMY RESEARCH OFFICE-DURHAM
DEPARTMENT OF THE ARMY
Project No. D0161102B33G
Proposal No. D-52

and

THE OFFICE OF NAVAL RESEARCH
DEPARTMENT OF THE NAVY
Contract No. N00014-67-A-0305-0010
Project No. NR 064-183

UNIVERSITY OF ILLINOIS
AT URBANA-CHAMPAIGN
AUGUST 1974

CIVIL ENGINEERING STUDIES
STRUCTURAL RESEARCH SERIES NO. 411

UILU-ENG-74-2023

WAVE PROPAGATION IN AN ELASTIC HALF SPACE DUE TO COUPLES APPLIED AT A POINT BENEATH THE SURFACE

by

T. E. Farewell
A. R. Robinson

A Joint Technical Report of
Research Programs Sponsored by the
U. S. ARMY RESEARCH OFFICE-DURHAM
DEPARTMENT OF THE ARMY
Project No. D0161102B33G
Proposal No. D-52

and

THE OFFICE OF NAVAL RESEARCH
DEPARTMENT OF THE NAVY
Contract No. N00014-67-A-0305-0010
Project No. NR 064-183

UNIVERSITY OF ILLINOIS AT
URBANA-CHAMPAIGN

AUGUST 1974

ACKNOWLEDGEMENT

This report was prepared as a doctoral dissertation by Cpt. T. E. Farewell, Assistant Professor, Department of Mechanics, U. S. Military Academy and was submitted to the Graduate College of the University of Illinois at Urbana-Champaign in partial fulfillment of the requirements for the degree of Doctor of Philosophy. The work was done under the supervision of Dr. A. R. Robinson, Professor of Civil Engineering, University of Illinois.

The investigation was conducted as part of research programs supported by the Army Research Office - Durham, Project No. D0161102B33G, Solution of Dynamic Problems by the Method of Self Similar Potentials, and by the Office of Naval Research, Contract N00014-67-A-0305-0010, Numerical and Approximate Methods of Stress Analysis.

The numerical results were obtained using the Honeywell-635 Computer System of the United States Military Academy at West Point, N.Y.

TABLE OF CONTENTS

1. INTRODUCTION

1.1 Objective and Scope

The application of dynamic loads to a body generates stress waves which propagate through the medium. Within a linearly elastic, isotropic, homogeneous solid both dilatational and distortional waves can exist. Solutions to elastic wave propagation problems are customarily sought in terms of potential functions which satisfy the wave equation and the boundary and initial conditions and determine the state of stress within the body. Application of the usual boundary conditions, however, results in an involved coupling of the potential functions which often makes the elastic wave propagation problem difficult to solve. Solving even relatively simple three-dimensional problems can be a major undertaking.

The objective of this study is to develop an efficient and useful technique for determining the three-dimensional wave propagation that results from couples applied at a point beneath the surface of an elastic half space. This problem is of distinct engineering importance because it provides a basis for earthquake modeling. The disturbances from couple sources simulate the elastic motion following a fault dislocation and occurring in the presence of an initial strain state. For example, the single couple of Fig. 3 might simulate the strike-slip dislocation of a point on a vertical fault. A review of

the literature shows that actually some controversy exists concerning what arrangement of couples best models a particular fault dislocation. This study does not intend to defend any specific model but to provide an approach that represents any arrangement of couple sources as a superposition of five fundamental "double force"* cases. Chapter 6 provides guidance for the application of these cases to some specific earthquake models.

This study seeks the solution to the fundamental double force cases with the aim of reducing the inherent complexity of the three-dimensional elastic wave propagation problem. Representation of the double force problem by the method of rotational superposition reduces the three-dimensional problem to more easily solved two-dimensional problems. These two-dimensional problems are expressed in terms of derivatives of the plane problems that evolve from formulation of the single force case by rotational superposition. An application of the method of self-similar potentials provides the solution to the plane problems associated with the double force by a slight modification of the potential functions for the plane problems associated with the single force. The time variation of the double force emerges in the most natural fashion as a linear function of time. Superposition can then yield other time variations of interest.

---

* A "double force" is a single couple applied at a point. A more detailed definition and discussion of this term is provided in Sec. 1.2

This approach to the solution of double force problems is very direct and allows clear identification of the wave front pattern during each stage of the solution process.

1.2 Concept of a Double Force

This study focuses on the double force as the building block for earthquake fault modeling. Definition of a double force and agreement on a notation for referring to the fundamental cases will aid the work that follows.

A "double force" is the limit of a situation involving two equal but opposite forces that are parallel or collinear. The magnitude of each force is $P(t) \cdot \Delta h^{-1}$, and Δh is the distance between the points of application of the forces. As Δh goes to zero, the forces increase in magnitude but the product of the magnitude and Δh remains constant. In the limit as Δh goes to zero, the double force becomes a loading at a point. The double force may be either a double force with moment (See Fig. 1) or a double force without moment (See Fig. 2). The description "double horizontal force" indicates the direction of the forces comprising the double force. This description provides a necessary distinction because a double horizontal force with moment and a double vertical force with moment produce different dynamic effects even though the double forces may be statically equivalent.

A convenient notation employed in this study permits quick reference to the fundamental double force cases. This notation consists of two letters, e.g., "Vh," plus, at most, two subscripts. The upper-case letter gives the orientation of the constituent forces and the lower-case letter indicates the orientation of the line drawn between the points of application of the forces. "V" indicates a vertical orientation and "h," the horizontal. This notation allows one to quickly visualize the double force as a couple. For example, "Vh" refers to the double vertical force with moment shown in Fig. 1. Subscripts, "n" and "e" for "north" and "east", respectively, indicate the relative orientation of horizontal forces and horizontal distances. Case H_nh_e is a double horizontal force with moment (See Fig. 3), and Case H_eh_e is a double horizontal force without moment (See Fig. 5). The five fundamental double force cases mentioned in Sec. 1.1 are shown in Figs. 1 thru 5 and can be listed using this notation as:

1. Case Vh; double vertical force with moment.
2. Case Vv; double vertical force without moment.
3. Case H_nh_e; double horizontal force with moment, forces in a horizontal plane.
4. Case Hv; double horizontal force with moment, forces in a vertical plane.
5. Case H_eh_e; double horizontal force without moment.

1.3 Previous Related Studies

Several methods have been employed in the past to solve problems of wave propagation in an elastic half space. Lamb* (1904) and Ewing, Jardetsky, and Press (1957) used harmonic wave techniques to solve some problems of transient loading of an elastic half space. Cagniard (1962) used two applications of Laplace transforms to solve Lamb's problem when the actual transformation was not necessary because of special conditions. Gakenheimer and Miklowitz (1969) used Laplace and double Fourier transforms to study a transient normal load on a half space. Both the harmonic wave and the transform techniques present well-known computational difficulties. With the former method one has the formidable task of evaluating a Fourier integral unless the source varies in a harmonic fashion. In the latter, the transformations are difficult to carry out except in special cases. The method of self similar potentials is a powerful alternative technique for solving two-dimensional dynamic problems and is simpler and more direct than the other techniques. Smirnov and Sobolev (1933) developed the method but its use outside the U.S.S.R. has been limited. Thompson and Robinson (1969) presented a description and bibliography of the method and applied the method to solve a dynamic contact problem.

---

* An author's name followed by a date of publication refers to entries in the List of References.

The difficulties encountered when applying most methods to two-dimensional problems are greatly compounded when a three-dimensional problem is attempted. Smirnov and Sobolev (1933) developed the method of rotational superposition to represent the three-dimensional problem as a superposition of two-dimensional problems. This permits the retention of the convenience of the method of self similar potentials in the three-dimensional problem. The method of rotational superposition was applied to some axially symmetric problems by Zvolinskii (1957) and Pod"yapol'ski (1959). Johnson and Robinson (1972) used the methods of rotational superposition and self similar potentials to solve the nonsymmetric problem of a horizontal force applied beneath the surface of a half space. This solution avoided the formidable mathematics associated with other methods and involved only one quadrature in the complex plane. The study contained herein is the first use of the methods of rotational superposition and self similar potentials to solve three-dimensional double force problems.

Others have conducted various studies concerning different types of double force disturbances. Ben-Menahem (1961) used double Fourier integrals to consider the displacements at long ranges due to Rayleigh and Love waves from a moving single couple source. Burridge, Lapwood, and Knopoff (1964) investigated the radiation patterns of first motions due to a "double couple" source on the surface using a Fourier integral technique. Gupta (1967) approximated the far-field

patterns caused by double force sources using the dynamic reciprocity theorem.

The application of the methods of rotational superposition and self similar potentials in this study permit efficient solution of double force problems for both near- and far-field locations. The solutions presented for the fundamental double force cases can be easily superposed to obtain a variety of seismic models. As in Johnson and Robinson's work, formidable mathematical manipulations are avoided and physical insight into the wave motions is maintained throughout the solution process.

1.4 Organization of the Study

Chapter 2 provides a review of the methods of rotational superposition and self similar potentials in order to give a basis for the developments in succeeding sections. The method of rotational superposition permits treatment of three-dimensional problems as a superposition of two-dimensional problems. The method of self similar potentials is an efficient technique for solving plane problems concerned with an elastic half space and is, therefore, a natural complement to the method of rotational superposition.

Chapter 3 presents the solutions for a dynamic vertical and a dynamic horizontal force applied at a point beneath the surface of an elastic half space using the above methods. The solutions in this form are essential to the subsequent solution of the double force

cases. Although Pekeris and Lifson (1957) have considered the problem of a subsurface vertical force, some of the intermediate results obtained by the method of self similar potentials are useful for solving double force problems. The solution of the problem of a subsurface horizontal force by rotational superposition and self similar potentials was carried out by Johnson and Robinson (1972) and only the results are summarized here.

Chapter 4 presents the procedures and relationships that permit the application of the methods of rotational superposition and self similar potentials to the solution of problems involving a dynamic double force. Arbitrarily inclined double forces are represented as a superposition of double vertical and double horizontal forces. Expressing the inclined double force as a superposition of fundamental double forces permits quick solution for a variety of cases once the fundamental solutions are in hand. Rotational superposition allows the double force to be represented as a superposition of two-dimensional problems that are in turn related to the two-dimensional problems associated with the single force. The relationship among the two-dimensional problems turns out to be more useful computationally than the more obvious relationship that exists among the three-dimensional problems. A particular application of the method of self similar potentials gives the solution to the plane

problems associated with the double force by a simple modification of the potential functions for the single force. The time variation of the double force examined in this way comes out directly and in a natural fashion as a linear function of time. Chapter 5 provides the solution for the displacements on the surface of the half space for the five fundamental double force cases shown in Figs. 1 thru 5.

Chapter 6 summarizes the developments in this study and gives guidance on the application of the results to some specific earthquake fault models. The use of the linear time variation of the double force to obtain other time variations is also discussed.

1.5 Notation

Symbols in this study are defined where they first appear. Those symbols used most frequently are listed below.

a	Speed of the P wave $(\sqrt{\frac{\lambda + 2\mu}{m}})$
b	Speed of the S wave $(\sqrt{\frac{\mu}{m}})$
c	Speed of Rayleigh wave
c_1	Same as a
c_2	Same as b
C, C_1, C_i, etc.	Contours of integration
C_ρ , C_L	Constants defined by Eqs. (3.44b) and (3.47a)

f_1, f_2	See Eq. (2.9)
G_1, G_{12}, etc.	See Eq. (3.21)
$H_n h_e$, Hv, $H_e h_e$	Double horizontal forces (See Sec. 1.2 for a complete description.)
i	$\sqrt{-1}$
$\bar{i}_\rho$, $\bar{i}_\omega$, $\bar{j}$	Unit vectors corresponding to (ρ, ω, Y) space coordinates
m	Mass density of the elastic solid
P	Magnitude of the load
P_i	See Eq. (2.22)
r	$\sqrt{x^2 + y^2}$
$R(\theta^2)$	Rayleigh function (See Eq. (2.31c))
t	Time coordinate
t_p, t_{ps}, t_{pp}, t_s	Arrival time of P, PS, PP, S, SS, SP and
t_{ss}, t_{sp}, t_H	head waves respectively
u_x, u_y	Components of the displacement field for the plane strain problems
u_z	Displacement field for the antiplane problem
u_X, u_Z, u_Y	Displacement field for the three-dimensional problem
$\bar{u}^V$, $\bar{u}^H$	Displacement field for a vertical and horizontal force respectively

u_x^f, u_x^d	Components of a two-dimensional field corresponding to a single force and a double force respectively
u_ρ^F, u_ρ^D	Components of a three-dimensional field corresponding to a single force and a double force respectively
u_ρ, u_ω, u_Y	Displacement field in cylindrical coordinates for the three-dimensional problem
Vh, Vv	Double vertical forces (See Sec. 1.2 for a complete description.)
$w(\theta_2)$	Self similar displacement function for the antiplane problem
X, Y, Z	Cartesian global space coordinates for the three-dimensional problem
x, y, z	Cartesian space coordinates for the two-dimensional problem
y_o	The y coordinate of the point of application of the load
α	Speed of expanding region within which a loading is applied
β	Angle of incidence (See Fig. 11.)

γ	Angle of orientation for an inclined double force (See Fig. 15.)
δ_1, δ_2	See Eqs. (3.8)
δ_{11}, δ_{12}	See Eqs. (3.10)
δ_{21}, δ_{22}	See Eqs. (3.15)
Δh	Distance between forces comprising a double force
η	Variable of integration ($= \omega - \omega_o$)
θ_1, θ_2	Complex variables defined by Eqs. (3.8)
θ_{11}, θ_{12}	Complex variables defined by Eqs. (3.10)
θ_{21}, θ_{22}	Complex variables defined by Eqs. (3.15)
θ_p, θ_s, θ_{pp}, θ_{ss}, θ_{ps}, θ_{sp}	Value of complex variable at arrival of the respective front
θ_i^{ℓ}, θ_i^{u}	Values of complex variable θ_i at the end points of integration
λ, μ	Lamé constants of elasticity
ν	Poisson's ratio
ρ, ω, Y	Cylindrical space coordinates corresponding to (X,Z,Y) (See Fig. 6a.)
σ_x, σ_y, τ_{yx}, etc.	Components of stress for plane problems
σ_X, σ_Y, τ_{XY}, etc.	Components of stress for three-dimensional problems
σ_ρ, σ_ω, $\tau_{\rho Y}$, etc.	Components of stress in cylindrical coordinates for three-dimensional problems

Σ_x, Σ_y, T_{zx}, etc.	Self similar stresses for plane problems
ϕ, ϕ_1, ϕ_{11}, ϕ_{12}	Scalar dilatational potentials
Φ, Φ_1, Φ_{11}, Φ_{12}	Complex dilatational potentials associated with ϕ, ϕ_1, ϕ_{11}, ϕ_{12}
ψ_z, ψ_2, ψ_{21}, ψ_{22}	Scalar distortional potentials
Ψ, Ψ_2, Ψ_{21}, Ψ_{22}	Complex distortional potentials associated with ψ_z, ψ_2, ψ_{21}, ψ_{22}
ω_o	Angle of orientation of plane problem with respect to XY plane
$(\quad)^P$, $(\quad)^S$, $(\quad)^{PS}$	Component associated with P, S, PS,
$(\quad)^R$, $(\quad)^H$	Rayleigh, and head waves respectively

2. THE METHODS OF ROTATIONAL SUPERPOSITION AND SELF SIMILAR POTENTIALS

2.1 General Equations

Wave propagation in a homogeneous, isotropic, linearly elastic solid is governed by the equations of motion,* which can be written in terms of displacements as:

$$
\begin{aligned}
(\lambda + \mu)\,\frac{\partial \Delta}{\partial X} + \mu\,\nabla^2 u_X &= m\,\frac{\partial^2 u_X}{\partial t^2} \\
(\lambda + \mu)\,\frac{\partial \Delta}{\partial Z} + \mu\,\nabla^2 u_Z &= m\,\frac{\partial^2 u_Z}{\partial t^2} \\
(\lambda + \mu)\,\frac{\partial \Delta}{\partial Y} + \mu\,\nabla^2 u_Y &= m\,\frac{\partial^2 u_Y}{\partial t^2}
\end{aligned}
\qquad (2.1)
$$

where (X, Y, Z) are cartesian coordinates, m is the mass density of the solid, λ and μ are the Lamé constants which define the elastic properties of the medium, and u_X, u_Y, and u_Z are the components of the displacement vector $\bar{u}$. The dilatation Δ and the Laplacian operator ∇^2 are defined by:

$$
\Delta = \frac{\partial u_X}{\partial X} + \frac{\partial u_Z}{\partial Z} + \frac{\partial u_Y}{\partial Y} \qquad (2.2)
$$

* The order (X,Z,Y) is used to correspond to the (ρ,ω,Y) coordinate system used later. (See Fig. 6a.)

$$\nabla^2 = \frac{\partial^2}{\partial X^2} + \frac{\partial^2}{\partial Z^2} + \frac{\partial^2}{\partial Y^2}$$

The Helmholtz Theorem (Schwartz et al., 1960) is customarily applied to the displacement vector to represent it by the sum of the gradient of a scalar potential and the curl of a vector potential. That is,

$$\bar{u} = \text{grad } \phi + \text{curl } \bar{\psi} \tag{2.3}$$

The scalar potential determines the irrotational (P) portion of the displacement; the vector potential, the equivoluminal (S) portion.

For the equations of motion to be satisfied, it is both a necessary and sufficient condition that the potentials satisfy the wave equations (Duhem, 1898),

$$\nabla^2 \phi = \frac{1}{a^2} \frac{\partial^2 \phi}{\partial t^2} \qquad \nabla^2 \psi_i = \frac{1}{b^2} \frac{\partial^2 \psi_i}{\partial t^2} \tag{2.4}$$

where $a = \sqrt{\frac{\lambda + 2\mu}{m}}$ and $b = \sqrt{\frac{\mu}{m}}$ are the P and S wave speeds, respectively.

For the case of plane strain in which the displacements are zero in the z* direction, the x and y components of $\bar{\psi}$ are zero. The

---

* Coordinates in lower-case letters refer to two-dimensional problems in this study; coordinates in upper-case letters, to three-dimensional problems.

solution to this two-dimensional wave propagation problem can then be expressed in terms of scalar potentials, ϕ and ψ_z, by:

$$\nabla^2\phi = \frac{1}{a^2}\frac{\partial^2\phi}{\partial t^2} \qquad \nabla^2\psi_z = \frac{1}{b^2}\frac{\partial^2\psi_z}{\partial t^2} \tag{2.5}$$

Another plane problem of interest in this study is one of the antiplane type for which the displacement vector is $(0, 0, u_z)$ and is a function of x, y, and t only. The equations of motion reduce to

$$\nabla^2 u_z = \frac{1}{b^2}\frac{\partial^2 u_z}{\partial t^2} \tag{2.6}$$

As will be demonstrated in the succeeding sections, the solution to the three-dimensional problems of interest can be represented by rotational superposition of appropriate two-dimensional plane strain and antiplane problems.

2.2 Rotational Superposition

2.2.1 General Approach

While a number of techniques are available for the solution of plane wave propagation problems, few techniques have been successfully developed for solution of three-dimensional problems. The method of rotational superposition simplifies the three-dimensional

problem by representing it as a superposition of more easily solved plane strain and antiplane problems. The fundamental concepts of this method are briefly reviewed here before the specific applications that follow in succeeding sections. Thompson and Robinson (1969) and Johnson and Robinson (1972) provide a more detailed treatment.

Consider the effect in three-dimensional space, (ρ, ω, Y)*, of applying a plane strain displacement field, u_x (x, y, t) and u_y (x, y, t), and an antiplane field, u_z (x, y, t), at an angle ω_o with respect to the XY plane. As indicated in Fig. 6b, the radial, circumferential and vertical displacements would be:

$$u_\rho = u_x \cos(\omega - \omega_o) + u_z \sin(\omega - \omega_o)$$

$$u_\omega = -u_x \sin(\omega - \omega_o) + u_z \cos(\omega - \omega_o) \qquad (2.7)$$

$$u_Y = u_y$$

The three-dimensional problem is obtained by multiplying each of the plane problems by a weighting function of ω_o and superposing the effects for all values of ω_o from 0 to π. This leads to:

---

* (ρ, ω, Y) are cylindrical coordinates corresponding to (X, Z, Y). Fig. 6a shows the relation between the two coordinate systems.

$$u_\rho = \int_0^\pi u_x \cos(\omega - \omega_o)\, f_1(\omega_o)\, d\omega_o$$

$$+ \int_0^\pi u_z \sin(\omega - \omega_o)\, f_2(\omega_o)\, d\omega_o$$

$$u_\omega = -\int_0^\pi u_x \sin(\omega - \omega_o)\, f_1(\omega_o)\, d\omega_o$$

$$+ \int_0^\pi u_z \cos(\omega - \omega_o)\, f_2(\omega_o)\, d\omega_o \qquad (2.8a)$$

$$u_Y = \int_0^\pi u_y\, f_1(\omega_o)\, d\omega_o$$

and

$$\sigma_\rho = \int_0^\pi \sigma_x\, f_1(\omega_o)\, d\omega_o$$

$$- \int_0^\pi 2\mu\epsilon_x \cos^2(\omega - \omega_o)\, f_1(\omega_o)\, d\omega_o$$

$$+ \int_0^\pi 2\tau_{xz} \cos(\omega - \omega_o) \sin(\omega - \omega_o)\, f_2(\omega_o)\, d\omega_o$$

$$\sigma_\omega = \int_0^\pi \sigma_x\, f_1(\omega_o)\, d\omega_o + \qquad (2.8b)$$

$$
\begin{aligned}
&- \int_0^{\pi} 2\mu\varepsilon_x \cos^2(\omega - \omega_o)\, f_1(\omega_o)\, d\omega_o \\
&- \int_0^{\pi} 2\tau_{xz} \sin(\omega - \omega_o) \cos(\omega - \omega_o)\, f_2(\omega_o)\, d\omega_o \\
\sigma_Y &= \int_0^{\pi} \sigma_y\, f_1(\omega_o)\, d\omega_o \\
\tau_{Y\rho} &= \int_0^{\pi} \tau_{yx} \cos(\omega - \omega_o)\, f_1(\omega_o)\, d\omega_o \\
&+ \int_0^{\pi} \tau_{yz} \sin(\omega - \omega_o)\, f_2(\omega_o)\, d\omega_o \\
\tau_{Y\omega} &= -\int_0^{\pi} \tau_{yx} \sin(\omega - \omega_o)\, f_1(\omega_o)\, d\omega_o \\
&+ \int_0^{\pi} \tau_{yz} \cos(\omega - \omega_o)\, f_2(\omega_o)\, d\omega_o \\
\tau_{\rho\omega} &= \int_0^{\pi} \tau_{xz} \cos 2\cdot(\omega - \omega_o)\, f_2(\omega_o)\, d\omega_o \\
&- \int_0^{\pi} 2\mu\varepsilon_x \sin(\omega - \omega_o) \cos(\omega - \omega_o)\, f_1(\omega_o)\, d\omega_o
\end{aligned}
\tag{2.8c}
$$

where

$$\varepsilon_x = \frac{\partial u_x}{\partial x}$$

The weighting functions are taken in the following form for the problems of interest:

$$f_1(\omega_o) = \cos n\omega_o \qquad f_2(\omega_o) = \sin n\omega_o \tag{2.9}$$

For problems exhibiting axial symmetry, n is taken as zero (Smirnov et al., 1933, and Zvolinskii, 1957)and thus only a plane strain problem is superposed. For the problem of a horizontal force parallel to the X axis, n is equal to one (Johnson and Robinson, 1972).

2.2.2 Determination of the Two-Dimensional Plane Strain Problem Corresponding to a Three-Dimensional Axisymmetric Problem

As indicated by Eqs. (2.8), a three-dimensional axisymmetric problem can be represented by a rotational superposition of a unique (Thompson and Robinson, 1969) plane strain problem. The inversion of this relationship, finding the two-dimensional boundary value problem defined by the three-dimensional problem, is the next major step of concern.

Before carrying out this inversion, some assumptions concerning the character of the plane problem can be made in order to simplify the general relations. The two-dimensional field associated with the axisymmetric three-dimensional problem will be symmetric. That is,

$$u_x(-x, y, t) = - u_x(x, y, t) \tag{2.10}$$

$$u_y(-x, y, t) = \quad u_y(x, y, t)$$

This assumption coupled with the change of variable, $\eta = \omega - \omega_o$, lead to the following simplification of Eqs. (2.8):

$$u_\rho = \int_0^\pi u_x \cos\eta \, d\eta$$

$$u_\omega = 0 \qquad (2.11a)$$

$$u_Y = \int_0^\pi u_y \, d\eta$$

$$\sigma_\rho = \int_0^\pi (\sigma_x - 2\mu \epsilon_x \sin^2\eta) \, d\eta$$

$$\sigma_\omega = \int_0^\pi (\sigma_z + 2\mu \epsilon_x \sin^2\eta) \, d\eta$$

$$\sigma_Y = \int_0^\pi \sigma_y \, d_y \qquad (2.11b)$$

$$\tau_{\rho Y} = \int_0^\pi \tau_{xy} \cos\eta \, d\eta$$

$$\tau_{\rho\omega} = \tau_{\omega Y} = 0$$

Note that the two-dimensional quantities such as u_x are functions of $\rho\cos\eta$, y, and t while the three-dimensional quantities such as u_ρ are functions of ρ, y, and t only.

The symmetry indicated by Eqs. (2.10) permits the last of Eqs. (2.11b) to be written:

$$\sigma_Y = 2\int_0^{\pi/2} \sigma_y \, d\eta \qquad (2.12)$$

$$\tau_{\rho Y} = 2\int_0^{\pi/2} \tau_{xy} \cos\eta \, d\eta$$

The change of variables, $\nu = \rho\cos\eta$, then yields:

$$\sigma_Y = 2\int_0^{\rho} \sigma_y \frac{d\,\nu}{\sqrt{\rho^2 - \nu^2}} \qquad (2.13)$$

$$\tau_{\rho Y} = \frac{2}{\rho}\int_0^{\rho} \tau_{xy} \frac{\nu\, d\,\nu}{\sqrt{\rho^2 - \nu^2}}$$

Solving these equations as Abel integral equations (Hamel, 1949) provides:

$$\sigma_y = \frac{1}{\pi}\frac{\partial}{\partial r}\int_0^{r} \sigma_Y \frac{\nu\, d\,\nu}{\sqrt{r^2 - \nu^2}} \qquad (2.14)$$

$$\tau_{xy} = \frac{1}{\pi r}\frac{\partial}{\partial r}\int_0^{r} \frac{\tau_{\rho Y}\, \nu^2 d\nu}{\sqrt{r^2 - \nu^2}}$$

where $r^2 = x^2 + y^2$.

Eqs. (2.14) provide the boundary conditions for the two-dimensional plane strain problem in terms of the boundary conditions for a three-dimensional axisymmetric problem. As will be discussed in Sec. 2.3, the plane problems can be solved with relative ease by the method of self similar potentials and then the three-dimensional problem can be reconstructed by direct rotational superposition. Note that if each two-dimensional problem satisfies the equations of motion the superposed problems satisfy the equation of motion and hence the three-dimensional problem satisfies the equation of motion.

2.2.3 Determination of the Two-Dimensional Plane Strain and Antiplane Problems Corresponding to a Single Force Perpendicular to the Axis of Rotation

This section considers the determination of the unique set of plane strain and antiplane problems associated with a particular three-dimensional problem. This amounts to a inversion of Eqs. (2.8) so as to define the two-dimensional boundary values in terms of the boundary values for the three-dimensional problem.

As before, some simplifying assumptions concerning the character of the plane problems can be made before proceeding to the actual inversion. The two-dimensional plane strain field associated with the three-dimensional problem of a single force parallel to the X axis is antisymmetric about the y axis. That is,

$$u_x(-x, y, t) = u_x(x, y, t)$$
$$u_y(-x, y, t) = -u_y(x, y, t) \qquad (2.15a)$$

The antiplane problem is symmetric, or

$$u_z(-x, y, t) = u_z(x, y, t) \qquad (2.15b)$$

These observations coupled with the change of variables, $\eta = \omega_o - \omega$, lead to the following simplifications of Eqs. (2.8):

$$u_\rho = \cos\omega \left\{ \int_0^\pi u_x \cos^2\eta \, d\eta - \int_0^\pi u_z \sin^2\eta \, d\eta \right\}$$
$$u_\omega = \sin\omega \left\{ -\int_0^\pi u_x \sin^2\eta \, d\eta + \int_0^\pi u_z \cos^2\eta \, d\eta \right\} \qquad (2.16a)$$
$$u_Y = \cos\omega \int_0^\pi u_y \cos\eta \, d\eta$$

and:

$$\sigma_\rho = \cos\omega \left\{ \int_0^\pi \sigma_x \cos\eta \, d\eta - 2\mu \int_0^\pi \epsilon_x \sin^2\eta \cos\eta \, d\eta \right.$$
$$\left. - 2 \int_0^\pi \tau_{zx} \sin^2\eta \cos\eta \, d\eta \right\}$$

$$\sigma_\omega = \cos\omega \left\{ \int_0^\pi \sigma_x \cos\eta \, d\eta - 2\mu \int_0^\pi \epsilon_x \cos^3\eta \, d\eta \right.$$
$$\left. + \int_0^\pi 2 \tau_{zx} \sin^2\eta \cos\eta \, d\eta \right\} \qquad (2.16b)$$

$$\sigma_Y = \cos\omega \int_0^\pi \sigma_y \cos\eta \, d\eta$$

$$\tau_{Y\rho} = \cos\omega \left\{ \int_0^\pi \tau_{yx} \cos^2\eta \, d\eta - \int_0^\pi \tau_{yz} \sin^2\eta \, d\eta \right\}$$

$$\tau_{Y\omega} = \sin\omega \left\{ \int_0^\pi -\tau_{yx} \sin^2\eta \, d\eta + \int_0^\pi \tau_{yz} \cos^2\eta \, d\eta \right\}$$

$$\tau_{\rho\omega} = \sin\omega \left\{ \int_0^\pi \tau_{zx}(\cos^2\eta - \sin^2\eta) \cos\eta \, d\eta \right.$$
$$\left. - 2\mu \int_0^\pi \epsilon_x \sin^2\eta \cos\eta \, d\eta \right\}$$

Note that all of the field quantities in the integrands are two-dimensional and are functions of $x = \rho\cos\eta$, y, and t. The strain, ϵ_x, is equal to $\partial u_x / \partial x$.

The stresses $\tau_{Y\rho}$ and $\tau_{Y\omega}$ can be written in the equivalent form:

$$\begin{aligned} \tau_{Y\rho} &= \cos\omega \left[\int_0^{\pi} \tau_1 \, d\eta + \int_0^{\pi} \tau_2 \cos 2\eta \, d\eta \right] \\ \tau_{Y\omega} &= \sin\omega \left[-\int_0^{\pi} \tau_1 \, d\eta + \int_0^{\pi} \tau_2 \cos 2\eta \, d\eta \right] \end{aligned} \tag{2.17a}$$

where

$$\tau_1 = \frac{\tau_{yx} - \tau_{yz}}{2} \tag{2.17b}$$

$$\tau_2 = \frac{\tau_{yx} + \tau_{yz}}{2}$$

For a disc of uniform horizontal traction τ in the X direction,

$$\tau_{yx} = -\tau_{yz} = \bar{\tau} \tag{2.18}$$

The boundary tractions then become:

$$\begin{aligned} \sigma_Y &= \cos\omega \int_0^{\pi} \sigma_y(\rho\cos\eta, y, t) \cos\eta \, d\eta \\ \tau_{Y\rho} &= \cos\omega \int_0^{\pi} \bar{\tau}(\rho\cos\eta, y, t) \, d\eta \\ \tau_{Y\omega} &= -\sin\omega \int_0^{\pi} \bar{\tau}(\rho\cos\eta, y, t) \, d\eta \end{aligned} \tag{2.19}$$

As in the previous section, these equations can be inverted by introducing the variable $\nu = \rho\cos\eta$, taking advantage of observed symmetry, and solving as Abel integral equations (Hamel, 1949). The results are:

$$\sigma_y[r, Y, t] = \frac{1}{\pi r}\frac{\partial}{\partial r}\int_0^r \frac{\sigma_Y(\nu, y, t)}{\cos\omega}\frac{\nu^2\, d\nu}{\sqrt{r^2 - \nu^2}}$$

$$\bar{\tau}[r, Y, t] = \frac{1}{\pi}\frac{\partial}{\partial r}\int_0^r \frac{\tau_{Y\rho}[\nu, y, t]}{\cos\omega}\frac{\nu\, d\nu}{\sqrt{r^2 - \nu^2}} \qquad (2.20)$$

$$= -\frac{1}{\pi}\frac{\partial}{\partial r}\int_0^r \frac{\tau_{Y\omega}[\nu, y, t]}{\sin\omega}\frac{\nu\, d\nu}{\sqrt{r^2 - \nu^2}}$$

$$= \tau_{yx} = -\tau_{yz}$$

Eqs. (2.20) provide the boundary conditions for the two-dimensional plane strain and antiplane problems in terms of the boundary conditions for the three-dimensional problem of a single force parallel to the X axis. In this way, the three-dimensional problem degenerates to a solution of plane problems which, as will be shown, can be conveniently handled using the method of self similar potentials.

2.3 The Method of Self Similar Potentials

The method of self similar potentials has proven to be an extremely efficient means of solving two-dimensional wave propagation problems. The method applies to self similar problems - those whose boundary and initial conditions are homogeneous functions of time and space. The method avoids formidable mathematical manipulation and, in fact, provides the solution to some problems almost by inspection. Unlike many wave propagation approaches, the method of self similar potentials engenders physical insight at every stage of the solution process.

This approach to two-dimensional wave propagation problems was developed by V.I. Smirnov and S.L. Sobolev (1933) but has not been widely used outside the U.S.S.R. Thompson and Robinson (1969) presented a motivation, development, and bibliography of the method. More recently, Johnson and Robinson (1972) explored the application of the method in conjunction with rotational superposition to solve three-dimensional problems involving a single force parallel to the surface of an elastic half space.

This section reviews only those elements of the method that are essential to the developments in this study. For additional details, see the aforementioned references.

2.3.1 General Comments

The homogeneity of the boundary values for self similar problems permits a reduction in the number of independent variables necessary to describe the motion of a body, e.g. (x, y, t) becomes (x/t, y/t). This reduction is accomplished by introducing an auxiliary function which is the general solution of the wave equation. The wave equation becomes a partial differential equation of new variables which are elliptic behind the wave front and hyperbolic beyond it. The plane strain and antiplane problems which form the three-dimensional problem by rotational superposition uncouple and may be solved separately. The solution for the plane strain problem involves P and SV waves; the antiplane solution consists of an SH wave only.

2.3.2 Solution of a Plane Strain Problem by Self Similar Potentials

Consider that the solution to the plane strain problem can be expressed in terms of the self similar potential functions, ϕ and ψ_z, which are the real parts of corresponding complex potential functions, Φ and Ψ. The complex potentials are functions of complex variables θ_1 and θ_2. That is,

$$\phi = \text{Re } \Phi(\theta_1) \qquad \psi_z = \text{Re } \Psi(\theta_2) \tag{2.21}$$

The variables θ_1 and θ_2 parameterize the characteristic surfaces of the wave equation and any function of the variable θ_i with continuous first and second derivatives automatically satisfies the wave equation. The following implicit function defines the variables θ_1 and θ_2,

$$\delta_i = t - \theta_i x - y \sqrt{c_i^{-2} - \theta_i^2} + P_i(\theta_i) = 0 \qquad (2.22)$$

where $i = 1,2$ and $c_1 = a$ and $c_2 = b$. For loadings at the origin of the (x, y, t) space, only the characteristic surfaces through the origin are of interest and $P_i(\theta_i) = 0$. Consider for this general discussion that the loading is applied at the origin. For the subsurface loadings considered in subsequent sections $P_i(\theta_i)$ will not be zero.

Solution of Eq. (2.22) provides the values of the θ_i variables and defines a mapping of the (x, y, t) space into the complex θ_i plane. For $x^2 + y^2 < c_i^2 t^2$,

$$\theta_i = \frac{t x + i y \sqrt{t^2 - \frac{r^2}{c_i^2}}}{r^2} \qquad (2.23a)$$

and for $x^2 + y^2 > c_i^2 t^2$,

$$\theta_i = \frac{t x + y \sqrt{\frac{r^2}{c_i^2} - t^2}}{r^2} \qquad \text{if } x < 0 \qquad (2.23b)$$

$$\theta_i = \frac{t\,x - y\sqrt{\frac{r^2}{c_i^2} - t^2}}{r^2} \qquad \text{if } x > 0$$

where $r^2 = x^2 + y^2$. The signs of the radical in the above equations conform to the definition of the radical $\sqrt{c_i^{-2} - \theta_i^2}$ in Eq. (2.22) as positive when θ_i is positive imaginary with a cut on the real θ_i axis from $-c_i^{-1}$ to c_i^{-1}. This definition is consistent with Smirnov's work (1964). Note that the variable θ_i is real beyond the wave front and complex behind it. The characteristic surfaces parameterized by θ_i are planes tangent to the cone $x^2 + y^2 = c_i^2\, t^2$ as shown in Fig. 7a. The value of θ_i is constant in a characteristic plane and the variables are equal at points on the surface $y = 0$ where the characteristic planes for θ_1 and θ_2 meet. As will be shown, this fact eases the solution of boundary value problems when $y = 0$ is the boundary.

The mapping defined by Eqs. (2.23) maps the lower half space into the upper half θ_i plane. Fig. 7b shows the mapping of some typical points. The surface $y = 0$ as well as the region outside and on the wave front map onto the real θ_i axis. The area inside the wave front maps into the region off the real θ_i axis. Since $\theta_1 = \theta_2$ on the $y = 0$ surface, the surface maps into the real θ_i axis independent of wave speed. Every value of θ_i between and including $-c_i^{-1}$ and $+c_i^{-1}$ represents a characteristic plane.

The complex displacements can be written in terms of the complex self similar potentials as:

$$u_x = \frac{\partial \Phi(\theta_1)}{\partial x} + \frac{\partial \Psi(\theta_2)}{\partial y}$$

$$u_y = \frac{\partial \Phi(\theta_1)}{\partial y} - \frac{\partial \Psi(\theta_2)}{\partial x} \qquad (2.24)$$

$$u_z = 0$$

No confusion will arise by referring to complex displacements; the real part is the physical displacement.

Eq. (2.22) defines the derivatives of θ_i as

$$\frac{\partial \theta_i}{\partial x} = \frac{\theta_i}{\delta_i'} \qquad \frac{\partial \theta_i}{\partial y} = \frac{\sqrt{c_i^{-2} - \theta_i^2}}{\delta_i'} \qquad \frac{\partial \theta_i}{\partial t} = -\frac{1}{\delta_i'} \qquad (2.25a)$$

where

$$\delta_i' = -x + \frac{y\,\theta_i}{\sqrt{c_i^{-2} - \theta_i^2}} \qquad (2.25b)$$

Hence,

$$u_x = \Phi'(\theta_1)\,\frac{\theta_1}{\delta_1'} + \Psi'(\theta_2)\,\frac{\sqrt{b^{-2} - \theta_2^2}}{\delta_2'} \qquad (2.26a)$$

$$u_y = \Phi'(\theta_1) \frac{\sqrt{a^{-2} - \theta_1^2}}{\delta_1'} - \Psi'(\theta_2) \frac{\theta_2}{\delta_2'}$$

where

$$\Phi' = \frac{\partial \Phi}{\partial \theta_1} \qquad \text{and} \qquad \Psi' = \frac{\partial \Psi}{\partial \theta_2} \tag{2.26b}$$

The displacements of Eqs. (2.26) can be written in a slightly more general form as:

$$u_x = \frac{\partial}{\partial t} \left[-\int_0^{\theta_1} \theta \, \Phi'(\theta) \, d\theta - \int_0^{\theta_2} \sqrt{b^{-2} - \theta^2} \, \Psi'(\theta) \, d\theta \right] \tag{2.27}$$

$$u_y = \frac{\partial}{\partial t} \left[-\int_0^{\theta_1} \sqrt{a^{-2} - \theta^2} \, \Phi'(\theta) \, d\theta + \int_0^{\theta_2} \theta \, \Psi'(\theta) \, d\theta \right]$$

The complex stresses are then:

$$\frac{\sigma_y}{\mu} = \frac{\partial^2}{\partial t^2} \left[\int_0^{\theta_1} (b^{-2} - 2\theta^2) \, \Phi'(\theta) \, d\theta - \int_0^{\theta_2} 2\theta \sqrt{b^{-2} - \theta^2} \, \Psi'(\theta) \, d\theta \right]$$

$$\frac{\sigma_x}{\mu} = \frac{\partial^2}{\partial t^2}\left[\int_0^{\theta_1} (b^{-2} + 2\theta^2 - 2a^{-2})\, \Phi'(\theta)\, d\theta + \int_0^{\theta_2} 2\theta \sqrt{b^{-2} - \theta^2}\, \Psi'(\theta)\, d\theta\right] \tag{2.28}$$

$$\frac{\tau_{yx}}{\mu} = \frac{\partial^2}{\partial t^2}\left[\int_0^{\theta_1} 2\theta \sqrt{a^{-2} - \theta^2}\, \Phi'(\theta)\, d\theta + \int_0^{\theta_2} (b^{-2} - 2\theta^2)\, \Psi'(\theta)\, d\theta\right]$$

$$\frac{\sigma_z}{\mu} = \frac{\partial^2}{\partial t^2}\left[\int_0^{\theta_1} (b^{-2} - 2a^{-2})\, \Phi'(\theta)\, d\theta\right]$$

The complex variables θ_i and hence the potential functions of Eqs. (2.27) are self similar. That is, they are homogeneous functions of degree zero. Any loading that is homogeneous in spatial and time coordinates can be represented by an appropriate integration or differentiation of Eqs. (2.27) depending on the degree of homogeneity. For example, a self similar loading, i.e., homogeneous boundary tractions of degree zero, is represented by:

$$u_x = \int_0^t -\left[\int_0^{\theta_1} \theta\, \Phi'(\theta)\, d\theta + \int_0^{\theta_2} \sqrt{b^{-2} - \theta^2}\, \Psi'(\theta)\, d\theta\right] d\tau \tag{2.29a}$$

$$u_y = \int_0^t -\left[\int_0^{\theta_1} \sqrt{a^{-2} - \theta^2}\, \Phi'(\theta)\, d\theta - \int_0^{\theta_2} \theta\, \Psi'(\theta)\, d\theta\right] d\tau$$

and,

$$\frac{\Sigma_x}{\mu} = \int_0^{\theta_1} (b^{-2} + 2\theta^2 - 2a^{-2})\, \Phi'(\theta)\, d\theta + \int_0^{\theta_2} 2\theta \sqrt{b^{-2} - \theta^2}\, \Psi'(\theta)\, d\theta$$

$$\frac{\Sigma_y}{\mu} = \int_0^{\theta_1} (b^{-2} - 2\theta^2)\, \Phi(\theta)\, d\theta - \int_0^{\theta_2} 2\theta \sqrt{b^{-2} - \theta^2}\, \Psi'(\theta)\, d\theta \qquad (2.29b)$$

$$\frac{T_{yx}}{\mu} = \int_0^{\theta_1} 2\theta \sqrt{a^{-2} - \theta^2}\, \Phi'(\theta)\, d\theta + \int_0^{\theta_2} (b^{-2} - 2\theta^2)\, \Psi'(\theta)\, d\theta$$

On the surface $y = 0$, $\theta_1 = \theta_2 = \bar{\theta} = t/x$ and Eqs. (2.29) become:

$$u_x = \int_0^t -\left[\int_0^{\bar{\theta}} [\theta\Phi'(\theta) + \sqrt{b^{-2} - \theta^2}\, \Psi'(\theta)]\, d\theta\right] d\tau \qquad (2.30a)$$

$$u_y = \int_0^t - \left[\int_0^{\bar{\theta}} \left[\sqrt{a^{-2} - \theta^2}\, \Phi'(\theta) - \theta\, \psi'(\theta) \right] d\theta \right] d\tau$$

$$\frac{\Sigma_x}{\mu} = \int_0^{\bar{\theta}} \left[(b^{-2} + 2\theta^2 - 2a^{-2})\, \Phi'(\theta) + 2\theta \sqrt{b^{-2} - \theta^2}\, \Psi'(\theta) \right] d\theta \qquad (2.30b)$$

$$\frac{\Sigma_y}{\mu} = \int_0^{\bar{\theta}} \left[(b^{-2} - 2\theta^2)\, \Phi'(\theta) - 2\theta \sqrt{b^{-2} - \theta^2}\, \Psi'(\theta) \right] d\theta$$

$$\frac{T_{yx}}{\mu} = \int_0^{\bar{\theta}} \left[2\theta \sqrt{a^{-2} - \theta^2}\, \Phi'(\theta) + (b^{-2} - 2\theta^2)\, \Psi'(\theta) \right] d\theta$$

The derivatives of the self similar potentials may now be found in terms of the derivatives of the complex boundary tractions from the last two of Eqs. (2.30b). The results are:

$$\Phi'(\theta_1) = \frac{1}{\mu} \frac{(b^{-2} - 2\theta_1^2)\, \Sigma_y'(\theta_1) + 2\theta_1 \sqrt{b^{-2} - \theta_1^2}\, T_{yx}'(\theta_1)}{R(\theta_1^2)}$$

$$\Psi'(\theta_2) = \frac{1}{\mu} \frac{(b^{-2} - 2\theta_2^2)\, T_{yx}' - 2\theta_2 \sqrt{a^{-2} - \theta_2^2}\, \Sigma_y'(\theta_2)}{R(\theta_2^2)} \qquad (2.31a)$$

where

$$\Sigma_y'(\theta_i) = \frac{\partial}{\partial\theta_i}\Sigma_y(\theta_i) \qquad T_{yx}'(\theta_i) = \frac{\partial}{\partial\theta_i}T_{yx}(\theta_i) \tag{2.31b}$$

and

$$R(\theta_i^2) = (b^{-2} - 2\theta_i^2)^2 + 4\theta_i^2\sqrt{a^{-2} - \theta_i^2}\sqrt{b^{-2} - \theta_i^2} \tag{2.31c}$$

is the Rayleigh function.

The complex tractions Σ_y and T_{yx} on the surface $y = 0$ are usually determined from the specified tractions by application of the Schwarz integral theorem (Churchill, 1960) for the half plane. The complex tractions on the boundary are then written as functions of $\bar{\theta} = t/x$. It is clear that once the complex tractions on the boundary are known, the complex self similar potentials are determined by Eqs. (2.31). The stresses and displacements throughout the half space are then determined by equations such as Eqs. (2.29).

2.3.3 Solution of an Antiplane Problem by Self Similar Potentials

The antiplane problem is solved in much the same manner as the plane strain problem. The principal difference occurs because the solution for the antiplane case is sought in terms of a complex self similar displacement function $w(\theta_2)$. The real part of this

displacement function constitutes the physical displacement for a problem whose displacements are self similar. θ_2 is defined by Eq. (2.22).

For a problem with self similar tractions, homogeneous tractions of degree zero, the displacements and stresses are found in a manner analogous to Sec. 2.3.2 to be:

$$u_z = \int_0^t \left[\int_0^{\theta_2} w'(\theta)\, d\theta \right] d\tau \tag{2.32a}$$

$$\frac{T_{yz}}{\mu} = -\int_0^{\theta_2} \sqrt{b^{-2} - \theta^2}\, w'(\theta)\, d\theta \tag{2.32b}$$

$$\frac{T_{zx}}{\mu} = -\int_0^{\theta_2} \theta\, w'(\theta)\, d\theta$$

The general approach outlined in the last paragraph of Sec. 2.3.2 applies equally well to the antiplane case.

3. SURFACE DISPLACEMENTS CAUSED BY A SUBSURFACE VERTICAL OR HORIZONTAL DYNAMIC FORCE

3.1 General Remarks

This section considers the effect in an elastic half space of applying a subsurface dynamic point force that varies as a step function in time. The solutions presented in this section for both a vertical and horizontal force as a rotational superposition of self similar problems are necessary to the solution of double force problems in subsequent sections.

Section 3.2 gives the solution for surface disturbances caused by a subsurface vertical force. Although Pekeris and Lifson (1957) have considered this problem, some of the intermediate results obtained by the method of self similar potentials are useful for solving double force problems. The solution in this form incidentally illustrates the application of the methods of rotational superposition and self similar potentials to a specific problem.

Johnson and Robinson (1972) formulated the solution to an interior horizontal point force by the method of self similar potentials. The solution in this form is also necessary to the work that follows and the results are briefly summarized in Sec. 3.3.

3.2 Surface Displacements Caused by a Subsurface Vertical Force

The solution for the vertical point force of Fig. 8a is

considered in two major stages. The first includes that period of time prior to incidence of the waves on the free surface and is identical to consideration of a point force in an infinite medium. The second stage considers time after the free surface is set in motion and is accomplished by superposition of the waves for a point force in an infinite medium with appropriate reflected waves to give a stress free condition on the surface.

3.2.1 Point Force in an Infinite Medium

A point force in an infinite medium can be treated by joining the two half spaces of Fig. 9a. The loading $Pt^2/4$ is the resultant of self similar stresses applied over an expanding circular region $\rho \leq \alpha t$ on the surface of each connecting half space. The self similar stresses applied on the surface of the lower half space are

$$\sigma_Y = -\frac{P}{4\pi\alpha^2} \quad \text{for } 0 \leq \rho \leq \alpha t$$
$$\sigma_Y = 0 \quad \text{for } \rho > \alpha t \tag{3.1}$$

and on the upper half space are

$$\sigma_Y = +\frac{P}{4\pi\alpha^2} \quad \text{for } 0 \leq \rho \leq \alpha t$$
$$\sigma_Y = 0 \quad \text{for } \rho > \alpha t \tag{3.2}$$

In addition, symmetry requires that u_ρ be zero on the surface of each of the connecting half spaces. In the limit as α goes to zero, the above boundary conditions describe a vertical concentrated load of magnitude $Pt^2/2$ acting at a point, $(0,y_o,0)$, in an infinite medium.

As previously indicated, any three-dimensional axisymmetric problem can be represented by rotational superposition of a two-dimensional plane strain problem. The boundary conditions for the two-dimensional problem corresponding to the lower half space are determined from the first of Eqs. (2.14), (3.2), and (2.11a) to be:

$$\sigma_Y = -\frac{P}{4\pi\alpha^2} \qquad \text{for } 0 < |x| \leq \alpha t$$

$$\sigma_Y = -\frac{P}{4\pi^2\alpha^2}\left[1 - \frac{1}{\sqrt{1-\alpha^2t^2/x^2}}\right] \qquad \text{for } |x| > \alpha t \qquad (3.3)$$

$$u_x = 0$$

Since these are self similar boundary tractions on the surface of a half space, they can be represented as functions of $\theta = t/x$ (See Sec. 2.3) by:

$$\Sigma_y = -\frac{P}{4\pi^2\alpha^2}\left[1 - \frac{1}{\sqrt{1-\alpha^2\theta^2}}\right] \qquad \text{for all } |x| \qquad (3.4)$$

$$u_x = 0$$

Note that as α goes to zero, Eqs. (3.4) supply the boundary conditions for the point load, $Pt^2/2$. The first derivatives of these complex self similar boundary tractions with respect to θ are:

$$\Sigma_y' = + \frac{P\theta}{4\pi^2} \left[\frac{1}{(1 - \alpha^2\theta^2)^{3/2}} \right]$$

$$u_x' = 0 \tag{3.5}$$

A suitable definition of the radical $\sqrt{1 - \alpha^2\theta^2}$ will allow the above expressions to apply to both the upper and lower half planes. In this study, the radical $\sqrt{1 - \alpha^2\theta^2}$ is defined to be positive for θ positive imaginary. This definition corresponds to previous studies (Johnson and Robinson, 1972). The limit of $\sqrt{1 - \alpha^2\theta^2}$ as α goes to zero is then -1 when approached from the lower half θ plane (the upper half space) and +1 when approached from the upper half θ plane.

In the limit as α goes to zero the boundary conditions for the upper half space become:

$$\Sigma_y' = - \frac{P\theta}{4\pi^2}$$

$$u_x' = 0 \tag{3.6}$$

Note that the imaginary portion of the boundary conditions is zero and

consequently the imaginary portion of the final solution should be zero. This fact will be computationally useful later.

As determined from the first of Eqs. (2.30a) and the second of (2.30b), the potentials for the plane strain problem are:

$$\Phi_1'(\theta_1) = -\frac{Pb^2}{4\pi^2\mu}\,\theta_1$$

$$\Psi_2'(\theta_2) = +\frac{Pb^2}{4\pi^2\mu}\,\frac{\theta_2^2}{\sqrt{b^{-2} - \theta_2^2}} \tag{3.7}$$

where θ_1 and θ_2 are implicitly defined by:

$$\delta_1 = t - \theta_1 x - (y - y_o)\sqrt{a^{-2} - \theta_1^2} = 0$$

$$\delta_2 = t - \theta_2 x - (y - y_o)\sqrt{b^{-2} - \theta_2^2} = 0 \tag{3.8}$$

For $[x^2 + (y - y_o)^2]^{\frac{1}{2}} > c_i t$, the solution of Eqs. (3.8) is

$$\theta_i = \frac{xt + (y - y_o)\sqrt{\dfrac{x^2 + (y - y_o)^2}{c_i^2} - t^2}}{x^2 + (y - y_o)^2} \tag{3.9a}$$

for $x > 0$ and $(y - y_o) < 0$

and $x < 0$ and $(y - y_o) > 0$

$$\frac{xt - (y - y_o)\sqrt{\frac{x^2 + (y - y_o)^2}{c_i^2} - t^2}}{x^2 + (y - y_o)^2}$$

for $x > 0$ and $(y - y_o) > 0$

and $x < 0$ and $(y - y_o) < 0$

and for $[x^2 + (y - y_o)^2]^{\frac{1}{2}} < c_i t$,

$$\theta_i = \frac{xt + (y - y_o)\, i \sqrt{t^2 - \frac{x^2 + (y - y_o)^2}{c_i^2}}}{x^2 + (y - y_o)^2} \qquad (3.9b)$$

As in Sec. 2.3, Eqs. (3.9) define a mapping of the (x,y,t) space into the complex θ_1 and θ_2 planes.

3.2.2 Solution for Time After the Free Surface is Set in Motion

The solution for time after incidence of the disturbance on the free surface can be found by superposing the incident potentials for the point force in an infinite medium and the reflected potentials to give a stress free condition on the boundary $y = 0$. This superposition may be conveniently considered as two separate uncoupled two-dimensional problems:

1. Incidence of the P wave portion resulting in reflected PP and PS waves.

2. Incidence of the S wave portion resulting in reflected SS and SP waves.

The three-dimensional problem can then be reconstructed by direct rotational superposition.

3.2.2.1 Incident P Wave Portion

The incident P wave is described by the incident dilatational potential Φ_1' given in Eqs. (3.7). The superposition of this potential field with that of the reflected PP and PS waves must provide a stress free condition on the boundary $y = 0$. Fig. 10 shows a typical wave front pattern for the P, PP, and PS waves.

The reflected waves may be considered to emanate from within a fictitious half space that lies above the surface $y = 0$. The reflected potentials Φ_{11}' and Ψ_{12}' are considered to be functions of the complex variables θ_{11} and θ_{12} respectively. As will be seen, the appropriate definitions of the complex variables are:

$$\delta_{11} = t - \theta_{11}x + (y + y_o)\sqrt{a^{-2} - \theta_{11}^2} = 0$$

$$\delta_{12} = t - \theta_{12}x + y\sqrt{b^{-2} - \theta_{12}^2} + y_o\sqrt{a^{-2} - \theta_{12}^2} = 0 \qquad (3.10)$$

The sign of the y term differs from that used in Eqs. (3.8) in order to describe a disturbance originating from the half space $y \leq 0$.

The variable θ_{11} specifically characterizes a disturbance originating at $(0, -y_o, 0)$. The forms of δ_{12} and δ_{22} are chosen to provide the same value for θ_{11}, θ_{12} and θ_{22} on the boundary. While δ_{11} can be solved for θ_{11} directly, θ_{12} must be found numerically off the surface.

The reflected potentials, $\Phi'_{11}(\theta_{11})$ and $\Psi'_{12}(\theta_{12})$ are found by setting the tractions in terms of potentials equal to zero to indicate a stress free surface. These stress-potential relations can be derived in the same manner as were the stress-potential relations when only two potentials were involved. The resulting relations in this case would be:

$$\begin{aligned}
\frac{\Sigma_y}{\mu} &= \int_0^{\theta_1} (b^{-2} - 2\theta^2)\, \Phi'_1(\theta)\, d\theta \\
&\quad + \int_0^{\theta_{11}} (b^{-2} - 2\theta^2)\, \Phi'_{11}(\theta)\, d\theta \\
&\quad + \int_0^{\theta_{12}} 2\theta \sqrt{b^{-2} - \theta^2}\, \Psi'_{12}(\theta)\, d\theta
\end{aligned} \tag{3.11}$$

$$\begin{aligned}
\frac{T_{yx}}{\mu} &= \int_0^{\theta_1} 2\theta \sqrt{a^{-2} - \theta^2}\, \Phi'_1(\theta)\, d\theta \\
&\quad - \int_0^{\theta_{11}} 2\theta \sqrt{a^{-2} - \theta^2}\, \Phi'_{11}(\theta)\, d\theta +
\end{aligned}$$

$$+\int_0^{\theta_{12}} (b^{-2} - 2\theta^2)\ \Psi'_{12}(\theta)\ d\theta$$

On the boundary, $\theta_1 = \theta_{11} = \theta_{12} = \theta$ and $\Sigma_y = T_{yx} = 0$. Hence the above equations can be solved for the reflected potentials. The results are:

$$\Phi'_{11}(\theta) = \frac{4\theta^2\ \sqrt{a^{-2} - \theta^2}\ \sqrt{b^{-2} - \theta^2} - (b^{-2} - 2\theta^2)^2}{R(\theta^2)}\ \Phi'_1(\theta)$$

$$\Psi'_{12}(\theta) = -\frac{4\theta(b^{-2} - 2\theta^2)\ \sqrt{a^{-2} - \theta^2}}{R(\theta^2)}\ \Phi'_1(\theta) \qquad (3.12)$$

where $R(\theta^2)$ is the Rayleigh function.

The values of the reflected potentials off the boundary are uniquely determined (Thompson and Robinson, 1969) by substituting the appropriate complex variable for θ in the above expressions. The expressions for the reflected potentials then become:

$$\Phi'_{11}(\theta_{11}) = \frac{4\theta_{11}^2\ \sqrt{a^{-2} - \theta_{11}^2}\ \sqrt{b^{-2} - \theta_{11}^2} - (b^{-2} - \theta_{11}^2)^2}{R(\theta_{11}^2)}\ \Phi'_1(\theta_{11})$$

$$\Psi'_{12}(\theta_{12}) = -\frac{4\theta_{12}(b^{-2} - 2\theta_{12}^2)\ \sqrt{a^{-2} - \theta_{12}^2}}{R(\theta_{12}^2)}\ \Phi'_1(\theta_{12}) \qquad (3.13)$$

The displacement field for the incident and reflected waves is simply:

$$u_x = \frac{\partial \theta_1}{\partial x} \Phi_1'(\theta_1) + \frac{\partial \theta_{11}}{\partial x} \Phi_{11}'(\theta_{11}) + \frac{\partial \theta_{12}}{\partial y} \Psi_{12}'(\theta_{12})$$

$$u_y = \frac{\partial \theta_1}{\partial y} \Phi_1'(\theta) + \frac{\partial \theta_{11}}{\partial y} \Phi_{11}'(\theta_{11}) - \frac{\partial \theta_{12}}{\partial x} \Psi_{12}'(\theta_{12}) \qquad (3.14)$$

3.2.2.2 Incident S Wave Portion

The incident S wave portion of the disturbance can generate both SS and SP waves. The reflected potentials are found in the same manner as were those for the incident P wave. Differences result, however, for angles of incidence less than arccos (b/a). For these angles of incidence the reflected P wave becomes a surface phenomenon and a head wave is formed. Figs. 11 and 12 show typical wave patterns for the two ranges of the angle of incidence.

As in the case of the incident P wave, the reflected potentials, Ψ_{21}' and Ψ_{22}', are implicitly defined in terms of complex variables. In this case:

$$\delta_{21} = t - \theta_{21}x + y\sqrt{a^{-2} - \theta_{21}^2} + y_o\sqrt{b^{-2} - \theta_{21}^2} = 0 \qquad (3.15)$$

$$\delta_{22} = t - \theta_{22}x + (y + y_o)\sqrt{b^{-2} - \theta_{22}^2} = 0$$

Note that θ_{22} clearly parameterizes a disturbance emerging from the point $(0, -y_o, 0)$. On the boundary both complex variables, θ_{21} and θ_{22}, are equal to θ_2 of the incident S wave. θ_{22} may be solved for directly from δ_{22} but θ_{21} must be found numerically for points not on the $y = 0$ surface.

As in the previous section, the reflected potentials are found by setting the stress in terms of the potentials equal to zero to indicate a stress free boundary and solving for the reflected potentials. The stress potential relations for the incident and reflected waves would be:

$$\begin{aligned}
\frac{\Sigma_y}{\mu} &= \int_0^{\theta_{21}} (b^{-2} - 2\theta^2)\, \Phi_{21}'(\theta)\, d\theta \\
&\quad - \int_0^{\theta_2} 2\theta \sqrt{b^{-2} - \theta^2}\, \Psi_2'(\theta)\, d\theta \\
&\quad + \int_0^{\theta_{22}} 2\theta \sqrt{b^{-2} - \theta^2}\, \Psi_{22}'(\theta)\, d\theta \\
\frac{T_{yx}}{\mu} &= -\int_0^{\theta_{21}} 2\theta \sqrt{a^{-2} - \theta^2}\, \Phi_{21}'(\theta)\, d\theta +
\end{aligned} \tag{3.16}$$

$$+\int_0^{\theta_2} (b^{-2} - 2\theta^2)\ \Psi_2'(\theta)\ d\theta$$

$$+\int_0^{\theta_{22}} (b^{-2} - 2\theta^2)\ \Psi_{22}'(\theta)\ d\theta$$

As before, the reflected potentials become:

$$\Phi_{21}'(\theta_{21}) = \frac{4\theta_{21}(b^{-2} - 2\theta_{21}^2)\ \sqrt{b^{-2} - \theta_{21}^2}}{R(\theta_{21}^2)}\ \Psi_2'(\theta_{21})$$

$$\Psi_{22}'(\theta_{22}) = \frac{4\theta_{22}^2\ \sqrt{a^{-2} - \theta_{22}^2}\ \sqrt{b^{-2} - \theta_{22}^2} - (b^{-2} - 2\theta_{22}^2)^2}{R(\theta_{22}^2)}\ \Psi_2'(\theta_{22}) \tag{3.17}$$

The plane strain displacement field is then:

$$u_x = \frac{\partial\theta_{21}}{\partial x}\ \Phi_{21}'(\theta_{21}) + \frac{\partial\theta_2}{\partial y}\ \Psi_2'(\theta_2) + \frac{\partial\theta_{22}}{\partial y}\ \Psi_{22}'(\theta_{22})$$

$$u_y = \frac{\partial\theta_{21}}{\partial y}\ \Phi_{21}'(\theta_{21}) - \frac{\partial\theta_2}{\partial x}\ \Psi_2'(\theta_2) - \frac{\partial\theta_{22}}{\partial x}\ \Psi_{22}'(\theta_{22}) \tag{3.18}$$

3.2.3 Three-Dimensional Displacement Field

The displacement field for the three-dimensional problem of a point force in an elastic half space can be reconstructed by direct

rotational superposition of the two-dimensional problems just considered. This superposition is expressed generally by Eqs. (2.11) and can be written as:

$$u_\rho = \int_0^\pi \left[\frac{\partial\theta_1}{\partial x}\,\Phi_1'(\theta_1) + \frac{\partial\theta_{11}}{\partial x}\,\Phi_{11}'(\theta_{11}) + \frac{\partial\theta_{12}}{\partial y}\,\Psi_{12}'(\theta_{12}) + \frac{\partial\theta_{21}}{\partial x}\,\Phi_{21}'(\theta_{21}) + \frac{\partial\theta_2}{\partial y}\,\Psi_2'(\theta_2) + \frac{\partial\theta_{22}}{\partial y}\,\Psi_{22}'(\theta_{22}) \right] \cos\eta\, d\eta$$

$$u_\omega = 0 \tag{3.19}$$

$$u_\gamma = \int_0^\pi \left[\frac{\partial\theta_1}{\partial y}\,\Phi_1'(\theta_1) + \frac{\partial\theta_{11}}{\partial y}\,\Phi_{11}'(\theta_{11}) - \frac{\partial\theta_{12}}{\partial x}\,\Psi_{12}'(\theta_{12}) + \frac{\partial\theta_{21}}{\partial y}\,\Phi_{21}'(\theta_{21}) - \frac{\partial\theta_2}{\partial x}\,\Psi_2'(\theta_2) - \frac{\partial\theta_{22}}{\partial x}\,\Psi_{22}'(\theta_{22}) \right] d\eta$$

Transformation of variables from η to θ provides:

$$u_\rho = \int_{C_1} -\frac{\theta_1\Phi_1'\cos\eta}{G_1}\,d\theta_1 + \int_{C_{11}} -\frac{\theta_{11}\Phi_{11}'\cos\eta}{G_{11}}\,d\theta_{11} + \int_{C_{12}} \frac{\sqrt{b^{-2} - \theta_{12}^{\,2}}\;\Psi_{12}'\cos\eta}{G_{12}}\,d\theta_{12} +$$

$$+ \int_{C_{21}} - \frac{\theta_{21}\Phi'_{21}\cos\eta}{G_{21}}\, d\theta_{12} \qquad (3.20)$$

$$+ \int_{C_2} - \frac{\sqrt{b^{-2} - \theta_2^{\,2}}\,\Psi'_2\cos\eta}{G_2}\, d\theta_2$$

$$+ \int_{C_{22}} \frac{\sqrt{b^{-2} - \theta_{22}^{\,2}}\,\Psi'_{22}\cos\eta}{G_{22}}\, d\theta_{22}$$

$$u_\omega = 0$$

$$u_Y = -\int_{C_1} \frac{\sqrt{a^{-2} - \theta_1^{\,2}}\,\Phi'_1}{G_1}\, d\theta_1$$

$$+ \int_{C_{11}} \frac{\sqrt{a^{-2} - \theta_{11}^{\,2}}\,\Phi'_{11}}{G_{11}}\, d\theta_{11}$$

$$+ \int_{C_{12}} \frac{\theta_{12}\Psi'_{12}}{G_{12}}\, d\theta_{12} + \int_{C_{21}} \frac{\sqrt{a^{-2} - \theta_{21}^{\,2}}\,\Phi'_{21}}{G_{21}}\, d\theta_{21}$$

$$+ \int_{C_2} \frac{\theta_2\Psi'_2}{G_2}\, d\theta_2 + \int_{C_{22}} \frac{\theta_{22}\Psi'_{22}}{G_{22}}\, d\theta_{22}$$

where, for $i = 1, 2$:

$$G_i = \{\rho^2\theta_i^{\,2} - [t - (y - y_o)\sqrt{c_i^{-2} - \theta_i^{\,2}}]^2\}^{\frac{1}{2}} \qquad (3.21a)$$

$$\cos\eta = \frac{t - (y - y_o)\ \sqrt{c_i^{-2} - \theta_i^2}}{\rho\theta_i}$$

and for ii = 11, 22:

$$G_{ii} = \{\rho^2\theta_{ii}^2 - [t + (y + y_o)\ \sqrt{c_i^{-2} - \theta_{ii}^2}]^2\}^{\frac{1}{2}}$$

$$\cos\eta = \frac{t + (y + y_o)\ \sqrt{c_i^{-2} - \theta_{ii}^2}}{\rho\theta_{ii}} \qquad (3.21b)$$

and for i = 1, j = 2 and i = 2, j = 1:

$$G_{ij} = \{\rho^2\theta_{ij}^2 - [t + y\ \sqrt{c_i^{-2} - \theta_{ij}^2} + y_o\ \sqrt{c_j^{-2} - \theta_{ij}^2}]^2\}^{\frac{1}{2}} \qquad (3.21c)$$

$$\cos\eta = \frac{t + y\ \sqrt{c_i^{-2} - \theta_{ij}^2} + y_o\ \sqrt{c_j^{-2} - \theta_{ij}^2}}{\rho\theta_{ij}}$$

The integrands of Eqs. (3.20) are analytic off the real axis except for the branch cuts for the G functions. These branch cuts are taken outward from the end points of integration, θ_i^u and θ_i^ℓ, to positive infinity. Fig. 13 shows the admissible contours of integration in the θ_i plane and Fig. 14 shows those for the θ_i^2 plane. Note that C_η is the contour corresponding to the variation of η from 0 to π.

On the surface y = 0, Eqs. (3.20) become:

$$u_\rho = -\int_{C_1} \frac{4\theta_1\, b^{-2}\, \sqrt{a^{-2} - \theta_1^2}\, \sqrt{b^{-2} - \theta_1^2}}{G_1 \cdot R(\theta_1^2)}\, \Phi_1'\, \cos\eta\, d\theta_1$$

$$- \int_{C_2} \frac{2b^{-2}(b^{-2} - 2\theta_2^2)\, \sqrt{b^{-2} - \theta_2^2}}{G_2 \cdot R(\theta_2^2)}\, \Psi_2'\, \cos\eta\, d\theta_2$$

$$u_\omega = 0 \tag{3.22}$$

$$u_Y = -\int_{C_1} \frac{2b^{-2}(b^{-2} - 2\theta_1^2)\, \sqrt{a^{-2} - \theta_1^2}}{G_1 \cdot R(\theta_1^2)}\, \Phi_1'\, d\theta_1$$

$$+ \int_{C_2} \frac{4\theta_2\, b^{-2}\, \sqrt{a^{-2} - \theta_2^2}\, \sqrt{b^{-2} - \theta_2^2}}{G_2 \cdot R(\theta_2^2)}\, \Psi_2'\, d\theta_2$$

where for $y = 0$:

$$G_i = \{\rho^2\theta_i^2 - [t + y_o\, \sqrt{c_i^{-2} - \theta_i^2}]^2\}^{\frac{1}{2}}$$

$$\cos\eta = \frac{t + y_o\, \sqrt{c_i^{-2} - \theta_i^2}}{\rho\theta_i} \tag{3.23}$$

For the incident potentials defined as in Eqs. (3.7), the displacements on the surface are:

$$\frac{2\pi^2\mu}{P}\, u_\rho = \int_{C_1} \frac{2\theta_1^2\, \sqrt{a^{-2} - \theta_1^2}\, \sqrt{b^{-2} - \theta_1^2}}{G_1\, R(\theta_1^2)}\, \cos\eta\, d\theta_1 +$$

$$-\int_{C_2} \frac{\theta_2^2(b^{-2} - 2\theta_2^2)}{G_2\, R(\theta_2^2)} \cos\eta\, d\theta_2$$

$$u_\omega = 0 \tag{3.24}$$

$$\frac{2\pi^2\mu}{P} u_Y = \int_{C_1} \frac{\theta_1(b^{-2} - 2\theta_1^2)\sqrt{a^{-2} - \theta_1^2}}{G_1\, R(\theta_1^2)} d\theta_1$$

$$+\int_{C_2} \frac{2\theta_2^3\sqrt{a^{-2} - \theta_2^2}}{G_2\, R(\theta_2^2)} d\theta_2$$

3.2.4 Disturbances on the Surface near the Wave Fronts

Although the equations of the previous section can provide numerical results for displacements throughout the half space, the specific character of the disturbances in the vicinity of the wave fronts is of particular interest. The following sections consider the disturbances on the surface near the wave fronts. Although not specifically studied here, disturbances off the surface could be examined without difficulty by a similar approach. The approach in this section parallels that of Johnson and Robinson (1972).

3.2.4.1 P, PP, and PS Wave Fronts

The first integral in each of Eqs. (3.24) defines the portion

of the disturbance caused by the P, PP, and PS waves. The end points of the contour of integration are defined for points on the surface by:

$$\theta_1{}^{\ell 2} = \theta_1{}^{u 2} = \left[\frac{\rho a t - y_o \sqrt{\rho^2 + y_o{}^2 - a^2 t^2}}{a(\rho^2 + y_o{}^2)} \right]^2 \qquad \text{for } t < t_p$$

$$\theta_1{}^{\ell 2} = \theta_1{}^{u 2} = \theta_p{}^2 = \frac{a^{-2}\rho^2}{\rho^2 + y_o{}^2} \qquad \text{for } t = t_p$$

$$\theta_1{}^{\ell 2} = \left[\frac{\rho a t - i\, y_o \sqrt{a^2 t^2 - (\rho^2 + y_o{}^2)}}{a(\rho^2 + y_o{}^2)} \right]^2 \qquad \text{for } t > t_p$$

$$t_p{}^2 = \frac{\rho^2 + y_o{}^2}{a^2} \qquad (3.25)$$

where t_p is the arrival time of the P, PP, and PS waves at the point of interest on the surface and θ_p is the corresponding θ_1 value. Note that for all values of time $\theta_1{}^{u 2} = \bar{\theta}_1{}^{\ell 2}$ and the end points lie on the same vertical line in the θ^2 plane. To determine the variation of $\theta_1{}^{\ell 2}$ near the wave front, it is convenient to rewrite it as

$$\theta_1{}^{\ell 2} = \left[\theta_p + \frac{\rho \Delta t - i\, y_o \sqrt{2 t \rho \Delta t + \Delta t^2}}{\rho^2 + y_o{}^2} \right]^2 \qquad (3.26)$$

where $\Delta t = t - t_p$. Eq. (3.26) shows that, for small values of Δt, the endpoints lie to the left of a^{-2}. The integrands of the first terms of Eqs. (3.24) are analytic to the left of a^{-2} and hence a straight line joining ${\theta_1}^{\ell^2}$ and ${\theta_1}^{u^2}$ would be an admissible contour of integration. Expanding the integrands in an infinite series and integrating term by term provides an estimate of the integrals to any desired degree of accuracy.

The integrands are of the form:

$$\int_{C_1} \frac{A({\theta_1}^2)}{G_1} \, d{\theta_1}^2 \tag{3.27}$$

$A({\theta_1}^2)$ is expanded about ${\theta_p}^2$ and G_1 about its branch points. Expanding $A({\theta_1}^2)$ about ${\theta_p}^2$ yields:

$$A({\theta_1}^2) \cong A_0 + A_1({\theta_1}^2 - {\theta_p}^2) + A_2 \frac{({\theta_1}^2 - {\theta_p}^2)^2}{2} + \ldots \tag{3.28a}$$

where

$$\begin{aligned} A_0 &= A({\theta_p}^2) \\ A_1 &= \left.\frac{d\, A({\theta_1}^2)}{d{\theta_1}^2}\right|_{{\theta_1}^2 = {\theta_p}^2} \qquad A_2 = \left.\frac{d^2 A({\theta_1}^2)}{d({\theta_1}^2)^2}\right|_{{\theta_1}^2 = {\theta_p}^2} \end{aligned} \tag{3.28b}$$

$G_1^2(\theta_1^2)$ can be rewritten (Zvolinski, 1957) before expanding to give

$$G_1^2(\theta_1^2) = (\rho^2 + y_o^2)\cdot\left(\sqrt{a^{-2} - \theta_1 u^2} - \sqrt{a^{-2} - \theta_1^2}\right)\cdot \left(\sqrt{a^{-2} - \theta_1^2} - \sqrt{a^{-2} - \theta_1 \ell^2}\right) \tag{3.29}$$

Dividing out the radicals $(\theta_1 u^2 - \theta_1^2)^{\frac{1}{2}}$ and $(\theta_1^2 - \theta_1 \ell^2)^{\frac{1}{2}}$ and expanding the first $\sqrt{a^{-2} - \theta_1^2}$ about $\theta_1 u^2$ and the second about $\theta_1 \ell^2$ in the remaining quantity yields:

$$G_1(\theta_1^2) \cong \frac{(\rho^2 + y_o^2)^{\frac{1}{2}} (\theta_1 u^2 - \theta_1^2)^{\frac{1}{2}} (\theta_1^2 - \theta_1 \ell^2)^{\frac{1}{2}}}{2(a^{-2} - \theta_1 u^2)^{\frac{1}{4}} (a^{-2} - \theta_1 \ell^2)^{\frac{1}{4}}} \cdot \left[1 + \frac{1}{4} \frac{(\theta_1^2 - \theta_1 u^2)}{(a^{-2} - \theta_1 u^2)} + \frac{1}{4} \frac{(\theta_1^2 - \theta_1 \ell^2)}{(a^{-2} - \theta_1 u^2)} + 0^* (\theta_1^2 - \theta_1 u^2)^2 + 0 (\theta_1^2 - \theta_1 \ell^2)^2 \right]^{\frac{1}{2}} \tag{3.30}$$

Term by term integration of Eq. (3.27) now yields:

$$\int_{C_1} \frac{A(\theta_1^2)}{G_1(\theta_1^2)} d\theta_1^2 \cong \frac{2(a^{-2} - \theta_1 u^2)^{\frac{1}{4}} (a^{-2} - \theta_1 \ell^2)^{\frac{1}{4}}}{(\rho^2 + y_o^2)^{\frac{1}{2}}} \cdot \tag{3.31}$$

---

* "0" refers to "on the order of".

$$\cdot \left[A_0\pi + A_1\pi \frac{\theta_1 u^2 + \theta_1 \ell^2 - 2\theta_p{}^2}{2} + O\left(\theta_1 u^2 - \theta_1 \ell^2\right)^2 \right]$$

If one uses Eqs. (3.25) to express $\theta_1 \ell^2$ and $\theta_1 u^2$ as functions of ρ, y, t, and t_p to examine the variation with time, Eq. (3.31) becomes

$$\int_{C_1} \frac{A(\theta_1{}^2)}{G_1(\theta_1{}^2)} d\theta_1{}^2 \cong - \frac{2\, y_o}{a^2(\rho^2 + y_o{}^2)} \cdot \left[A_0\pi + A_1\pi \frac{\rho^2 - y_o{}^2}{(\rho^2 + y_o{}^2)^2} (t^2 - t_p{}^2) + O\left(t^2 - t_p{}^2\right)^2 \right] \tag{3.32}$$

The displacements on the surface in the vicinity of the fronts can now be expressed for $t \geq t_p$ as

$$u_\rho{}^P \cong - \frac{P\, y_o\, \theta_p \sqrt{a^{-2} - \theta_p{}^2}\, \sqrt{b^{-2} - \theta_p{}^2}}{a^2 \pi \mu (\rho^2 + y_o{}^2)\, R(\theta_p{}^2)} + O(t - t_p)$$

$$u_\omega{}^P = 0 \tag{3.33}$$

$$u_Y^P \cong - \frac{P\, y_o \sqrt{a^{-2} - \theta_p^2}\,(b^{-2} - 2\theta_p^2)}{2a^2\pi\mu(\rho^2 + y_o^2)\, R(\theta_p^2)} + O(t - t_p)$$

Eq. (3.33) shows that the radial and vertical surface displacements experience a step discontinuity upon arrival of the combined P, PP, and PS wave fronts and vary linearly thereafter.

3.2.4.2 S, SS, SP, and Head Wave Fronts

The character of the distortional portion of the disturbance depends on the angle of incidence, β (See Fig. 11). When the angle of incidence is greater than arccos (b/a), no head wave is formed, the wave front pattern is like that shown in Fig. 11, and the S, SP, and SS fronts are coincident on the surface. When the angle of incidence is less than arccos (b/a), a head wave is formed, the wave front pattern is like that shown in Fig. 12 and, on the surface, the SP front is coincident with the head wave front and the S front is coincident with the SS wave front. For the latter range of β, the S front is totally reflected as an SS front and the SP wave exists only as a surface phenomenon.

The distortional portion of the disturbance on the surface of the half space appears as the second integral in each of Eqs. (3.24). The endpoints of the contours of integration are:

$$\theta_2{}^{\ell 2} = \theta_2{}^{u 2} = \left[\frac{bt\rho - y_o\sqrt{\rho^2 + y_o{}^2 - b^2t^2}}{b(\rho^2 + y_o{}^2)}\right]^2 \qquad \text{for } t < t_s$$

$$\theta_2{}^{\ell 2} = \theta_2{}^{u 2} = \frac{\rho^2 b^{-2}}{\rho^2 + (-y_o)^2} = \theta_s{}^2 \qquad \text{for } t = t_s$$

$$\theta_2{}^{\ell 2} = \left[\frac{bt\rho - i\, y_o\sqrt{b^2t^2 - \rho^2 - y_o{}^2}}{b(\rho^2 + y_o{}^2)}\right]^2 \qquad \text{for } t > t_s$$

$$t_s{}^2 = \frac{\rho^2 + y_o{}^2}{b^2} \qquad (3.34)$$

where t_s is the arrival time of the S wave at the point of interest and θ_s is the corresponding θ_2 value. As in the P wave case, $\theta_2{}^{u 2} = \bar{\theta}_2{}^{\ell 2}$. Note that $\theta_s{}^2$ is always less than or equal to b^{-2}. If no head wave passes through the point of interest, $\theta_s{}^2$ is also less than a^{-2}. If a head wave does pass through the point of interest, $\theta_s{}^2$ will be greater than a^{-2} but less than b^{-2}.

Consider first the case when the point on the surface has an angle of incidence greater than arccos b/a, no head wave is formed, and $\theta_2{}^{\ell 2}$ lies to the left of a^{-2}. The integrands of Eqs. (3.24) are analytic to the left of a^{-2} and hence the method just used for the P wave may be employed. The results for the combined S, SP, and SS fronts

on the surface are:

$$u_\rho^S \simeq -\frac{Py_o}{2\pi\mu b^2} \quad \frac{b^{-2} - 2\theta_s^2}{(\rho^2 + y_o^2)\, R(\theta_s^2)} + O(t - t_s)$$

$$u_\omega^S = 0 \tag{3.35}$$

$$u_Y^S \simeq -\frac{Py_o}{\pi\mu b^2} \quad \frac{\sqrt{a^{-2} - \theta_s^2}}{p^2 + y_o^2} \quad \frac{\theta_s^2}{R(\theta_s^2)} + O(t - t_s)$$

Eqs. (3.35) show that the radial and vertical displacements on the surface experience a step discontinuity upon arrival of the combined S, SS, and SP wave fronts and vary linearly thereafter.

Now consider the case where the point of interest on the surface has an angle of incidence less than arccos b/a. A head wave is formed in this case and the wave fronts for the SP and H (head) waves coincide on the surface. The fronts of the S and SS waves also coincide on the surface (See Fig. 12). The ends of the contour of integration in this case lie between θ_s^2 and a^{-2} and are determined by the first of Eqs. (3.34). The contour of integration is then a path connecting the endpoints and crossing the real axis to the left of a^{-2} (See Fig. 13). The front of this reflected distortional wave is defined by:

$$b^2t^2 = \rho^2 + (y + y_o)^2 \qquad \text{for } \frac{\rho}{y} < \frac{bt}{\sqrt{\rho_\ell^2 + y_o^2 - b^2t^2}}$$

$$t = \rho\, a^{-2} + (y + y_o)\sqrt{b^{-2} - a^{-2}} \qquad \text{for } \frac{\rho}{y} > \frac{bt}{\sqrt{\rho_\ell^2 + y_o^2 - b^2t^2}} \tag{3.36}$$

where

$$\rho_\ell = a\,t - y_o\sqrt{a^2/b^2 - 1}$$

The first expression defines the SS wave front; the second, the head wave front.

To examine the character of disturbances in the vicinity of the head wave front, it is convenient to rationalize the denominators of the integrands by multiplying by the complex conjugate of the Rayleigh function. To illustrate the calculation, consider the radial displacement,

$$u_\rho^H = -\frac{P}{4\pi^2\mu}\int_C \frac{\theta_2 \cos\eta(b^{-2} - 2\theta_2^2)}{G_2\, R(\theta_2^2)}\, d\theta_2^2$$

$$= -\frac{P}{4\pi^2\mu}\int_C \frac{\theta_2 \cos\eta(b^{-2} - 2\theta_2^2)^3}{G_2\, R(\theta_2^2)\cdot\bar{R}(\theta_2^2)}\, d\theta_2^2 \qquad (3.37)$$

$$+ \frac{P}{4\pi^2\mu}\int_C \left[(\theta_2^3 \cos\eta\,(b^{-2} - 2\theta_2^2)\cdot \frac{4\sqrt{a^{-2} - \theta^2}\ \sqrt{b^{-2} - \theta_2^2}}{G_2\, R(\theta_2^2)\cdot\bar{R}(\theta_2^2)} \right] d\theta_2^2$$

The first integrand of Eq. (3.37) is analytic to the left of b^{-2} and, hence, contributes nothing to the solution. The character of the disturbance in the vicinity of the head wave front is then determined by the last integral. To the right of a^{-2} for the upper half space, the radical $\sqrt{a^{-2} - \theta^2}$ is defined to be negative imaginary below the branch cut and positive imaginary above it. Eqs. (3.37) therefore reduce to

$$u_\rho{}^H = -\frac{2\ Pi}{\pi^2\mu}\int_{\theta_\ell^2}^{a^{-2}} \left[\theta_2^3 \cos\eta(b^{-2} - 2\theta_2^2)\cdot \frac{4\sqrt{\theta_2^2 - a^{-2}}\ \sqrt{b^{-2} - \theta_2^2}}{G_2\cdot R(\theta_2^2)\cdot R(\theta_2^2)} \right] d\theta_2^2 \qquad (3.38)$$

To perform the calculation, the integrand is expanded in an infinite series and integrated term-wise. Consider the integral to be of the form

$$u_\rho{}^H = -\frac{8\ Pi}{\pi^2\mu}\int_{\theta_\ell{}^2}^{a^{-2}} \frac{A(\theta_2{}^2)}{G_2(\theta_2{}^2)}\ \sqrt{\theta_2 - a^{-2}}\ d\theta_2{}^2 \qquad (3.39a)$$

where

$$A(\theta_2{}^2) = \frac{\theta_2{}^3\cos\eta(b^{-2} - 2\theta_2{}^2)\ \sqrt{b^{-2} - \theta_2{}^2}}{R(\theta_2{}^2)\cdot\bar{R}(\theta_2{}^2)} \qquad (3.39b)$$

Expanding $A(\theta_2{}^2)$ in a Taylor's series about a^{-2} provides

$$A(\theta_2{}^2) \tilde{=} A_0 + O(\theta_2{}^2 - a^{-2}) \qquad (3.40a)$$

where

$$A_0 = \frac{a^{-2}(t + y_o\ \sqrt{b^{-2} - a^{-2}})\ \sqrt{b^{-2} - a^{-2}}}{\rho(b^{-2} - 2a^{-2})^3} \qquad (3.40b)$$

Expanding $G_2{}^2(\theta_2{}^2)$ of Eq. (3.21a) about $\theta_2{}^{\ell^2}$ yields

$$G_2(\theta_2\ ) \tilde{=} i\ \sqrt{\rho^2 + y_o{}^2}\ \sqrt{\theta_\ell{}^2 - \theta_2{}^2}\ \cdot$$

$$[B_0 + B_1(\theta_2{}^2 - \theta_2{}^{\ell^2}) + \ldots\ ]^{\frac{1}{2}} \qquad (3.41)$$

where

$$B_0 = 1 + \frac{y_o t}{(\rho^2 + y_o^2)\sqrt{b^{-2} - \theta_2 \ell^2}}$$

$$B_1 = \frac{y_o t}{4(\rho^2 + y_o^2)(b^{-2} - \theta_2 \ell^2)^{3/2}}$$

Carrying out the integration of Eq. (3.39a) provides

$$u_\rho^H \cong \frac{P A_o}{\pi\mu(\rho^2 + y_o^2)^{\frac{1}{2}} B_0^{\frac{1}{2}}} (\theta_2 \ell^2 - a^{-2}) + O(\theta_2 \ell^2 - a^{-2}) \tag{3.42}$$

The following approximation for $(\theta_2 \ell^2 - a^{-2})$ can be obtained from Eqs. (3.34),

$$\theta_2 \ell^2 - a^{-2} \cong - \frac{2(t - t_H)\sqrt{b^{-2} - a^{-2}}}{a\rho\sqrt{b^{-2} - a^{-2}} - y_o} + O(t - t_H)^2 \tag{3.43}$$

where t_H is the arrival time of the head wave. The character of the disturbance in the vicinity of the head wave front may now be written as:

$$u_\rho^H = 0 \qquad \text{for } t < t_H \tag{3.44a}$$

$$= 2A_0\, C_\rho \frac{(t - t_H)}{(\rho^2 + y_o^2)^{\frac{1}{2}}} + O(t - t_H)^2 \quad \text{for } t \geq t_H$$

where

$$C_\rho = - \frac{P}{\pi\mu B_0^{\frac{1}{2}}} \frac{\sqrt{b^{-2} - a^{-2}}}{a\rho \sqrt{b^{-2} - a^{-2}} - y_o} \tag{3.44b}$$

By the same approach the expression for vertical displacement would be

$$u_Y^H = 0 \qquad \text{for } t < t_H$$

$$\cong \frac{a^{-2}}{(b^{-2} - 2\theta^2)^2} C_\rho \frac{(t - t_H)}{(\rho^2 + y_o^2)^{\frac{1}{2}}} \tag{3.45a}$$

$$+ O(t - t_H)^2 \qquad \text{for } t \geq t_H$$

Note that B_0 is zero at the arrival of the S wave and, hence, C_ρ and the indicated displacements become infinite. To examine this singularity, expand $A(\theta_2^2)$ and $G_2(\theta_2^2)$ of Eq. (3.39a) about $\theta_\ell^2 = \theta_s^2$ to obtain:

$$G_2(\theta_2^2) \cong - (\rho^2 + y_o^2)^{\frac{1}{2}} (\theta_s^2 - \theta_2^2) \cdot$$

$$[B_1 + O(\theta_2^2 - \theta_s^2)^3]^{\frac{1}{2}} \tag{3.46}$$

$$A(\theta_2^2) \cong [C_0 + O(\theta_2^2 - \theta_s^2)]$$

where

$$B_1 = \frac{y_o t}{4(\rho^2 + y_o^2)\,(b^{-2} - \theta_s^2)^{3/2}}$$

$$= -\frac{tb^3\ \sqrt{\rho^2 + y_o^2}}{4(-y_o)^2}$$

and

$$C_0 = \frac{\theta_s^2(b^{-2} - 2\theta_s^2)\,(t + y_o\ \sqrt{b^{-2} - \theta_s^2})\ \sqrt{b^{-2} - \theta_s^2}}{\rho\ R(\theta_s^2)\cdot\bar{R}(\theta_s^2)}$$

Performing the integration indicated by Eq. (3.39a) expresses the logarithmically singular portion as

$$u_\rho^{\,L} = C_0 \cdot C_L \quad \ln\left[1 - \frac{bt}{\sqrt{\rho^2 + y_o^2}}\right] \tag{3.47a}$$

where

$$C_L = \frac{2Py_o(\theta_s^2 - a^{-2})^{\frac{1}{2}}}{\pi^2 \mu b\ \sqrt{bt}(\rho^2 + y_o^2)^{3/4}}$$

By the same approach,

$$u_Y^L = \frac{\theta_s^2(b^{-2} - 2\theta_s^2)^2}{R(\theta_s^2)\cdot\bar{R}(\theta_s^2)} C_L \ln\left[1 - \frac{bt}{\sqrt{\rho^2 + y_o^2}}\right] \quad (3.47b)$$

Eqs. (3.44) and (3.45) show that, in the region on the surface where a head wave is formed, the displacements caused by the SP and head wave fronts are continuous on arrival and vary linearly thereafter. The rate of variation with time is inversely proportional to the distance from the origin of the disturbance. As shown by Eqs. (3.47) a logarithmic singularity occurs behind the head wave front near the combined S and SS front. This singularity does not occur when the load is applied on the surface and occurs for the subsurface loading only when a head wave is formed.

3.2.4.3 Surface Wave Front

For the subsurface loading, no physical point maps into the complex plane at the Rayleigh pole at $\pm c^{-1}$. Consequently, no point experiences an infinite displacement due to the Rayleigh wave but points near the Rayleigh pole will be significantly affected.

To examine the Rayleigh effect on the surface, Eqs. (3.24) are written in the form

$$u_\rho = + \frac{P}{2\pi^2\mu} \int_{C_1} \left[\frac{I_1(\theta_1^2)}{G_1 R(\theta_1^2)} - \frac{(\rho^2 + y_o^2)^{-\frac{1}{2}} \cdot I_1(c^{-2})}{R'(c^{-2}) \cdot (\theta_1^2 - c^{-2}) \sqrt{(\theta_1 - \theta_1^{\ell})(\theta_1 - \theta_1^{u})}} \right] d\theta_1^2$$

$$+ \frac{P}{2\pi^2\mu} \int_{C_1} \frac{(\rho^2 + y_o^2)^{-\frac{1}{2}} I_1(c^{-2})}{R'(c^{-2}) \cdot (\theta_1^2 - c^{-2}) \sqrt{(\theta_1 - \theta_1^{\ell})(\theta_1 - \theta_1^{u})}} d\theta_1^2$$

$$+ \frac{P}{4\pi^2\mu} \int_{C_2} \left[\frac{I_2(\theta_2^2)}{G_2 R(\theta_2^2)} - \frac{(\rho^2 + y_o^2)^{-\frac{1}{2}} \cdot I_2(c^{-2})}{R'(c^{-2}) \cdot (\theta_2^2 - c^{-2}) \sqrt{(\theta_2^2 - \theta_2^{\ell})(\theta_2 - \theta_2^{u})}} \right] d\theta_2^2 \qquad (3.48a)$$

$$+ \frac{P}{4\pi^2\mu} \int_{C_2} \frac{(\rho^2 + y_o^2)^{-\frac{1}{2}} I_2(c^{-2})}{R'(c^{-2}) \cdot (\theta_2^2 - c^{-2}) \sqrt{(\theta_2 - \theta_2^{\ell})(\theta_2 - \theta_2^{u})}} d\theta_2^2$$

where

$$I_1(\theta_1^2) = \theta_1 \cos\eta \sqrt{a^{-2} - \theta_1^2} \sqrt{b^{-2} - \theta_1^2}$$

$$I_2(\theta_2^2) = \theta_2 \cos\eta (b^{-2} - 2\theta_2^2) \qquad (3.48b)$$

$$R'(c^{-2}) = \frac{d}{d\theta^2} R(\theta^2) \Bigg|_{\theta^2 = c^{-2}} \tag{3.48c}$$

Only the second and fourth integrals of Eq. (3.48) vary rapidly near the front of the surface wave. Evaluation of these integrals gives

$$u_\rho^R = \frac{Pi(\rho^2 + y_o^2)^{-\frac{1}{2}}}{2\pi\mu\, R'(c^{-2})} \left[\frac{2\, I_1(c^{-2})}{\sqrt{(c^{-1} - \theta_1^{\ell})(c^{-1} - \theta_1^{u})}} + \frac{I_2(c^{-2})}{\sqrt{(c^{-1} - \theta_2^{\ell})(c^{-1} - \theta_2^{u})}} \right] \tag{3.49}$$

Writing all $\sin\eta$ and $\cos\eta$ terms as functions of t, y, and $\xi = (\rho^2 + y_o^2)^{\frac{1}{2}} - ct$ and expanding in a binomial series approximates the Rayleigh portion of the radial displacement as:

$$u_\rho^R = \frac{Pci(\rho^2 + y_o^2)^{-\frac{1}{4}}}{4\sqrt{2}\,\pi\mu\, R'(c^{-2})} \left[\frac{2\sqrt{(a^{-2} - c^{-2})(b^{-2} - c^{-2})}}{(\xi + iy_o\sqrt{1 - c^2/a^2})^{\frac{1}{2}}} + \frac{b^{-2} - 2c^{-2}}{(\xi + iy_o\sqrt{1 - c^2/b^2})^{\frac{1}{2}}} \right] + O(\xi + iy_o\sqrt{1 - c^2/a^2})^{\frac{1}{2}}$$

$$+ O(\xi + iy_o\sqrt{1 - c^2/b^2})^{\frac{1}{2}} \tag{3.50a}$$

In a similar manner,

$$u_Y^R \cong -\frac{Pi}{2\sqrt{2}\,\pi\mu\, R'(c^{-2})(\rho^2 + y_o^2)^{\frac{1}{4}}} \cdot \frac{\sqrt{a^{-2} - c^{-2}}}{} \tag{3.50b}$$

$$\left[\frac{b^{-2} - 2c^{-2}}{(\xi + iy_o\ \sqrt{1 - c^2/a^2})^{\frac{1}{2}}} + \frac{2c^{-2}}{(\xi + iy_o\ \sqrt{1 - c^2/b^2})^{\frac{1}{2}}} \right]$$

$$+ \quad O(\xi + iy_o\ \sqrt{1 - c^2/a^2})^{\frac{1}{2}} + O(\xi + iy_o\ \sqrt{1 - c^2/b^2})^{\frac{1}{2}}$$

Eqs. (3.50) show that the displacements in the vicinity of the surface wave depend on:

1. The distance from the source.
2. The distance from the surface wave.
3. The relative values of ξ and y_o.

For points beneath the surface, a slight complication arises because θ_{21} and θ_{12} are not explicitly known. Although not considered in this study, the effect in this region could be examined numerically.

3.2.5 Numerical Results on the Surface

Numerical evaluation of Eqs. (3.24) for Poisson's ratio equal to .25 provide results identical to those of Pekeris and Lifson

(1957). The integration involves a simple quadrature in the complex plane and the techniques employed are discussed in the Appendix. The numerical results also demonstrate the singularities and nature of the displacements in the vicinity of the wave fronts that were derived in detail in the previous section.

3.3 Surface Displacements Caused by a Subsurface Horizontal Force

This section provides the solution by the methods of rotational superposition and self similar potentials for the displacements of the surface of an elastic half space which are caused by the subsurface horizontal force of Fig. 8b. This formulation was obtained by Johnson and Robinson (1972) and is summarized here only to the extent necessary to support the developments that follow.

The solution for the horizontal force that varies as a step function in time is obtained in much the same fashion as that for the vertical force. Differences arise because the loading is not axisymmetric and consequently an antiplane as well as a plane strain problem must be superposed to obtain the three-dimensional problem. The potential functions for the plane strain problem in the upper portion of an infinite medium are:

$$\Phi_1' = -\frac{Pb^2}{4\pi^2\mu}\frac{\theta_1^2}{\sqrt{a^{-2} - \theta_1^2}} \tag{3.51a}$$

$$\Psi_2' = - \frac{Pb^2}{4\pi^2\mu} \theta_2$$

These functions are comparable to those obtained for the vertical force in Eqs. (3.7). The displacement potential that defines the associated antiplane problem is

$$w_2' = - \frac{P}{4\pi^2\mu} \frac{\theta_2}{\sqrt{b^{-2} - \theta_2^2}} \tag{3.51b}$$

The potentials* of Eqs. (3.51a) describe the incident P and SV waves. The displacement potential* of Eq. (3.51b) describes an incident SH wave.

Insertion of the incident potentials of Eqs. (3.51a) into Eqs. (3.13)** and (3.17) determines the reflected PP, PS, SS, and SP waves generated at the y = 0 surface by the incident P and SV waves. In a similar fashion, the displacement potential for the reflected SH wave caused by the incident SH wave is determined by

$$w_{22}'(\theta_{22}) = w_2'(\theta_2) \tag{3.52}$$

The antiplane displacement field for the combined incident

---

* A factor of $\frac{1}{2}$ has been applied to these potentials to represent a force of magnitude P instead of 2P.

** Note that the subscripts "12" and "21" used by Johnson and Robinson have been interchanged in this study to provide direct correspondence with the geophysical terms PS and SP, respectively.

and reflected SH portion is

$$u_z = w_2' \frac{\partial \theta_2}{\partial t} + w_{22}' \frac{\partial \theta_{22}}{\partial t} \tag{3.53}$$

Rotational superposition of the two-dimensional problems described by the incident and reflected potentials along with an appropriate change of variables provides the following expressions for displacements on the surface of the half space:

$$\frac{u_\rho}{\cos\omega} = \int_{C_1} - \frac{\theta_1 \Phi_1' \cos^2\eta}{G_1} \cdot \frac{4b^{-2} \sqrt{a^{-2} - \theta_1^2}\ \sqrt{b^{-2} - \theta_1^2}}{R(\theta_1^2)}\, d\theta_1$$

$$- \int_{C_2} \frac{\Psi_2' \cos^2\eta}{G_2} \cdot \frac{2b^{-2}(b^{-2} - 2\theta_2^2)\ \sqrt{b^{-2} - \theta_2^2}}{R(\theta_2^2)}\, d\theta_2$$

$$- \int_{C_2} \frac{2w_2' \sin^2\eta}{G_2}\, d\theta_2 \tag{3.54}$$

$$\frac{u_\omega}{\sin\omega} = \int_{C_1} \frac{\theta_1 \Phi_1' \sin^2\eta}{G_1} \cdot \frac{4b^{-2}\sqrt{a^{-2} - \theta_1^2}\sqrt{b^{-2} - \theta_1^2}}{R(\theta_1^2)} d\theta_1$$

$$+ \int_{C_2} \frac{\Psi_2' \sin^2\eta}{G_2} \cdot \frac{2b^{-2}(b^{-2} - 2\theta_2^2)\sqrt{b^{-2} - \theta_2^2}}{R(\theta_2^2)} d\theta_2$$

$$+ \int_{C_2} \frac{2w_2' \cos^2\eta}{G_2} d\theta_2$$

$$\frac{u_Y}{\cos\omega} = -\int_{C_1} \frac{\Phi_1' \cos\eta}{G_1} \frac{2b^{-2}(b^{-2} - 2\theta_1^2)\sqrt{a^{-2} - \theta_1^2}}{R(\theta_1^2)} d\theta_1$$

$$+ \int_{C_2} \frac{\theta_2 \Psi_2' \cos\eta}{G_2} \frac{4b^{-2}\sqrt{a^{-2} - \theta_2^2}\sqrt{b^{-2} - \theta_2^2}}{R(\theta_2^2)} d\theta_2$$

where G_i, $\sin\eta$, and $\cos\eta$ are defined as in Sec. 3.2.3. See Johnson and Robinson (1972) for a discussion of the numerical results for

Eqs. (3.54) as well as a discussion of the wave front characteristics. Note, however, that the numerical results graphed in Johnson and Robinson's work should be divided by a factor of π^4 to provide the correct results.

4. APPLICATION OF THE METHODS OF ROTATIONAL SUPERPOSITION AND SELF SIMILAR POTENTIALS TO THE SOLUTION OF DOUBLE FORCE PROBLEMS

4.1 General Remarks

The objective of this section is to develop the procedures and relationships that permit the application of the method of rotational superposition and, in turn, the method of self similar potentials to dynamic problems involving a double force applied at a point beneath the surface of an elastic half space. This section focuses on those double force problems that are used in simulation of earthquake fault dislocations. The approach developed herein can also be applied to other nuclei of strain problems.

The two general orientations of double forces used in simulating earthquake fault dislocations are shown in Figs. 15 and 16. The forces comprising the double force of Fig. 15 are parallel to the strike* of the fault. The forces comprising the double force of Fig. 16 lie in a plane that is perpendicular to the strike. As shown in Sec. 4.2, these general double forces can be obtained by an appropriate superposition of five fundamental double vertical and double horizontal forces. In Sec. 4.3 the method of rotational superposition represents these fundamental double force problems as a superposition

---

* The "strike" is the compass direction of a horizontal line in an inclined plane.

of plane problems. This formulation permits the relationship between single and double force problems to occur between the two-dimensional problems instead of the three-dimensional ones. As derived in Sec. 4.4, an application of the method of self similar potentials gives the potential functions for these plane problems as a product of the potential functions for the single force and a simple function of the complex θ_i variable. The time variation of the double force problem formulated in this manner emerges in a natural fashion as a linear function of time.

4.2 Representation of an Inclined Double Force with Moment as a Superposition of Double Horizontal and Double Vertical Forces

Expressing an arbitrarily inclined double force as a superposition of fundamental double horizontal and double vertical forces permits one to obtain quick solution to any orientation by linear superposition once the fundamental solutions are in hand. The next two sections present this representation for two categories of inclined double forces - the double force at an arbitrary angle in a vertical plane (Fig. 16) and the double horizontal force in an inclined plane (Fig. 15). These double forces represent the two general orientations used in simulating fault dislocations because they correspond to dip-slip and strike-slip directions.

4.2.1 Double Force at an Arbitrary Angle in a Vertical Plane

Consider the forces of magnitude $P \cdot \Delta h^{-1}$ shown in Fig. 16a. In the limit as Δh goes to zero, this force system becomes a double force with moment applied at a point. Before taking the limit, resolve each of the constituent forces into vertical and horizontal components to obtain the force systems R and Q of Fig. 16b. Consider these systems separately in Figs. 17a and 17b respectively.

At point g in Fig. 17a, apply two equal and opposite forces of magnitude $R = P \cdot \Delta h^{-1} \cdot \sin\gamma$. Assume that the displacement field for a downward vertical force at point g and of magnitude P would be $\bar{u}^V(X,Y,Z,t)$. The displacement field of the force system shown in Fig. 17a would then be

$$\bar{u}^R = \sin\gamma \frac{\bar{u}^V(X,Y,Z,t) - \bar{u}^V(X,Y+\Delta h \cdot \cos\gamma,Z,t)}{\Delta h} - \sin\gamma \frac{\bar{u}^V(X,Y,Z,t) - \bar{u}^V(X-\Delta h \cdot \sin\gamma,Y,Z,t)}{\Delta h} \tag{4.1}$$

Multiplying the first term by $\cos\gamma \cdot (\cos\gamma)^{-1}$ and the second by $\sin\gamma \cdot (\sin\gamma)^{-1}$ yields

$$\bar{u}^R = (\sin\gamma)(\cos\gamma) \frac{\bar{u}^V(X,Y,Z,t) - \bar{u}^V(X,Y+\Delta h \cdot \cos\gamma,Z,t)}{\Delta h \cdot \cos\gamma} + \tag{4.2}$$

$$- \sin^2\gamma \frac{\bar{u}^V(X,Y,Z,t) - \bar{u}^V(X-\Delta h \cdot \sin\gamma, Y, Z, t)}{\Delta h \cdot \sin\gamma}$$

In the limit as Δh goes to zero, the above expression becomes

$$\bar{u}^R = - (\sin\gamma)(\cos\gamma) \frac{\partial \bar{u}^V}{\partial Y} - \sin^2\gamma \frac{\partial \bar{u}^V}{\partial X} \tag{4.3}$$

The first term of Eq. (4.3) is of the form of a double vertical force without moment (Case Vv); the second, of a double vertical force with moment (Case Vh).

By the same procedure the displacement field of force system Q of Fig. 17b could be written as

$$\bar{u}^Q = \sin\gamma \cos\gamma \frac{\partial \bar{u}^H}{\partial X} + \cos^2\gamma \frac{\partial \bar{u}^H}{\partial Y} \tag{4.4}$$

where $\bar{u}^H(X,Y,Z,t)$ represents the displacement field of a horizontal force of magnitude P applied in the positive X direction at point g in Fig. 17b. The first term of Eq. (4.4) is of the form of a double horizontal force without moment (Case $H_e h_e$); the second, of a double horizontal force with moment (Case Hv).

Since the superposition of $\bar{u}^R$ and $\bar{u}^Q$ provides the double force of Fig. 16a, it is clear that any arbitrarily inclined double force in a vertical plane can be represented by a superposition of fundamental double horizontal and double vertical forces. The angle

of inclination, γ, of the force determines the magnitude of the fundamental double forces that are superposed to obtain the inclined double force.

4.2.2 Double Horizontal Force in an Inclined Plane

Consider the double force with moment that is shown in Fig. 15a. Let the magnitude of each force be $P \cdot \Delta h^{-1}$. Add two equal but opposite forces at point d as shown in Fig. 15b. Assume that $\bar{u}^H(X,Y,Z,t)$ is the displacement field for a horizontal force of magnitude P and applied at point d in the positive X direction. The displacement field for the force system of Fig. 15b would then be

$$\bar{u} = \frac{\bar{u}^H(X,Y,Z,t) - \bar{u}^H(X,Y,Z-\Delta h \cdot \sin\gamma,t)}{\Delta h} - \frac{\bar{u}^H(X,Y,Z,t) - \bar{u}^H(X,Y+\Delta h \cos\gamma,Z,t)}{\Delta h} \tag{4.5}$$

By multiplying the first term by $\sin\gamma \cdot (\sin\gamma)^{-1}$ and the second by $\cos\gamma \cdot (\cos\gamma)^{-1}$, Eq. (4.5) becomes

$$\bar{u} = \sin\gamma \frac{\bar{u}^H(X,Y,Z,t) - \bar{u}^H(X,Y,Z-\Delta h \sin\gamma,t)}{\Delta h \cdot \sin\gamma} + \tag{4.6}$$

$$- \cos\gamma \frac{\bar{u}^H(X,Y,Z,t) - \bar{u}^H(X,Y+\Delta h \cos\gamma,Z,t)}{\Delta h \cdot \cos\gamma}$$

In the limit as Δh goes to zero, Eq. (4.6) becomes

$$u = \sin\gamma \frac{\partial \bar{u}^H}{\partial Z} + \cos\gamma \frac{\partial \bar{u}^H}{\partial Y} \tag{4.7}$$

Eq. (4.7) shows that the double horizontal force in an inclined plane can be represented by a superposition of the fundamental double horizontal forces of Cases $H_n h_e$ and Hv. The magnitude of the double forces so combined depends on the angle, γ.

4.3 Representation of Double Horizontal and Double Vertical Force Problems by Rotational Superposition

The last section showed that an inclined double force can be obtained by a linear superposition of double horizontal and double vertical forces. We now proceed to develop a convenient method for solving the fundamental double force cases.

The ease with which two-dimensional problems can be solved as compared with three-dimensional problems motivates us to explore the use of rotational superposition as a technique for solving the fundamental double force cases. This method expresses the three-dimensional problem as a superposition of plane problems rotated about an axis - hence, the name rotational superposition. Although the method has

proven quite suitable for single force problems (Johnson and Robinson, 1972), it has not been applied to double force or other nuclei of strain cases.

This section presents the derivation of the expressions which represent the fundamental double force problems by rotational superposition of associated two-dimensional problems. This formulation makes it possible to relate the two-dimensional problems instead of the three-dimensional single and double force problems. Later, in Sec. 4.4, an adaptation of the method of self similar potentials will provide the basis for solving the plane problems that evolve from this formulation.

The adaptation of the method of rotational superposition in this section is presented first in Sec. 4.3.1 for double vertical forces and then in Sec. 4.3.2 for double horizontal forces.

4.3.1 Double Vertical Force

4.3.1.1 Case Vh

Fig. 1 shows Case Vh, a double vertical force with moment. The following analysis leads to representation of this double force as a rotational superposition of plane strain fields.

Consider that the plane strain displacement field, $\Delta h^{-1} \cdot \bar{u}^f(x,y,t)$,* is related to the axisymmetric displacement field for a vertical force by Eqs. (2.11a). Apply this field at an angle ω_o with respect to the XY plane (See Fig. 18). Next apply an equal but opposite field, $-\Delta h^{-1} \cdot \bar{u}^f(x-\Delta x,y,t)$, at the same angle but shifted by an incremental amount Δh in the positive X direction. Superposition of these displacement fields yields:

$$u_x^d = \frac{u_x^f(x,y,t) - u_x^f(x-\Delta x,y,t)}{\Delta h}$$

$$u_y^d = \frac{u_y^f(x,y,t) - u_y^f(x-\Delta x,y,t)}{\Delta h} \qquad (4.8)$$

Note that since the plane strain field is not a function of z, only the x coordinate is affected by the incremental shift. The increments are related by $\Delta h \cdot \cos\omega_o = \Delta x$. In the limit as Δh goes to zero, the combined fields become

$$u_x^d = + \cos\omega_o \frac{\partial}{\partial x} u_x^f(x,y,t) \qquad (4.9)$$

---

* The "f" superscript will be employed to denote two-dimensional fields associated with a single force; the "d", two-dimensional fields associated with double forces. The upper-case superscripts "F" and "D", denote the corresponding three-dimensional fields.

$$u_y^{\,d} = + \cos\omega_o \frac{\partial}{\partial x} u_y^{\,f}(x,y,t)$$

where $(u_x^{\,f}, u_y^{\,f})$ is the two-dimensional displacement field corresponding to a vertical force.

If the applied loading is symmetric with respect to the y axis, then the associated two-dimensional fields will be symmetric. That is,

$$\begin{aligned} u_x^{\,f}(x,y,t) &= - u_x^{\,f}(-x,y,t) \\ u_y^{\,f}(x,y,t) &= \quad u_y^{\,f}(-x,y,t) \end{aligned} \tag{4.10}$$

The spatial derivatives of the displacement field and hence the double force field will necessarily be antisymmetric. That is,

$$\begin{aligned} u_x^{\,d}(x,y,t) &= \quad u_x^{\,d}(-x,y,t) \\ u_y^{\,d}(x,y,t) &= - u_y^{\,d}(-x,y,t) \end{aligned} \tag{4.11}$$

The three-dimensional double force field can now be constructed by applying the method of rotational superposition as in Eqs. (2.8a) and taking advantage of the symmetry just observed. The resulting three-dimensional field for the double vertical force of Case Vh is:

$$u_\rho^{\,D} = \cos\omega \int_0^\pi \frac{\partial u_x^{\,f}}{\partial x} \cos^2\eta \, d\eta$$

$$u_\omega^D = -\sin\omega \int_0^\pi \frac{\partial u_x^f}{\partial x} \sin^2\eta \, d\eta \tag{4.12}$$

$$u_Y^D = \cos\omega \int_0^\pi \frac{\partial u_y^f}{\partial x} \cos\eta \, d\eta$$

where (u_x^f, u_y^f) is the plane strain field associated with an axially symmetric force such as that considered in Sec. 3.

It will be noted that in the presentation just given the differentiation with respect to a variable to obtain the double force is obtained before integrating the two-dimensional problems. It is natural to ask what occurs if this order is reversed. Consider that the three-dimensional displacement fields, $\Delta h^{-1} \cdot \bar{u}^F(\rho,Y,t)$ and minus $\Delta h^{-1} \cdot \bar{u}^F(\rho-\Delta\rho,Y,t)$, are superposed as in Fig. 19. The first field is symmetric about the Y axis. The second field is equal but opposite to the first and is displaced by an incremental distance, Δh, in the positive X direction. The superposition of these fields can be expressed as:

$$u_\rho^D = \frac{u_\rho^F(\rho,Y,t) - \cos\Delta\omega \cdot u_\rho^F(\rho-\Delta\rho,Y,t)}{\Delta h}$$

$$u_\omega^D = \frac{\sin\Delta\omega \cdot u_\rho^F(\rho-\Delta\rho,Y,t)}{\Delta h} \tag{4.13}$$

$$u_Y^D = \frac{u_Y^F(\rho,Y,t) - u_Y^F(\rho-\Delta\rho,Y,t)}{\Delta h} .$$

Noting that $\Delta h \cdot \cos\omega = -\Delta\rho$ and $\Delta h \cdot \sin\omega \approx \rho \cdot \Delta\omega$ and taking the limit as Δh approaches zero provide:

$$u_\rho^D = + \cos\omega \frac{\partial u_\rho^F}{\partial\rho}$$

$$u_\omega^D = - \frac{\sin\omega}{\rho} u_\rho^F \qquad (4.14)$$

$$u_Y^D = + \cos\omega \frac{\partial u_Y^F}{\partial\rho}$$

As before, the displacement field for the axially symmetric force is expressed as a superposition of associated two-dimensional plane fields by:

$$u_\rho^F = \int_0^\pi u_x^f \cos\eta \, d\eta$$

$$u_\omega^F = 0 \qquad (4.15)$$

$$u_Y^F = \int_0^\pi u_y^f \, d\eta$$

Substitution of Eqs. (4.15) into the former expressions then gives:

$$u_\rho^D = +\cos\omega \int_0^\pi \frac{\partial u_x^f}{\partial x} \cos^2\eta \, d\eta$$

$$u_\omega^D = -\frac{\sin\omega}{\rho} \int_0^\pi u_x^f \cos\eta \, d\eta = -\sin\omega \int_0^\pi \frac{\partial u_x^f}{\partial x} \sin^2\eta \, d\eta$$

$$u_Y^D = +\cos\omega \int_0^\pi \frac{\partial u_y^f}{\partial x} \cos\eta \, d\eta \qquad (4.16)$$

Eqs. (4.16) are obviously identical to those previously developed in Eqs. (4.12).

Vectorially what has just been done can be expressed more compactly by taking a partial derivative of the vector field for a force. Let the three-dimensional axisymmetric displacement field of Eqs. (4.15) be written in vector form as:

$$\bar{u}^F = \int_0^\pi u_x^f \cos\eta \, d\eta \, \bar{i}_\rho + \int_0^\pi u_y^f \, d\eta \, \bar{j}$$

$$= u_\rho^F \, \bar{i}_\rho + u_Y^F \, \bar{j} \qquad (4.17)$$

The vector displacement field for the double force of Case Vh could be described by

$$\bar{u}^D = \frac{\partial \bar{u}^F}{\partial x} \qquad (4.18)$$

Considering that $X = \rho\cos\omega$ and $Z = \rho\sin\omega$, one may write Eq. (4.18) as

$$\bar{u}^D = \frac{\partial u_\rho^F}{\partial \rho} \frac{\partial \rho}{\partial} \bar{i}_\rho + u_\rho^F \frac{\partial}{\partial X} \bar{i}_\rho + \frac{\partial u_Y^F}{\partial \rho} \frac{\partial \rho}{\partial X} \bar{j} \tag{4.19}$$

It can easily be shown that Eqs. (4.19) may be simplified to give

$$\begin{aligned} \bar{u}^D = & \cos\omega \int_0^\pi \frac{\partial u_x^f}{\partial x} \cos^2\eta \, d\eta \, \bar{i}_\rho \\ & - \frac{\sin\omega}{\rho} \int_0^\pi u_x^f \cos\eta \, d\eta \, \bar{i}_\omega \\ & + \cos\omega \int_0^\pi \frac{\partial u_y^f}{\partial x} \cos\eta \, d\eta \, \bar{j} \end{aligned} \tag{4.20}$$

An integration by parts will show that Eq. (4.20) is equivalent to Eqs. (4.12).

4.3.1.2 Case Vv

The following analysis leads to representation of Case Vv (Fig. 2) as a rotational superposition of plane strain fields.

Consider that a plane strain displacement field, $\Delta h^{-1} \cdot \bar{u}^f(x,y,t)$, is related to the three-dimensional axisymmetric displacement field for a vertical interior force by Eqs. (2.11a). Apply this field at an angle ω_o with respect to the XY plane as was

done for Case Vh in Fig. 18. Next apply an equal but opposite field, $-\Delta h^{-1}\cdot\bar{u}^{f}(x,y-\Delta y,t)$, at the same angle but shifted by an amount Δh in the positive Y direction. Superposition of these fields yields:

$$u_x^d = \frac{u_x^f(x,y,t) - u_x^f(x,y-\Delta h,t)}{\Delta h}$$
$$u_y^d = \frac{u_y^f(x,y,t) - u_y^f(x,y-\Delta h,t)}{\Delta h} \qquad (4.21)$$

In the limit as Δh gives to zero, the combined fields become simply:

$$u_x^d = \frac{\partial u_x^f}{\partial y}$$
$$u_y^d = \frac{\partial u_y^f}{\partial y} \qquad (4.22)$$

The displacement field of the applied vertical force is symmetric with respect to the y axis as indicated by Eqs. (2.10). The field indicated by Eqs. (4.22) will also be symmetric. That is,

$$u_x^d(x,y,t) = -u_x^d(-x,y,t)$$
$$u_y^d(x,y,t) = u_y^d(-x,y,t) \qquad (4.23)$$

Substitution into Eqs. (2.8a) and taking advantage of the symmetry indicated above provide:

$$u_\rho^D = \int_0^\pi \frac{\partial u_x^f}{\partial y} \cos\eta \, d\eta$$

$$u_\omega^D = 0 \qquad (4.24)$$

$$u_Y^D = \int_0^\pi \frac{\partial u_y^f}{\partial y} \, d\eta$$

Eqs. (4.24) depict the three-dimensional problem of a double vertical force without moment (Case Vv) as a rotational superposition of plane strain problems which are related to the single force problem.

4.3.2 Double Horizontal Force

The three fundamental double horizontal force cases are Cases H_nh_e, Hv, and H_eh_e and are shown in Figs. 3, 4, and 5, respectively. The following sections present the representation of these cases by rotational superposition.

4.3.2.1 Case $H_n h_e$

Case $H_n h_e$ is a double horizontal force with moment with the forces in a horizontal plane. The following analysis leads to representation of this double force as a rotational superposition of plane strain fields.

Consider that the two-dimensional fields associated with a horizontal force of magnitude, $P \cdot \Delta h^{-1}$, and oriented as in Fig. 8b are a plane strain displacement field, $\Delta h^{-1} \cdot \bar{u}^f(x,y,t)$, and an antiplane displacement field, $\Delta h^{-1} \cdot u_x{}^f(x,y,t)$. Apply these fields at an angle ω_o with respect to the XY plane as in Fig. 20.

Next consider that equal but opposite fields, $\Delta h^{-1} \cdot \bar{u}^f(x-\Delta x,y,t)$ and $\Delta h^{-1} \cdot \bar{u}_z{}^f(x-\Delta x,y,t)$, are applied at the same angle but are shifted by an incremental amount Δh in the positive z direction. The superposition of these fields can then be represented by:

$$u_x{}^d = \frac{u_x{}^f(x,y,t) - u_x{}^f(x-\Delta x,y,t)}{\Delta h}$$

$$u_y{}^d = \frac{u_y{}^f(x,y,t) - u_y{}^f(x-\Delta x,y,t)}{\Delta h} \qquad (4.25)$$

$$u_z{}^d = \frac{u_z{}^f(x,y,t) - u_z{}^f(x-\Delta x,y,t)}{\Delta h}$$

Note that $\Delta h \cdot \sin\omega_o = \Delta x$ and thus, in the limit as Δh approaches zero, the above relations become:

$$u_x^d = \sin\omega_o \frac{\partial u_x^f}{\partial x}$$

$$u_y^d = \sin\omega_o \frac{\partial u_y^f}{\partial x} \qquad (4.26a)$$

$$u_z^d = \sin\omega_o \frac{\partial u_z^f}{\partial x} \qquad (4.26b)$$

Eqs. (4.26) express the two-dimensional fields associated with the double horizontal force of Fig. 3 in terms of the two-dimensional fields associated with a single horizontal force.

In Eqs. (2.15), the plane strain field associated with a single horizontal force was taken as antisymmetrical and the antiplane field symmetrical. The plane strain field in Eqs. (4.26a) will then necessarily be symmetrical and the antiplane field in Eq. (4.26b) will be antisymmetrical. That is,

$$u_x^d(x,y,t) = -u_x^d(-x,y,t)$$

$$u_y^d(x,y,t) = u_y^d(-x,y,t) \qquad (4.27a)$$

$$u_z^d(x,y,t) = -u_z^d(-x,y,t) \qquad (4.27b)$$

Rotational superposition together with the observed symmetry yield:

$$
\begin{aligned}
u_\rho^D &= \sin\omega\cos\omega\left[\int_0^\pi \frac{\partial u_x^f}{\partial x}\cos\eta\cos 2\eta\, d\eta\right. \\
&\qquad \left. - 2\int_0^\pi \frac{\partial u_z^f}{\partial x}\cos\eta\sin^2\eta\, d\eta\right] \\
u_\omega^D &= \cos 2\omega \int_0^\pi \frac{\partial u_x^f}{\partial x}\sin^2\eta\cos\eta\, d\eta \\
&\quad + \sin^2\omega \int_0^\pi \frac{\partial u_z^f}{\partial x}\cos\eta\, d\eta \\
&\quad + \cos 2\eta \int_0^\pi \frac{\partial u_z^f}{\partial x}\cos\eta\sin^2\eta\, d\eta \\
u_Y^D &= \sin\omega\cos\omega \int_0^\pi \frac{\partial u_y^f}{\partial x}\cos 2\eta\, d\eta
\end{aligned}
\tag{4.28}
$$

Eqs. (4.28) express the three-dimensional displacement field for Case $H_n h_e$ (See Fig. 3) as a rotational superposition of more easily determined plane fields.

The interchange of the order of differentiation and superposition in this case leads to the correct result as well but yields a

more complicated form than that of Eqs. (4.28). Consider the displacement field, $\Delta h^{-1}\cdot(u_\rho{}^F,\ u_\omega{}^F,\ u_Y{}^F)$, of a force $P\cdot(\Delta h)^{-1}$ in the positive X direction. This field can be expressed as a rotational superposition of plane strain and antiplane fields by:

$$\begin{aligned}
\Delta h^{-1}\cdot u_\rho{}^F(\rho,\omega,Y,t) &= \Delta h^{-1}\cdot\cos\omega\left[\int_0^\pi u_x{}^f \cos^2\eta\, d\eta\right. \\
&\qquad \left. -\int_0^\pi u_z{}^f \sin^2\eta\, d\eta\right] \\
\Delta h^{-1}\cdot u_\omega{}^F(\rho,\omega,Y,t) &= \Delta h^{-1}\cdot\sin\omega\left[-\int_0^\pi u_x{}^f \sin^2\eta\, d\eta\right. \\
&\qquad \left. +\int_0^\pi u_z{}^f \cos^2\eta\, d\eta\right] \\
\Delta h^{-1}\cdot u_Y{}^F(\rho,\omega,Y,t) &= \Delta h^{-1}\cdot\cos\omega \int_0^\pi u_y{}^f \cos\eta\, d\eta
\end{aligned} \tag{4.29}$$

Superpose over this field one corresponding to an equal but opposite force that is shifted an incremental distance Δh in the positive Z direction. This superposition can be expressed as:

$$\begin{aligned}
u_\rho = \frac{u_\rho{}^F(\rho,\omega,Y,t)}{\Delta h} &- \frac{u_\rho{}^F(\rho+\Delta\rho,\omega+\Delta\omega,Y,t)\cos\Delta\omega}{\Delta h} \\
&- \frac{u_\rho\,(\rho+\Delta\rho,\omega+\Delta\omega,Y,t)\,(-\sin\Delta\omega)}{\Delta h}
\end{aligned}$$

$$u_\omega = \frac{u_\omega^F(\rho,\omega,Y,t)}{\Delta h} - \frac{u_\omega^F(\rho+\Delta\rho,\omega+\Delta\omega,Y,t)\ \cos\ \Delta\omega}{\Delta h} \qquad (4.30)$$

$$- \frac{u_\rho^F(\rho+\Delta\rho,\omega+\Delta\omega,Y,t)\ (\sin\ \Delta\omega)}{\Delta h}$$

$$u_Y = \frac{u_Y^F(\rho,\omega,Y,t)}{\Delta h} \quad \frac{u_Y^F(\rho+\Delta\rho,\omega+\Delta\omega,Y,t)}{\Delta h}$$

Noting that $\Delta h \cdot \cos\omega \approx -\rho \cdot \Delta\omega$ and $\Delta h \cdot \sin\omega = -\Delta\rho$ and taking the limit as Δh goes to zero yields:

$$u_\rho = \sin\omega \frac{\partial u_\rho^F}{\partial\rho} + \frac{\cos\omega}{\rho} \cdot \frac{\partial u_\rho^F}{\partial\omega} - \frac{\cos\omega}{\rho} u_\omega^F$$

$$u_\omega = \sin\omega \frac{\partial u_\omega^F}{\partial\rho} + \frac{\cos\omega}{\rho} \cdot \frac{\partial u_\omega^F}{\partial\omega} + \frac{\cos\omega}{\rho} u_\rho^F \qquad (4.31)$$

$$u_Y = \sin\omega \frac{\partial u_Y^F}{\partial\rho} + \frac{\cos\omega}{\rho} \cdot \frac{\partial u_Y^F}{\partial\omega}$$

Substitution of Eqs. (4.29) into (4.31) yields expressions which are equivalent to Eqs. (4.28), although this equivalence is not immediately apparent. The form of Eqs. (4.28) is preferred because the derivatives are of the same order in each term.

4.3.2.2 Case Hv

The following analysis leads to representation of the double horizontal force of Case Hv (See Fig. 4) as a rotational superposition of plane fields.

Consider that a plane strain displacement field, $\Delta h^{-1} \cdot \bar{u}^f(x,y,t)$ and the antiplane field, $\Delta h^{-1} \cdot u_z{}^f(x,y,t)$, are related to a three-dimensional displacement field for a horizontal force of magnitude $P \cdot \Delta h^{-1}$ by Eqs. (2.16a). Apply these plane fields at an angle ω_o with respect to the XY plane. Next apply equal but opposite fields, $\Delta h^{-1} \cdot \bar{u}^f(x,y-\Delta y,t)$ and $\Delta h^{-1} \cdot u_z{}^f(x,y-\Delta y,t)$, at the same angle but shifted by an incremental amount Δh in the positive Y direction. The resulting displacement field is:

$$u_x{}^d = \frac{u_x{}^f(x,y,t) - u_x{}^f(x,y-\Delta y,t)}{\Delta h}$$

$$u_y{}^d = \frac{u_y\,(x,y,t) - u_y\,(x,y-\Delta y,t)}{\Delta h} \qquad (4.32)$$

$$u_z{}^d = \frac{u_z{}^f(x,y,t) - u_z{}^f(x,y-\Delta y,t)}{\Delta h}$$

Note that $\Delta h = \Delta y$ and, in the limit as Δh goes to zero, Eqs. (4.32) become:

$$u_x^d = \frac{\partial u_x^F}{\partial y}$$

$$u_y^d = \frac{\partial u_y^f}{\partial y} \qquad (4.33a)$$

$$u_z^d = \frac{\partial u_z^f}{\partial y} \qquad (4.33b)$$

where (u_x^f, u_y^f, u_z^f) is the two-dimensional displacement field corresponding to an interior horizontal force in three dimensions.

Some observations concerning the character of this displacement field can be made. The plane strain field is antisymmetric and antiplane field is symmetric (See Eqs. 2.15). The expressions of Eqs. (4.33a) will then necessarily be antisymmetric and Eq. (4.33b) will be symmetric. That is,

$$u_x^d(x,y,t) = + u_x^d(-x,y,t)$$

$$u_y^d(x,y,t) = - u_y^d(-x,y,t) \qquad (4.34)$$

$$u_z^d(x,y,t) = - u_z^d(-x,y,t)$$

Rotational superposition of the fields expressed by Eqs. (4.26) and simplifying according to the symmetry noted in Eqs. (4.27) yield:

$$u_\rho^D = \cos\omega \left[\int_0^\pi \frac{\partial u_x^f}{\partial y} \cos^2\eta \, d\eta - \int_0^\pi \frac{\partial u_z^f}{\partial y} \sin^2\eta \, d\eta \right]$$

$$u_\omega^D = -\sin\omega \left[\int_0^\pi \frac{\partial u_x^f}{\partial y} \sin^2\eta \, d\eta - \int_0^\pi \frac{\partial u_z^f}{\partial y} \cos^2\eta \, d\eta \right] \qquad (4.35)$$

$$u_Y^D = \cos\omega \int_0^\pi \frac{\partial u_y^f}{\partial y} \cos\eta \, d\eta$$

Eqs. (4.35) express the three-dimensional displacement field for the double horizontal force of Case Hv as a rotational superposition of more easily determined plane fields.

4.3.2.3 Case $H_e h_e$

The following analysis leads to representation of the double horizontal force without moment of Case $H_e h_e$ (See Fig. 5) as a rotational superposition of plane fields.

Consider that a plane strain field, $\Delta h^{-1} \cdot \bar{u}^f(x,y,t)$ and an antiplane field, $\Delta h^{-1} \cdot u_z^f(x,y,t)$, are related to the three-dimensional

field for a horizontal force of magnitude $P \cdot \Delta h^{-1}$ by Eqs. (2.16a). Apply these plane fields at an angle ω_o with respect to the XY plane (See Fig. 21). Next apply equal but opposite fields, $\Delta h^{-1} \cdot \bar{u}^f(x-\Delta x,y,t)$ and $\Delta h^{-1} \cdot \bar{u}_z{}^f(x-\Delta x,y,t)$, at the same angle but shifted by an incremental amount Δh in the positive X direction. The combined displacement field is:

$$u_x{}^d = \frac{u_x{}^f(x,y,t) - u_x{}^f(x-\Delta x,y,t)}{\Delta h}$$

$$u_y{}^d = \frac{u_y{}^f(x,y,t) - u_y{}^f(x-\Delta x,y,t)}{\Delta h} \qquad (4.36)$$

$$u_z{}^d = \frac{u_z{}^f(x,y,t) - u_z{}^f(x-\Delta x,y,t)}{\Delta h}$$

Note that $\Delta h \cdot \cos\omega_o = \Delta x$ and, in the limit as Δh goes to zero, the above expressions become:

$$u_x{}^d = \cos\omega_o \frac{\partial u_x{}^f}{\partial x}$$

$$u_y{}^d = \cos\omega_o \frac{\partial u_y{}^f}{\partial x} \qquad (4.37)$$

$$u_z^{\,d} = \cos\omega_o \frac{\partial u_z^{\,f}}{\partial x}$$

Eqs. (4.37) express the two-dimensional fields associated with Case $H_e h_e$ in terms of the plane fields associated with a single horizontal force.

Rotational superposition of the above plane fields using Eqs. (2.8) coupled with the simplifications of symmetry provided by Eqs. (4.27) yield:

$$\begin{aligned}
u_\rho^{\,D} = &\quad \cos 2\omega \int_0^\pi \cos^3\eta \frac{\partial u_x^{\,f}}{\partial x} d\eta \\
&+ \sin^2\omega \int_0^\pi \cos\eta \frac{\partial u_x^{\,f}}{\partial x} d\eta \\
&- \cos 2\omega \int_0^\pi \cos\eta \sin^2\eta \frac{\partial u_z^{\,f}}{\partial x} d\eta \\
u_\omega^{\,D} = &- \sin\omega \cos\omega \int_0^\pi 2 \sin^2\eta \cos\eta \frac{\partial u_x^{\,f}}{\partial x} d\eta \\
&+ \sin\omega \cos\omega \int_0^\pi \frac{\partial u_z^{\,f}}{\partial x} \cos 2\eta \cos\eta \, d\eta
\end{aligned} \qquad (4.38)$$

$$u_Y^D = \cos 2\omega \int_0^{\pi} \cos^2\eta \frac{\partial u_y^f}{\partial x} d\eta + \sin^2\omega \int_0^{\pi} \frac{\partial u_y^f}{\partial x} d\eta$$

Eqs. (4.38) express the three-dimensional displacement field for the double force Case $H_e h_e$ as a rotational superposition of more easily solved plane problems.

4.4 Application of the Method of Self Similar Potentials to Two-Dimensional Problems Associated with a Three-Dimensional Double Force

The last section explained the formulation of a double force applied at a point as a rotational superposition of two-dimensional problems. This section completes the general theory required for solution of double force problems by adapting the self similar potentials which have already been found for the single force case to handle the two-dimensional problems that evolved in the last section. In fact, as the derivation shows, the two-dimensional field associated with a double force can be obtained by simply multiplying the two-dimensional potentials for the single force case by an appropriate function of the complex variable, θ_i, of Sec. 3.2.1.

The two-dimensional fields of Sec. 4.3 for the double force loadings are related in each case to the two-dimensional displacement fields for the single vertical or horizontal force by a partial derivative with respect to x or y. A simpler relation exists as a result of the nature of the method of self similar potentials and is proven by the arguments that follow. Consider that $\bar{u}^f$ is the two-dimensional displacement field associated by rotational superposition with a single force that varies as a step function in time. As discussed in Sec. 2.3.2, the components of this displacement field can be expressed in terms of self similar potentials by Eqs. (2.27). As shown in Sec. 4.3, the components of the two-dimensional field for the double force are of the form

$$u_x^d = \frac{\partial}{\partial x} u_x^f \tag{4.39}$$

Inserting the first of Eqs. (2.27) into Eq. (4.39) yields

$$\begin{aligned} u_x^d = &- \frac{\partial}{\partial t} \frac{\partial}{\partial x} \int_0^{\theta_1} \theta \, \Phi_1' \, d\theta \\ &- \frac{\partial}{\partial t} \frac{\partial}{\partial x} \int_0^{\theta_2} \sqrt{b^{-2} - \theta^2} \, \Psi' \, d\theta \end{aligned} \tag{4.40}$$

Recognizing the relationship between time and space derivatives in Eq. (2.25a), one obtains

$$u_x^{\,d} = -\frac{\partial}{\partial t}\left[\ \theta_1\ \Phi_1' \cdot (-\theta_1)\ \frac{\partial \theta_1}{\partial t}\ \right] \qquad (4.41)$$

$$-\frac{\partial}{\partial t}\left[\ \sqrt{b^{-2} - \theta_2^{\,2}}\ \Psi_2' \cdot (-\theta_2)\ \frac{\partial \theta_2}{\partial t}\right]$$

Letting $E'(\theta_1)$ and $F'(\theta)$ equal $-\theta_1\Phi'$ and $-\theta_2\Psi_2'$, respectively, yields

$$u_x^{\,d} = -\frac{\partial}{\partial t}\left[\ \theta_1\ E'\ \frac{\partial \theta_1}{\partial t}\ \right] \qquad (4.42)$$

$$-\frac{\partial}{\partial t}\left[\ \sqrt{b^{-2} - \theta_2^{\,2}}\ F'\ \frac{\partial \theta_2}{\partial t}\right]$$

which can be rewritten as

$$u_x^{\,d} = -\frac{\partial^2}{\partial t^2}\left[\int_0^{\theta_1} \theta\ E'\ d\theta\right] \qquad (4.43)$$

$$-\frac{\partial^2}{\partial t^2}\left[\int_0^{\theta_2} \sqrt{b^{-2} - \theta^2}\ F'\ d\theta\right]$$

or

$$\int_0^t u_x^{\,d}\ d\tau = -\frac{\partial}{\partial t}\left[\int_0^{\theta_1} \theta\ E'\ d\theta\right] \qquad (4.44)$$

$$-\frac{\partial}{\partial t}\left[\int_0^{\theta_2} \sqrt{b^{-2} - \theta^2}\ F'\ d\theta\right]$$

Note that the form of Eq. (4.44) is identical to that of the first of Eqs. (2.27) except that E' and F' have replaced the potentials Φ' and Ψ'. The first time integral of u_x^d is then simply a two-dimensional displacement component associated with a double force that varies as a linear function in time. Hence, formal replacement of the potentials, Φ' and Ψ', of the single force varying as a step function by the potentials E' and F' in the method of self similar potentials provides the two-dimensional field associated with a double force that varies as a linear function in time. The modified potentials are the product of the potentials for the single force and a simple function of θ_i. This function of θ_i comes from the relation between the time and space derivatives of Eqs. (2.25a). The relationships between the potential functions Φ' and E' and between Ψ' and F' may be summarized as follows: For a double force related to a single force by $\frac{\partial}{\partial x}$,

$$E' = -\theta_1 \Phi'$$
$$F' = -\theta_2 \Psi' \tag{4.45}$$

For a double force related to a single force by $\frac{\partial}{\partial y}$,

$$E' = -\sqrt{a^{-2} - \theta_1^2}\, \Phi'$$
$$F' = -\sqrt{b^{-2} - \theta_2^2}\, \Psi' \tag{4.46}$$

As a result of the above representation, the convenience of the self similar method in the single force problem is retained in the double force problem. See the next chapter for specific applications of this derivation.

5. SURFACE DISPLACEMENTS CAUSED BY A SUBSURFACE DOUBLE VERTICAL OR DOUBLE HORIZONTAL FORCE

5.1 General Remarks

The previous chapters have provided the theory necessary to solve wave propagation problems involving a dynamic double force in an elastic half space. This chapter demonstrates the application of these developments by solving for the surface displacements caused by the five fundamental double forces shown in Figs. 1 thru 5. As will be discussed in Chapter 6, superposition of these fundamental cases can yield a variety of models for simulation of earthquake fault dislocations. The time variations of the moments of the double forces considered in this chapter are taken to be linear because the method of self similar potentials (See Sec. 4.4) naturally leads to this time variation. As will be discussed in Chapter 6, superposition can provide other time variations of interest.

5.2 Double Vertical Force

5.2.1 Case Vh; Double Vertical Force with Moment

The derivation of Sec. 4.3.1.1 showed that the double vertical force with moment, of Fig. 1 can be expressed as a rotational superposition of plane fields by:

$$u_\rho = \cos\omega \int_0^\pi \frac{\partial u_x^f}{\partial x} \cos^2\eta \, d\eta$$

$$u_\omega = -\sin\omega \int_0^\pi \frac{\partial u_x^f}{\partial x} \sin^2\eta \, d\eta \qquad (5.1)$$

$$u_Y = \cos\omega \int_0^\pi \frac{\partial u_y^f}{\partial x} \cos\eta \, d\eta$$

where (u_x^f, u_y^f) is the plane strain field associated with a single vertical force.

Application of the derivation of Sec. 4.4 yields the following expressions for the partial derivatives in Eq. (5.1) when the moment of the double force described by Eqs. (5.1) varies as a linear function in time:

$$\frac{\partial u_x^f}{\partial x} = -\frac{\partial \theta_1}{\partial x}\theta_1\Phi_1' - \frac{\partial \theta_{11}}{\partial x}\theta_{11}\Phi_{11}' - \frac{\partial \theta_{12}}{\partial y}\theta_{12}\Psi_{12}'$$

$$- \frac{\partial \theta_{21}}{\partial x}\theta_{21}\Phi_{21}' - \frac{\partial \theta_2}{\partial y}\theta_2\Psi_2' - \frac{\partial \theta_{22}}{\partial y}\theta_{22}\Psi_{22}'$$

$$\frac{\partial u_y^f}{\partial x} = -\frac{\partial \theta_1}{\partial y}\theta_1\Phi_1' - \frac{\partial \theta_{11}}{\partial y}\theta_{11}\Phi_{11}' + \frac{\partial \theta_{12}}{\partial x}\theta_{12}\Psi_{12}' \qquad (5.2)$$

$$- \frac{\partial \theta_{21}}{\partial y}\theta_{21}\Phi_{21}' + \frac{\partial \theta_2}{\partial x}\theta_2\Psi_2' + \frac{\partial \theta_{22}}{\partial x}\theta_{22}\Psi_{22}'$$

The potentials in Eqs. (5.2) are those for the single vertical force and are defined by Eqs. (3.7), (3.13), and (3.17). Insertion of Eqs. (5.2) into Eqs. (5.1) and transformation of variables from η to the appropriate θ variable provides:

$$\frac{u_\rho}{\cos\omega} = \int_{C_1} \frac{\theta_1^2 \cos^2\eta}{G_1} \Phi_1' \, d\theta_1 + \int_{C_{11}} \frac{\theta_{11}^2 \cos^2\eta}{G_{11}} \Phi_{11}' \, d\theta_{11}$$

$$- \int_{C_{12}} \frac{\theta_{12} \sqrt{b^{-2} - \theta_{12}^2}}{G_{12}} \cos^2\eta \, \Psi_{12}' \, d\theta_{12}$$

$$+ \int_{C_{21}} \frac{\theta_{21} \cos^2\eta}{G_{21}} \Phi_{21}' \, d\theta_{21}$$

$$+ \int_{C_2} \frac{\theta_2 \sqrt{b^{-2} - \theta_2^2}}{G_2} \cos^2\eta \, \Psi_2' \, d\theta_2$$

$$- \int_{C_{22}} \frac{\theta_{22} \sqrt{b^{-2} - \theta_{22}^2}}{G_{22}} \cos^2\eta \, \Psi_{22}' \, d\theta_{22}$$

$$\frac{u_\omega}{\sin\omega} = -\int_{C_1} \frac{\theta_1^2 \sin^2\eta}{G_1} \Phi_1' \, d\theta_1 - \int_{C_{11}} \frac{\theta_{11}^2 \sin^2\eta}{G_{11}} \Phi_{11}' \, d\theta_{11}$$

$$+ \int_{C_{12}} \frac{\theta_{12} \sqrt{b^{-2} - \theta_{12}^2}}{G_{12}} \sin^2\eta \, \Psi_{12}' \, d\theta_{12} - \qquad (5.3)$$

$$+ \int_{C_{21}} \frac{\theta_{21}^2 \sin^2\eta}{G_{21}} \Phi'_{21}\, d\theta_{21}$$

$$- \int_{C_2} \frac{\theta_2 \sqrt{b^{-2} - \theta_2^2}}{G_2} \sin^2\eta\, \Psi'_2\, d\theta_2$$

$$+ \int_{C_{22}} \frac{\theta_{22} \sqrt{b^{-2} - \theta_{22}^2}}{G_{22}} \sin^2\eta\, \Psi'_{22}\, d\theta_{22}$$

$$\frac{u_Y}{\cos\omega} = + \int_{C_1} \frac{\theta_1 \sqrt{a^{-2} - \theta_1^2}}{G_1} \cos\eta\, \Phi'_1\, d\theta_1$$

$$- \int_{C_{11}} \frac{\theta_1 \sqrt{a^{-2} - \theta_{11}^2}}{G_{11}} \cos\eta\, \Phi'_{11}\, d\theta_{11}$$

$$- \int_{C_{12}} \frac{\theta_{12}^2 \cos\eta}{G_{12}} \Psi'\, d\theta_{12}$$

$$- \int_{C_{21}} \frac{\theta_{21} \sqrt{a^{-2} - \theta_{21}^2}}{G_{21}} \Phi'_{21}\, d\theta_{21}$$

$$- \int_{C_2} \frac{\theta_2^2 \cos\eta}{G_2} \Psi'_2\, d\theta_2$$

$$- \int_{C_{22}} \frac{\theta_{22}^2 \cos\eta}{G_{22}} \Psi'_{22}\, d\theta_{22}$$

where the G functions are defined as in Eqs. (3.21).

For points on the surface, the displacements for Case Vh can be expressed in terms of the incident potentials for the single vertical force by:

$$\frac{u_\rho}{\cos\omega} = \int_{C_1} \frac{H_1\ \Phi_1'}{G_1\ R(\theta_1^2)} \cos^2\eta\ d\theta_1^2 + \int_{C_2} \frac{H_2\ \Psi_2'}{G_2\ R(\theta_2^2)} \cos^2\eta\ d\theta_2^2$$

$$\frac{u_\omega}{\sin\omega} = -\int_{C_1} \frac{H_1\ \Phi_1'}{G_1\ R(\theta_1^2)} \sin^2\eta\ d\theta_1^2 - \int_{C_2} \frac{H_2\ \Psi_2'}{G_2\ R(\theta_2^2)} \sin^2\eta\ d\theta_2^2 \qquad (5.4a)$$

$$\frac{u_Y}{\cos\omega} = \int_{C_1} \frac{I_1\ \Phi_1'}{G_1\ R(\theta_1^2)} \cos\eta\ d\theta_1^2 + \int_{C_2} \frac{I_2\ \Psi_2'}{G_2\ R(\theta_2^2)} \cos\eta\ d\theta_2^2$$

where

$$
\begin{aligned}
H_1 &= 2\theta_1 \; b^{-2} \sqrt{a^{-2} - \theta_1^2} \sqrt{b^{-2} - \theta_1^2} \\
H_2 &= \quad b^{-2}(b^{-2} - 2\theta_2^2) \sqrt{b^{-2} - \theta_2^2} \\
I_1 &= \quad b^{-2}(b^{-2} - 2\theta_1^2) \sqrt{a^{-2} - \theta_1^2} \\
I_2 &= -2\theta_2 \; b^{-2} \sqrt{a^{-2} - \theta_2^2} \sqrt{b^{-2} - \theta_2^2}
\end{aligned}
\tag{5.4b}
$$

Inserting the values for the incident potentials yields:

$$
\begin{aligned}
\frac{2\pi^2\mu}{P} \frac{u_\rho}{\cos\omega} &= -\int_{C_1} \frac{2\theta_1^3 \sqrt{a^{-2} - \theta_1^2} \sqrt{b^{-2} - \theta_1^2}}{G_1 \, R(\theta_1^2)} \cos^2\eta \, d\theta_1 \\
&\quad + \int_{C_2} \frac{\theta_2^3(b^{-2} - 2\theta_2^2)}{G_2 \, R(\theta_2^2)} \cos^2\eta \, d\theta_2 \\
\frac{2\pi^2\mu}{P} \frac{u_\omega}{\sin\omega} &= +\int_{C_1} \frac{2\theta_1^3 \sqrt{a^{-2} - \theta_1^2} \sqrt{b^{-2} - \theta_1^2}}{G_1 \, R(\theta_1^2)} \sin^2\eta \, d\theta_1 \\
&\quad - \int_{C_2} \frac{\theta_2^3(b^{-2} - 2\theta_2^2)}{G_2 \, R(\theta_2^2)} \sin^2\eta \, d\theta_2 \qquad (5.5) \\
\frac{2\pi^2\mu}{P} \frac{u_Y}{\cos\omega} &= -\int_{C_1} \frac{\theta_1^2(b^{-2} - 2\theta_1^2) \sqrt{a^{-2} - \theta_1^2}}{G_1 \, R(\theta_1^2)} \cos\eta \, d\theta_1 +
\end{aligned}
$$

$$-\int_{C_2} \frac{2\theta_2^4 \sqrt{a^{-2} - \theta_2^2}}{G_2 R(\theta_2^2)} \cos\eta \, d\theta_2$$

Note for computational convenience that placing a $-\theta\cos\eta$ in the integrands of Eqs. (3.24) produces integrals identical to those in the first and third of Eqs. (5.5).

5.2.2 Case Vv; Double Vertical Force without Moment

The double vertical force of Case Vv can be expressed by a rotational superposition of plane fields by Eqs. (4.24). An application of the derivation of Sec. 4.4 expresses the partial derivatives in the integrands of Eqs. (4.24) as:

$$\frac{\partial u_x^f}{\partial y} = -\frac{\partial \theta_1}{\partial x} \sqrt{a^{-2} - \theta_1^2}\, \Phi_1' + \frac{\partial \theta_{11}}{\partial x} \sqrt{a^{-2} - \theta_{11}^2}\, \Phi_{11}'$$

$$+ \frac{\partial \theta_{12}}{\partial y} \sqrt{b^{-2} - \theta_{12}^2}\, \Psi_{12}' + \frac{\partial \theta_{21}}{\partial x} \sqrt{a^{-2} - \theta_{21}^2}\, \Phi_{21}'$$

$$- \frac{\partial \theta_2}{\partial y} \sqrt{b^{-2} - \theta_2^2}\, \Psi_2' + \frac{\partial \theta_{22}}{\partial y} \sqrt{b^{-2} - \theta_{22}^2}\, \Psi_{22}' \quad (5.6)$$

$$\frac{\partial u_y^f}{\partial y} = -\frac{\partial \theta_1}{\partial y} \sqrt{a^{-2} - \theta_1^2}\, \Phi_1' + \frac{\partial \theta_{11}}{\partial y} \sqrt{a^{-2} - \theta_{11}^2}\, \Phi_{11}' -$$

$$+ \frac{\partial\theta_{12}}{\partial x} \sqrt{b^{-2} - \theta_{12}^2}\, \Psi'_{12} + \frac{\partial\theta_{21}}{\partial y} \sqrt{a^{-2} - \theta_{21}^2}\, \Phi'_{21}$$

$$+ \frac{\partial\theta_2}{\partial x} \sqrt{b^{-2} - \theta_2^2}\, \Psi'_2 - \frac{\partial\theta_{22}}{\partial x} \sqrt{b^{-2} - \theta_{22}^2}\, \Psi'_{22}$$

where the potentials are for the single vertical force and are defined by Eqs. (3.7), (3.13), and (3.17). Insertion of Eqs. (5.6) into Eqs. (4.24) and transformation of variables from η to the appropriate θ value yield the following expression for the surface displacements caused by the double force of Case Vv:

$$u_\rho = -\int_{C_1} \frac{2\theta_1\, b^{-2}(b^{-2} - 2\theta_1^2) \sqrt{a^{-2} - \theta_1^2}}{G_1 R(\theta_1^2)} \Phi'_1 \cos\eta\, d\theta_1$$

$$+ \int_{C_2} \frac{4\theta_2^2\, b^{-2} \sqrt{a^{-2} - \theta_2^2} \sqrt{b - \theta_2^2}}{G_2 R(\theta_2^2)} \Psi'_2 \cos\eta\, d\theta_2$$

$$u_\omega = 0 \qquad (5.7)$$

$$u_Y = \int_{C_1} \frac{4\theta_1 (2a^{-2} - b^{-2}) \sqrt{a^{-2} - \theta_1^2} \sqrt{b^{-2} - \theta_1^2}}{G_1 R(\theta_1^2)} \Phi'\, d\theta_1$$

$$+ \int_{C_2} \frac{2\theta_2 (2a^{-2} - b^{-2})(b^{-2} - 2\theta_2^2) \sqrt{b^{-2} - \theta_2^2}}{G_2 R(\theta_2^2)} \Psi'_2\, d\theta_2$$

where Φ_1' and Ψ_2' are defined by Eqs. (3.7).

5.3 Double Horizontal Force

5.3.1 Case $H_n h_e$; Double Horizontal Force with Moment, Forces in a Horizontal Plane

The double horizontal force of Case $H_n h_e$ can be expressed by a rotational superposition of plane fields by Eqs. (4.28). As before, the partial derivatives of the plane strain fields may be written as in Eqs. (5.2) but with the incident potential functions now defined in Eqs. (3.51a) for the horizontal force. Application of the derivation of Sec. 4.4 permits expression of the derivatives of the anti-plane field in Eqs. (4.28) as

$$\frac{\partial u_z^f}{\partial x} = - \theta_2 w_2' \frac{\partial \theta_2}{\partial t} - \theta_{22} w_{22}' \frac{\partial \theta_{22}}{\partial t} \tag{5.8}$$

where w_2' and w_{22}' are defined by Eqs. (3.51b) and (3.52).

Substituting into Eqs. (4.28) and transforming variables from η to the appropriate θ variable yields the following expressions for surface displacements for Case $H_n h_e$:

$$\frac{u_\rho}{\sin\omega \cos\omega} = \int_{C_1} \frac{H_1 \Phi_1'}{G_1 R(\theta_1^2)} \cos\eta \cos 2\eta \, d\theta_1 +$$

$$+ \int_{C_2} \frac{H_2 \Psi_2'}{G_2 R(\theta_2^2)} \cos\eta \cos 2\eta \, d\theta_2$$

$$+ 2 \int_{C_2} \frac{w_2'}{G_2} \cos\eta \sin^2\eta \, d\theta_2^2$$

$$\frac{u_\omega}{\cos 2\omega} = \int_{C_1} \frac{H_1 \Phi_1'}{G_1 R(\theta_1^2)} \sin^2\eta \cos\eta \, d\theta_1^2$$

$$+ \int_{C_2} \frac{H_2 \Psi_2'}{G_2 R(\theta_2^2)} \sin^2\eta \cos\eta \, d\theta_2^2 \qquad (5.9)$$

$$- \int_{C_2} \frac{w_2'}{G_2} \sin^2\eta \cos\eta \, d\theta_2^2$$

$$- \frac{\sin^2\omega}{\cos 2\omega} \int_{C_2} \frac{w_2'}{G_2} \cos\eta \, d\theta_2^2$$

$$\frac{u_Y}{\sin\omega \cos\omega} = \int_{C_1} \frac{I_1 \Phi_1'}{G_1 R(\theta_1^2)} \cos 2\eta \, d\theta_1^2$$

$$+ \int_{C_2} \frac{I_2 \Psi_2'}{G_2 R(\theta_2^2)} \cos 2\eta \, d\theta_2^2$$

where H_1, H_2, I_1, and I_2 are defined in Eqs. (5.4b).

5.3.2 Case Hv; Double Horizontal Force with Moment, Forces in a Vertical Plane

The double horizontal force of Case Hv can be expressed by a rotational superposition of plane fields by Eqs. (4.35). The partial derivatives of the plane strain fields may be written as in Eqs. (5.6) but with the incident potentials now defined in Eqs. (3.51a) for the horizontal force. Application of the derivation of Sec. 4.4 permits expression of the derivatives of the antiplane field in Eqs. (4.35) as

$$\frac{\partial u_z^f}{\partial y} = - \sqrt{b^{-2} - \theta_2^2}\, w_2' \frac{\partial \theta_2}{\partial t} + \sqrt{b^{-2} - \theta_{22}^2}\, w_{22}' \frac{\partial \theta_{22}}{\partial t} \tag{5.10}$$

Note that $w_2' = w_{22}'$ and hence, the surface where $\theta_2 = \theta_{22}$, the above derivative is zero.

As before, substitution into Eqs. (4.35) and transformation of variables lead to the following expressions for surface displacements for Case Hv:

$$\frac{2\pi^2\mu}{P}\frac{u_\rho}{\cos\omega} = \int_{C_1} \frac{\theta_1^3(b^{-2} - 2\theta_1^2)}{G_1 R(\theta_1^2)} \cos^2\eta \, d\theta_1$$

$$- \int_{C_2} \frac{2\theta_2^3 \sqrt{a^{-2} - \theta_2^2}\ \sqrt{b^{-2} - \theta_2^2}}{G_2 R(\theta_2^2)} \cos^2\eta \, d\theta_2$$

$$\frac{2\pi^2\mu}{P}\frac{u_\omega}{\sin\omega} = -\int_{C_1} \frac{\theta_1^3(b^{-2} - 2\theta_1^2)}{G_1 R(\theta_1^2)} \sin^2\eta \, d\theta_1 \qquad (5.11)$$

$$+ \int_{C_2} \frac{2\theta_2^3 \sqrt{a^{-2} - \theta_2^2}\ \sqrt{b^{-2} - \theta_2^2}}{G_2 R(\theta_2^2)} \sin^2\eta \, d\theta_2$$

$$\frac{2\pi^2\mu}{P}\frac{u_Y}{\cos\omega} = -\int_{C_1} \frac{2\theta_1^4(2a^{-2} - b^{-2})\ \sqrt{b^{-2} - \theta_1^2}}{G_1 R(\theta_1^2)} \cos\eta \, d\theta_1$$

$$- \int_{C_2} \left[\frac{\theta_2^2(2a^{-2} - b^{-2})\ \sqrt{b^{-2} - \theta_1^2}}{G_2 R(\theta_2^2)} \cdot \right.$$

$$\left. (b^{-2} - 2\theta_2^2) \cos\eta \right] d\theta_2$$

5.3.3 Case H_eh_e; Double Horizontal Force without Moment

The double horizontal force of Case H_eh_e can be expressed by a rotational superposition of plane problems by Eqs. (4.38). As before, the partial derivatives of the plane strain field in Eqs. (4.38) may be written as in Eqs. (5.2) with the incident potentials defined for the single horizontal force. The derivative for the antiplane field is as shown in Eq. (5.8).

In the same manner as before, the surface displacements for Case H_eh_e become:

$$u_\rho = \cos 2\omega \int_{C_1} \frac{H_1 \Phi_1'}{G_1 R(\theta_1^2)} \cos^3\eta \, d\theta_1^2$$

$$+ \cos 2\omega \int_{C_2} \frac{H_2 \Psi_2'}{G_2 R(\theta_2^2)} \cos^3\eta \, d\theta_2^2$$

$$+ \sin^2\omega \int_{C_1} \frac{H_1 \Phi_1'}{G_1 R(\theta_1^2)} \cos\eta \, d\theta_1^2$$

$$+ \sin^2\omega \int_{C_2} \frac{H_2 \Psi_2'}{G_2 R(\theta_2^2)} \cos\eta \, d\theta_2^2$$

$$+ \cos 2\omega \int_{C_2} \frac{2\theta_2 W_2'}{G_2} \cos\eta \sin 2\eta \, d\theta_2^2$$

$$\frac{u_\omega}{\sin\omega\cos\omega} = -2\int_{C_1} \frac{H_1\Phi_1'}{G_1R(\theta_1^2)}\sin^2\eta\cos\eta\, d\theta_1^2$$

$$-2\int_{C_2} \frac{H_2\Psi_2'}{G_2R(\theta_2^2)}\sin^2\eta\cos\eta\, d\theta_2^2 \qquad (5.12)$$

$$-\int_{C_2} \frac{2\theta_2 W_2'}{G_2}\cos^2\eta\cos\eta\, d\theta_2^2$$

$$u_Y = \cos2\omega\int_{C_1} \frac{I_1\Phi_1'}{G_1R(\theta_1^2)}\cos^2\eta\, d\theta_1^2$$

$$+\cos2\omega\int_{C_2} \frac{I_2\Psi_2'}{G_2R(\theta_2^2)}\cos^2\eta\, d\theta_2^2$$

$$+\sin^2\omega\int_{C_1} \frac{I_1\Phi_1'}{G_1R(\theta_1^2)}\, d\theta_1^2$$

$$+\sin^2\omega\int_{C_2} \frac{I_2\Psi_2'}{G_2R(\theta_2^2)}\, d\theta_2^2$$

where the incident potentials are for the horizontal force and are defined by Eqs. (3.51).

5.4 Disturbances Near the Wave Fronts

This section presents the determination of the character of the displacements on the surface in the vicinity of the wave fronts for each of the fundamental cases except Case Vv. The wave front analysis for Case Vv is almost identical to that for the vertical force of Sec. 3.1 and is not included here. As before, the analysis is performed in the θ^2 plane. The procedures are identical to those outlined in detail in Sec. 3 and only the results are presented here.

5.4.1 Case Vh

The expressions for displacement of the surface in the vicinity of the combined P, PP, and PS wave fronts are:

$$\frac{u_\rho^P}{\cos\omega} \cong \frac{P}{\pi\mu} \frac{y_o}{a^2(\rho^2 + y_o^2)} [A_0 + O(t - t_p)]$$

$$\frac{u_\omega^P}{\sin\omega} \cong \frac{P}{\pi\mu} \frac{y_o}{\rho^2(\rho^2 + y_o^2)^{\frac{1}{2}}} [A_0(t - t_p) + O(t - t_p)^2] \quad (5.13)$$

$$\frac{u_Y^P}{\cos\omega} \cong \frac{P}{\pi\mu} \frac{y_o}{a^2(\rho^2 + y_o^2)} [A_0 + O(t - t_p)]$$

where A_0 is the value of the first integrand in each of Eqs. (5.4) when $\sin^2\eta$ and G_1 are omitted and $\theta_1^2 = \theta_p^2$. The foregoing equations

show that the radial and vertical displacements on the surface experience a step discontinuity on arrival of the combined P, PP, and PS wave fronts; the circumferential displacement is continuous.

For angles of incidence greater than arccos (b/a), the following variations of surface displacements occur in the vicinity of the combined S, SS, and SP wave fronts:

$$\frac{u_\rho^S}{\cos\omega} \simeq -\frac{P}{\pi\mu}\frac{y_o}{b^2(\rho^2 + y_o^2)}[A_0 + O(t - t_s)]$$

$$\frac{u_\omega^S}{\sin\omega} \simeq -\frac{P}{\pi\mu}\frac{y_o}{\rho^2(\rho^2 + y_o^2)^{\frac{1}{2}}}[A_0(t - t_p) + O(t - t_s)^2] \qquad (5.14)$$

$$\frac{u_Y^S}{\cos\omega} \simeq +\frac{P}{\pi\mu}\frac{y_o}{b^2(\rho^2 + y_o^2)}[A_0 + O(t - t_s)]$$

where A_0 is the value of the second integrand in each of Eqs. (5.4) when $\sin^2\eta$ and G_1 are omitted and $\theta_2^2 = \theta_s^2$. The above equations indicate that the radial and vertical displacements on the surface experience a step discontinuity on arrival of the combined S, SS, SP front; the circumferential displacement is continuous.

For angles of incidence less than arccos (b/a) the head wave contribution to displacement of the surface is:

$$\frac{u_\rho^H}{\cos\omega} \tilde{=} C_\rho \frac{2a^{-2}(t + y_o\sqrt{b^{-2} - a^{-2}})^2 \sqrt{b^{-2} - a^{-2}}}{\rho^2(b^{-2} - 2a^{-2})^3}$$

$$\frac{t - t_H}{(\rho^2 + y_o^2)^{\frac{1}{2}}} + O(t - t_H)^2$$

$$\frac{u_\omega^H}{\sin\omega} \tilde{=} - C_h \frac{2a^{-4}\sqrt{b^{-2} - a^{-2}}}{(b^{-2} - 2a^{-2})^3} \frac{\sqrt{\rho^2 + y_o^2}}{\rho^2} (t - t_H)^2 \qquad (5.15a)$$

$$+ \quad O(t - t_H)^3$$

$$\frac{u_Y^H}{\cos\omega} \tilde{=} - C_\rho \frac{a^{-2}(t + y_o\sqrt{b^{-2} - a^{-2}})}{\rho^2(b^{-2} - 2a^{-2})^2} \frac{t - t_H}{(\rho^2 + y_o^2)^{\frac{1}{2}}} + O(t - t_H)^2$$

where C_ρ is defined by Eq. (3.44b) and

$$C_h = - \frac{PB_0^{\frac{1}{2}}}{4\pi\mu} \frac{a^2 \sqrt{b^{-2} - a^{-2}}}{a\rho\sqrt{b^{-2} - a^{-2}} - y_o} \qquad (5.15b)$$

The coefficient C_ρ becomes infinite in the vicinity of the S wave front and a logarithmic singularity occurs. The form of this singularity is:

$$\frac{u_\rho^L}{\cos\omega} \tilde{=} C_L \ln\left[1 - \frac{bt}{\sqrt{\rho^2 + y_o^2}}\right] \cdot \left| \frac{4\theta_2^4 \cos^2\eta(b^{-2} - 2\theta_2^2)(b^{-2} - \theta_2^2)^{\frac{1}{2}}}{2R(\theta_2^2)\cdot\bar{R}(\theta_2^2)} \right|_{\theta_2^2 = \theta_s^2}$$

$$\frac{u_\omega^L}{\sin\omega} = 0 \qquad (5.16)$$

$$\frac{u_Y^L}{\cos\omega} \tilde{=} C_L \ln\left[1 - \frac{bt}{\sqrt{\rho^2 + y_o^2}}\right] \cdot \left| \frac{\theta_2^3 \cos\eta(b^{-2} - 2\theta_2^2)^2(a^{-2} - \theta_2^2)^{\frac{1}{2}}}{R(\theta_2^2)\cdot R(\theta_2^2)} \right|_{\theta_2^2 = \theta_s^2}$$

where C_L is defined as in Eq. (3.47a).

The above equations show that all displacements are continuous on arrival of the head wave and that the radial and vertical displacements experience a logarithmic singularity on arrival of the S wave.

The variation of the displacements in the vicinity of the surface wave may be expressed by:

$$\frac{u_\rho^R}{\cos\omega} = -\frac{Pi(\rho^2 + y_o^2)^{3/4}}{\pi\mu c^3 \rho^2 (2)^{\frac{1}{2}} R'(c^{-2})} \cdot$$

$$\left[\frac{(c^{-2} - a^{-2})^{\frac{1}{2}}(c^{-2} - b^{-2})^{\frac{1}{2}}}{\left[\xi - iy_o \sqrt{1 - \frac{c^2}{a^2}}\right]^{\frac{1}{2}}} \right.$$

$$\left. - \frac{b^{-2} - 2c^{-2}}{2\left[\xi - iy_o \sqrt{1 - \frac{c^2}{b^2}}\right]^{\frac{1}{2}}} \right]$$

$$+ \; 0\left[\xi - iy_o \sqrt{1 - \frac{c^2}{a^2}}\right]^{\frac{1}{2}} + 0\left[\xi - iy_o \sqrt{1 - \frac{c^2}{b^2}}\right]^{\frac{1}{2}}$$

$$\frac{u_\omega^R}{\sin\omega} \simeq \frac{Pi}{\pi\mu} \frac{(2)^{\frac{1}{2}}(\rho^2 + y_o^2)^{\frac{1}{4}}}{cR'(c^{-2})} \qquad (5.17)$$

$$\left[(c^{-2} - a^{-2})^{\frac{1}{2}}(c^{-2} - b^{-2})^{\frac{1}{2}} \left[\xi - iy_o \sqrt{1 - \frac{c^2}{a^2}}\right]^{\frac{1}{2}} \right.$$

$$\left. - \frac{1}{2}(b^{-2} - 2c^{-2}) \left[\xi - iy_o \sqrt{1 - \frac{c^2}{b^2}}\right]^{\frac{1}{2}} \right]$$

$$+ \; 0\left[\xi - iy_o \sqrt{1 - \frac{c^2}{a^2}}\right]^{3/2}$$

$$+ \; 0\left[\xi - iy_o \sqrt{1 - \frac{c^2}{b^2}}\right]^{3/2}$$

$$\frac{u_Y^R}{\cos\omega} \simeq -\frac{Pi(\rho^2 + y_o^2)^{\frac{1}{4}}}{\pi\mu\, R'(c^{-2})\ \rho c^2 (2)^{\frac{1}{2}}} \cdot$$

$$\left[\frac{(b^{-2} - 2c^{-2})(a^{-2} - c^{-2})^{\frac{1}{2}}}{2\left[\xi - iy_o\sqrt{1 - \frac{c^2}{a^2}}\right]^{\frac{1}{2}}} + \frac{(a^{-2} - c^{-2})^{\frac{1}{2}}}{\left[\xi - iy_o\sqrt{1 - \frac{c^2}{b^2}}\right]^{\frac{1}{2}}} \right]$$

$$+ \quad 0\left[\xi - iy_o\sqrt{1 - \frac{c^2}{a^2}}\right]^{\frac{1}{2}} + 0\left[\xi - iy_o\sqrt{1 - \frac{c^2}{b^2}}\right]^{\frac{1}{2}}$$

where $R'(c^{-2})$ is defined by Eq. (3.48b) and $\xi = [(\rho^2 + y_o^2)^{\frac{1}{2}} - ct]$.

5.4.2 Case $H_n h_e$

The expressions for the displacement of the surface in the vicinity of the combined P, PP, and PS fronts are:

$$\frac{u_\rho^P}{\sin\omega\cos\omega} \simeq \frac{P}{\pi\mu}\frac{y_o}{a^2(\rho^2 + y_o^2)}[A_0 + O(t - t_p)]$$

$$\frac{u_\omega^P}{\cos 2\omega} \simeq -\frac{P}{\pi\mu}\frac{y_o}{\rho^2(\rho^2 + y_o^2)^{\frac{1}{2}}}[A_0(t - t_p) + O(t - t_p)^2] \qquad (5.18)$$

$$\frac{u_Y^P}{\sin\omega\cos\omega} = \frac{P}{\pi\mu}\frac{y_o}{a^2(\rho^2 + y_o^2)}[A_0 + O(t - t_p)]$$

where A_0 is the value of the first integrand in each of Eqs. (5.9) when $\sin^2\eta$ and G_1 are omitted and $\theta_1^2 = \theta_p^2$. The above equations show that the radial and vertical displacements experience a step discontinuity on arrival; the circumferential displacement is continuous.

For angles of incidence greater than arccos (b/a), the variation of the surface displacements in the vicinity of the combined S, SS, and SP wave fronts is:

$$\frac{u_\rho^S}{\sin\omega\cos\omega} \cong -\frac{P}{\pi\mu}\frac{y_o}{b^2(\rho^2 + y_o^2)}\left[\frac{(b^{-2} - 2\theta_s^2)\ (b^{-2} - \theta_s^2)^{\frac{1}{2}}\theta_s}{R(\theta_s^2)} + O(t - t_p)\right]$$

$$u_\omega^S \cong \cos 2\omega \frac{P}{2\pi\mu}\frac{y_o}{\rho^2(\rho^2 + y_o^2)^{\frac{1}{2}}} \cdot \qquad (5.19)$$

$$\left[\frac{\theta_s(2\theta_s^2 - b^{-2})(b^{-2} - \theta_s^2)^{\frac{1}{2}}}{R(\theta_s^2)}(t - t_p) + \theta_s\ (b^{-2} - \theta_s^2)^{-\frac{1}{2}}(t - t_p) + \right.$$

$$+ \qquad O(t - t_p)^2 \Bigg]$$

$$+ \quad \sin^2\omega \, \frac{P}{2\pi\mu} \, \frac{y_o}{a^2(\rho^2 + y_o^2)} \, (b^{-2} - \theta_2^2)^{-\frac{1}{2}} \, \theta_s$$

$$+ \quad O(t - t_p)$$

$$\frac{u_Y^S}{\sin\omega \cos\omega} \cong \frac{P}{\pi\mu} \, \frac{y_o}{b^2(\rho^2 + y_o^2)} \, .$$

$$\left[\frac{\theta_s^2 (a^{-2} - \theta_s^2)^{\frac{1}{2}} (b^{-2} - \theta_s^2)^{\frac{1}{2}}}{R(\theta_s^2)} + O(t - t_p) \right]$$

The above equations show that the displacements experience a discontinuity on arrival of the combined S, SS, and SP wave front except for the circumferential displacement when sinω is zero.

For angles of incidence less than arccos (b/a), the variation on the surface in the vicinity of the head wave is:

$$\frac{u_\rho^H}{\sin\omega \cos\omega} \cong - C_\rho \, \frac{2(b^{-2} - a^{-2})}{\rho \, (b^{-2} - 2a^{-2})^3} \, (t + y_o \sqrt{b^{-2} - a^{-2}}) \, .$$

$$[\,2(t + y_o\sqrt{b^{-2} - a^{-2}}) - a^{-2}\,] \cdot$$

$$\frac{t - t_H}{(\rho^2 + y_o^2)^{\frac{1}{2}}} + O(t - t_H)^2$$

$$\frac{u_\omega^H}{\sin^2\omega} \tilde{=} - C_\rho \frac{a^{-2}\, y_o}{2(b^{-2} - a^{-2})^{\frac{1}{2}}} \frac{t - t_H}{(\rho^2 + y_o^2)^{\frac{1}{2}}}$$

$$+ O(t - t_H)^2$$

$$\frac{u_Y^H}{\sin\omega\cos\omega} \tilde{=} - C_\rho \frac{(b^{-2} - a^{-2})^{\frac{1}{2}}}{(b^{-2} - 2a^{-2})^2} \frac{t - t_H}{\rho^2(\rho^2 + y_o^2)^{\frac{1}{2}}} \cdot$$

$$[2(t + y_o\sqrt{b^{-2} - a^{-2}})^2 - a^{-2}] + O(t - t_H)^2$$

where C_ρ is defined as before. The above equations show that all displacements are continuous on arrival of the head wave. As before, C_ρ becomes infinite in the vicinity of the S wave front and hence the displacements experience a logarithmic singularity.

The variation of the displacements in the vicinity of the surface wave may be expressed by:

$$\frac{u_\rho R}{\sin\omega\cos\omega} \simeq \frac{Pi(b^{-2} - c^{-2})^{\frac{1}{2}}(\rho^2 + y_o^2)^{\frac{1}{4}}}{\sqrt{2}\,\pi\mu c^2 R'(c^{-2})} \cdot$$

$$\left\{ \frac{y_o^2 - \rho^2}{c^2\rho^3} \left[\xi - iy\sqrt{1 - \frac{c^2}{a^2}}\right]^{-\frac{1}{2}} \right.$$

$$+ \frac{(b^{-2} - 2c^{-2})(y_o^2 - \rho^2)}{2c\rho^3} \cdot$$

$$\left. \left[\xi - iy_o\sqrt{1 - \frac{c^2}{b^2}}\right]^{-\frac{1}{2}} \right\}$$

$$+ 0\left[\xi - iy_o\sqrt{1 - \frac{c^2}{a^2}}\right]^{\frac{1}{2}}$$

$$+ 0\left[\xi - iy_o\sqrt{1 - \frac{c^2}{b^2}}\right]^{\frac{1}{2}}$$

$$\frac{u_\omega R}{\cos 2\omega} \simeq -\frac{\sqrt{2}\,Pi(b^{-2} - c^{-2})^{\frac{1}{2}}(\rho^2 + y_o^2)^{3/4}}{c^2\rho\pi\mu R'(c^{-2})} \cdot \qquad (5.21)$$

$$\left\{ \left[\xi - iy_o\sqrt{1 - \frac{c^2}{a^2}}\right]^{\frac{1}{2}} \right.$$

$$\left. + \frac{b^{-2} - 2c^{-2}}{2c^{-2}} \left[\xi - iy\sqrt{1 - \frac{c^2}{b^2}}\right]^{\frac{1}{2}} \right\}$$

$$+ \quad 0\left[\xi - iy_o\sqrt{1-\frac{c^2}{a^2}}\right]^{3/2}$$

$$+ \quad 0\left[\xi - iy_o\sqrt{1-\frac{c^2}{b^2}}\right]^{3/2}$$

$$\frac{u_Y R}{\sin\omega\cos\omega} \cong \frac{Pi(\rho^2 + y_o{}^2)^{-\frac{1}{4}}}{\sqrt{2}\,\pi\mu c^3 R(c^{-2})\rho^2} \cdot$$

$$\left[\frac{(b^{-2} - 2c^{-2})(y_o{}^2 - \rho^2)}{2} \cdot \right.$$

$$\left[\xi - iy_o\sqrt{1-\frac{c^2}{a^2}}\right]^{-\frac{1}{2}}$$

$$+ \quad (b^{-2} - c^{-2})^{\frac{1}{2}}(a^{-2} - c^{-2})^{\frac{1}{2}}(y_o{}^2 - \rho^2) \cdot$$

$$\left.\left[\xi - iy_o\sqrt{1-\frac{c^2}{b^2}}\right]^{-\frac{1}{2}}\right]$$

$$+ \quad 0\left[\xi - iy_o\sqrt{1-\frac{c^2}{a^2}}\right]^{\frac{1}{2}}$$

$$+ \quad 0\left[\xi - iy_o\sqrt{1-\frac{b^2}{a^2}}\right]^{\frac{1}{2}}$$

5.4.3 Case Hv

The similarity between the form of Eqs. (5.4a) and Eqs. (5.11) causes the variation of the displacements in the vicinity of the wave fronts for Case Hv to be of the same form as those for Case Vh. Only the coefficients will differ and these can be easily obtained using the approach of Sec. 3.2.4.

5.4.4 Case $H_e h_e$

The expressions for displacement of the surface in the vicinity of the combined P, PP, and PS fronts are:

$$u_\rho{}^P \simeq \frac{P}{\pi\mu} \frac{y_o}{a^2(\rho^2 + y_o{}^2)} \cdot$$

$$\left\{ \cos 2\omega \frac{2\theta_\rho{}^3(b^{-2} - \theta_\rho{}^2)^{\frac{1}{2}}}{R(\theta_\rho{}^2)} \right.$$

$$\left. + \sin^2\omega \frac{2\theta_\rho{}^3(b^{-2} - \theta_\rho{}^2)^{\frac{1}{2}}}{R(\theta_\rho{}^2)} + O(t - t_p) \right\}$$

$$u_\omega{}^P \simeq \frac{P}{\pi\mu} \frac{y_o}{\rho^2(\rho^2 + y_o{}^2)^{\frac{1}{2}}} \cdot \qquad (5.22)$$

$$\sin\omega\cos\omega\,\frac{4\theta_\rho{}^3(b^{-2}-\theta_\rho{}^2)^{\frac{1}{2}}}{R(\theta_\rho{}^2)}\,(t-t_p)$$

$$+\quad O(t-t_p)^2$$

$$u_Y{}^P \cong \frac{P}{\pi\mu}\,\frac{y_o}{a^2(\rho^2+y_o{}^2)}\cdot$$

$$\left\{\quad\cos2\omega\,\frac{\theta_\rho{}^3(b^{-2}-2\theta_\rho{}^2)}{R(\theta_\rho{}^2)}\right.$$

$$\left.-\quad\sin^2\omega\,\frac{\theta_\rho{}^3(b^{-2}-2\theta_\rho{}^2)}{R(\theta_\rho{}^2)}+O(t-t_p)\right\}$$

For angles of incidence greater than arccos (b/a), the variation of the surface displacements in the vicinity of the combined S, SS, and SP wave fronts is:

$$\frac{u_\rho{}^S}{\cos^2\omega} \cong \frac{P}{\pi\mu}\,\frac{y_o}{b^2(\rho^2+y_o{}^2)}\cdot$$

$$\frac{\theta_s{}^2(b^{-2}-2\theta_s{}^2)(b^{-2}-\theta_s{}^2)^{\frac{1}{2}}}{R(\theta_s{}^2)}+O(t-t_s)$$

$$\frac{u_\omega^S}{\sin\omega\cos\omega} \simeq -\frac{P}{\pi\mu}\frac{y_o}{\rho^2(\rho^2+y_o^2)^{\frac{1}{2}}}\cdot \qquad (5.23)$$

$$\frac{\theta_s^2}{(b^{-2}-\theta_s^2)^{\frac{1}{2}}} + O(t-t_s)$$

$$\frac{u_Y^S}{\cos 2\omega} \simeq \frac{P}{\pi\mu}\frac{y_o}{b^2(\rho^2+y_o^2)}\cdot$$

$$\frac{2\theta_s^3(a^{-2}-\theta_s^2)^{\frac{1}{2}}(b^{-2}-\theta_s^2)^{\frac{1}{2}}}{R(\theta_s^2)} + O(t-t_s)$$

The above equations show that all displacements experience a step discontinuity on arrival of the combined S, SS, and SP fronts.

For angles of incidence less than arccos (b/a), the variation of the surface displacements in the vicinity of the head wave is:

$$u_\rho^H = -C_\rho \frac{4a^{-2}(b^{-2}-a^{-2})}{(b^{-2}-2a^{-2})^3}\cdot$$

$$\left\{ \cos 2\omega \frac{(t+y_o\sqrt{b^{-2}-a^{-2}})}{\rho^3 a^{-2}} \frac{t-t_H}{(\rho^2+y_o^2)^{\frac{1}{2}}}\right.$$

$$+ \quad \sin^2\omega \, \frac{(t + y_o \sqrt{b^{-2} - a^{-2}})}{2\rho} \, \frac{t - t_H}{(\rho^2 + y_o^2)^{\frac{1}{2}}} \Bigg\}$$

$$+ \quad O(t - t_H)^2$$

$$\frac{u_\omega^H}{\sin\omega \cos\omega} \simeq - C_\rho \, \frac{a^{-2}}{2(b^{-2} - a^{-2})^{\frac{1}{2}}} \, \frac{t - t_H}{(\rho^2 + y_o^2)^{\frac{1}{2}}} \tag{5.24}$$

$$+ \quad O(t - t_H)^2$$

$$u_Y^H = - C_\rho \, \frac{(b^{-2} - a^{-2})^{\frac{1}{2}}}{(b^{-2} - 2a^{-2})^2} \cdot$$

$$\Bigg\{ \quad \cos 2\omega \, (t + y_o \sqrt{b^{-2} - a^{-2}}) \, \frac{t - t_H}{\rho^2(\rho^2 + y_o^2)^{\frac{1}{2}}}$$

$$+ \quad \sin^2\omega \, \frac{t - t_H}{a^2(\rho^2 + y_o^2)^{\frac{1}{2}}} \Bigg\}$$

$$+ \quad O(t - t_H)^2$$

As before, C_ρ becomes infinite in the vicinity of the S wave front and hence the displacements which contain C_ρ experience a logarithmic singularity.

The variation of the displacements in the vicinity of the Rayleigh surface wave may be expressed by:

$$u_\rho^R \simeq - \frac{Pi(b^{-2} - c^2)^{\frac{1}{2}}(\rho^2 + y_o^2)^{\frac{1}{4}}}{\pi\mu R'(c^{-2})\ \sqrt{2}\ c^4\rho} \cdot$$

$$\left[\cos 2\omega\ \frac{\rho^2 + y_o^2}{\rho^2} + \sin^2\omega\right] \cdot$$

$$\left[\left[\xi - iy_o\sqrt{1 - \frac{c^2}{a^2}}\right]\right.$$

$$\left. + \quad 0\left[\xi - iy_o\sqrt{1 - \frac{c^2}{a^2}}\right]^{\frac{1}{2}}\right]$$

$$\simeq \frac{Pi(b^{-2} - c^{-2})^{\frac{1}{2}}(\rho^2 + y_o^2)^{\frac{1}{4}}(b^{-2} - 2c^{-2})}{\pi\mu R'(c^{-2})\ 2\ \sqrt{2}\ c^2\rho} \cdot$$

$$\left[\cos 2\omega\ \frac{\rho^2 + y_o^2}{\rho^2} + \sin\ \omega\right] \cdot \qquad (5.25)$$

$$\left[\xi - iy_o \sqrt{1 - \frac{c^2}{b^2}}\right]^{-\frac{1}{2}}$$

$$+ \quad 0\left[\xi - iy_o \sqrt{1 - \frac{c^2}{c_i^2}}\right]^{\frac{1}{2}}$$

$$\frac{u_\omega^R}{\sin\omega \cos\omega} \cong \frac{Pi \sqrt{2}\,(b^{-2} - c^{-2})^{\frac{1}{2}}(\rho^2 + y_o^2)^{3/4}}{\pi\mu R'(c^{-2})\rho^2} \cdot$$

$$\left\{ \quad 2 \left[\xi - iy_o \sqrt{1 - \frac{c^2}{a^2}}\right]^{\frac{1}{2}}\right.$$

$$+ \quad \frac{(b^{-2} - 2c^{-2})}{2c^{-2}} \left[\xi - iy \sqrt{1 - \frac{c^2}{b^2}}\right]^{\frac{1}{2}}$$

$$+ \quad 0 \left[\xi - iy_o \sqrt{1 - \frac{c^2}{a^2}}\right]^{3/2}$$

$$\left. + \quad 0 \left[\xi - iy_o \sqrt{1 - \frac{c^2}{b^2}}\right]^{3/2} \right\}$$

$$u_Y^R \cong - \frac{Pi(\rho^2 + y_o^2)^{-\frac{1}{4}}(b^{-2} - c^{-2})}{\pi\mu R'(c^{-2})c^3\ 2 \quad 2\ \rho^2} \cdot$$

$$\left[(\rho^2 + y_o^2)\cos\omega - y_o^2 \sin\omega\right] .$$

$$\cdot \left\{ \left[\xi - iy_o \sqrt{1 - \frac{c^2}{a^2}} \right]^{-\frac{1}{2}} \right.$$

$$\left. 0 \left[\xi - iy_o \sqrt{1 - \frac{c^2}{a^2}} \right]^{\frac{1}{2}} \right\}$$

$$- \frac{Pi(a^{-2} - c^{-2})^{\frac{1}{2}} (b^{-2} - c^{-2})^{\frac{1}{2}}}{\pi\mu R'(c^{-2}) c^3 \quad 2\rho^2(\rho^2 + y_o^2)^{\frac{1}{4}}} \cdot$$

$$\left[(\rho^2 + y_o^2) \cos\omega - y_o^2 \sin\omega \right] \cdot$$

$$\left\{ \left[\xi - iy_o \sqrt{1 - \frac{c^2}{b^2}} \right]^{-\frac{1}{2}} \right.$$

$$+ \quad \left. 0 \left[\xi - iy_o \sqrt{1 - \frac{c^2}{c_i^2}} \right]^{\frac{1}{2}} \right\}$$

5.5 Numerical Results

Numerical evaluation of the integrands of Secs. 4.2 and 4.3 provide with relative ease a time history of the displacements on the surface for any focal depth. Sample results for the fundamental cases are shown in Figs. 23 through 28. These results were obtained using a value of Poisson's ratio of .25. The numerical results are actually of higher quality than indicated by the figures

because the slight roughness is actually a result of the graphical output equipment.

No attempt is made in this study to compare the various cases or their variation with focal depth. As indicated in Sec. 6.2, any desired comparison of the fundamental cases or comparison of any models derived therefrom can easily be made using the information provided in this study.

6. SUMMARY AND PROPOSED APPLICATIONS

6.1 Summary

In this study, the methods of rotational superposition and self similar potentials have been extended to solve problems involving a dynamic double force acting at a point beneath the surface of an elastic half space. Solutions have been obtained for five fundamental double vertical and double horizontal forces. These solutions can be superposed to yield a wide variety of models for earthquake fault dislocations. As a necessary intermediate step, the case of a vertical force applied at a point within a half space was solved by the same methods.

The combined use of the methods of rotational superposition and self similar potentials has proven to be a direct and useful approach to the solution of double force problems. A particular application of the method of rotational superposition represents the three-dimensional double force problem as a superposition of plane problems related to the single force case. When the moment produced by the double force varies as a linear function in time, the solutions for the plane problems are obtained by a simple modification of the self similar potentials for the single force. The resulting integrals are easily evaluated on the surface of the half space and involve only quadrature in the complex plane. The simplicity of the

computations makes superposition of these solutions to obtain specific fault models a simple matter. In addition, the solution process involves physically meaningful quantities at every stage. The positions of the wave fronts to include the head wave are always apparent and the specific character of the disturbances on the surface can be extracted without difficulty.

In summary, this extension of the methods of self similar potentials and rotational superposition to solve double force problems clearly illustrates the power and convenience of these methods for solving practical dynamic problems in elasticity.

6.2 Applications to Earthquake Modeling

The relationship between a double force at a point and an elementary slip which might simulate part of an earthquake source at a point is not a straightforward one. Indeed, the literature indicates that considerable controversy exists concerning what arrangement of forces best models a particular fault dislocation. The two primary contenders are the single couple (double force) of Nakano (1930) and the so-called double couple* (pair of double forces) of Honda (1957). Figure 16a shows a single couple model for a dip-slip fault with a dip angle, γ. Figure 22a shows the corresponding pair of couples that is

* The "double couple" used in this context in the literature refers to a pair of couples and does not imply the same relationship between couples as exists between a single force and a double force.

used to represent the same dip-slip fault dislocation. Actually, some controversy even exists concerning selection of the orientation of the double force with the fault plane. See Stauder (1962) and Benioff (1964) for a detailed review and bibliography of this and other aspects of the controversy over fault models. On first consideration, the single couple model presents obvious correspondence with Reid's (1910) elastic strain theory for fault mechanisms. The single couple does, however, produce a net moment whereas the pair of couples does not. Studies of seismograms have provided support for both models but neither has received general acceptance. Obviously, more research is necessary before conclusive decisions on model selection can be made. The fundamental double force solutions supplied in this study will assist this research by permitting quick solution to a variety of models and permit easy variation of the orientation of the fault plane. Table 1 (next page) illustrates how the fundamental double force solutions may be superposed to give various models. This table gives the contribution of each fundamental double force solution to a dip-slip and a strike-slip model formulated first by a single couple and then by pairs of couples.

Many models other than those in Table 1 can be formed using the solutions presented in this study. For example, Case $H_e h_e$ of Fig. 5 with the forces in the opposite direction is the simplest model for a tensile fault. Burridge, Lapwood, and Knopoff (1964)

TABLE 1.

FACTORS FOR SUPERPOSITION OF FUNDAMENTAL CASES
TO OBTAIN DIP-SLIP AND STRIKE-SLIP MODELS

	Vv	Vh	$H_n h_e$	Hv	$H_e h_e$
Single Couple,					
Dip-Slip	$-\sin\gamma \cos\gamma$	$-\sin^2\gamma$	0	$\cos^2\gamma$	$\sin\gamma \cos\gamma$
Strike-Slip	0	0	$\sin\gamma$	$\cos\gamma$	0
Pair of Couples,					
Dip-Slip	$-\sin^2\gamma$	$\cos^2\gamma$	0	$\cos^2\gamma$	$\sin^2\gamma$
Strike-Slip	0	$\cos\gamma$	$\sin\gamma-\sin\gamma$*	$\cos\gamma$	0

* This case requires that coordinates X and Z be substituted for coordinates Z and negative X, respectively, to give the correct orientation.

give a description of a more involved tensile fault model that can also be formed from fundamental double force solutions. By superposition, faults of finite length may also be modeled. Using the "pair of couples" as the basic model, a dip-slip fault dislocation of finite length may be modeled as in Fig. 22b. Propagating faults may be modeled by considering the point models to originate at different times. In addition, Johnson and Robinson (1972) provide guidelines for extending the self similar solution to consider multilayered media.

6.3 Superposition of the Fundamental Linear Time Variation to Obtain Other Time Variations

The time variation of the moment produced by the double forces in this study is linear. Other time variations of interest may be obtained by superposition of this fundamental ramp variation. As the succeeding derivation shows, any variation of loading that is initially zero and has a finite first derivative can be obtained by this approach. The versed sine time variation that has been used in the past (Newmark et al., 1972) possesses these characteristics and could be obtained from the fundamental ramp variation.

Let $M(t)$ represent the loading of interest as a function of time and consider $U(t)$ to be the response to this general time variation. If $u(t)$ is the response to a unit ramp, the response to the loading $M(t)$ can be expressed by the superposition integral as

$$U(t) = \int_0^t M'(t - \tau) \cdot \frac{\partial u(\tau)}{\partial \tau} \, d\tau \quad \text{when } M(0) = 0 \qquad (6.1)$$

where $M'(t - \tau)$ is the first derivative of the loading $M(t)$. The partial derivative of $u(\tau)$ with respect to τ is, of course, the response to a unit step. Integration of Eq. (6.1) by parts gives

$$U(t) = \left| M'(t - \tau) \cdot u(\tau) \right|_{\tau=0}^{\tau=t} + \int_0^t M''(t - \tau) \cdot (\tau) \, d\tau \qquad (6.2)$$

and finally,

$$U(t) = M_o' \cdot u(t) + \int_0^t M''(\tau) \cdot u(t - \tau)\, d\tau \qquad (6.3)$$

where M_o' is the first derivative of $M(t)$ at $t = 0$ and M'' is the second derivative of $M(t)$.

The foregoing derivation shows that the fundamental ramp time variation that emerges naturally by the method of self similar potentials is useful for obtaining other desired time variations.

LIST OF REFERENCES

Benioff, H. (1964). "Earthquake Source Mechanisms," Science, Vol. 143, 1399-1404.

Ben-Menahem (1961). "Radiation of Seismic Surface Waves from Finite Moving Sources," Bulletin of the Seismological Society of America, Vol. 51, 401-435.

Burridge, R., Lapwood, E. R., and Knopoff, L. (1964). "Body Force Equivalents for Seismic Dislocations," Bulletin of the Seismological Society of America, Vol. 54, 1875-1888.

Cagniard, L. (1962). Reflection and Refraction of Progressive Seismic Waves, International Series in the Earth Sciences, McGraw-Hill, New York.

Churchill, R. V. (1960). Complex Variables and Applications, Second Edition, McGraw-Hill, New York.

Duhem, P. (1898). "Sur l'intégrale des Equations des Petits Mouvements d'un Solide Isotrope," Mem. Soc. Sci. Bordeaux Sér. V, Vol. 3, 317-329.

Ewing, W. N., Jardetzky, W. S., and Press, F. (1957). Elastic Waves in Layered Media, International Series in the Earth Sciences, McGraw-Hill, New York.

Gakenheimer, D. C. and Miklowitz, J. (1969). "Transient Excitation of an Elastic Half Space by a Point Load Traveling on the Surface," J. Appl. Mech., Vol. 36, 505-515.

Gupta, I. N. (1967). "Body Wave Radiation Patterns from Elementary Sources within a Half Space," Bulletin of the Seismological Society of America, Vol. 57, 657-674.

Hamel, G. (1949). Integralgleichungen, Springer-Verlag, Berlin.

Honda, H. (1957). "The Mechanism of the Earthquakes," Sci. Repts. Tôhoku Univ., Ser. 5: Gophys., Suppl. 9, 1-46.

Jeffreys, H. and Jeffreys, B.S. (1956). Methods of Mathematical Physics, Third Edition, Cambridge University Press, Cambridge.

Johnson, J. J. and Robinson, A. R. (1972). "Wave Propagation in a Half Space Due to an Interior Point Load Parallel to the Surface," Civil Engineering Studies, SRS 388, University of Illinois, Urbana, Illinois.

Lamb, H. (1904). "On the Propagation of Tremors over the Surface of an Elastic Solid," Phil. Trans. Royal Soc. A, 203, 1-42.

Nakano, H. (1930). "Some Problems Concerning the Propagation of the Disturbances in and on a Semi-Infinite Elastic Solid," Geophys. Mag., Vol. 2, 189-348.

Newmark, N. M., Robinson, A. R., Ang, A. H. S., Lopez, L. A., and Hall, W. J. (1972). "Methods for Determining Site Characteristics," Proc. Int. Conf. on Microzonation, Seattle Wash., Oct., 1972.

Pekeris, C. L. and Lifson, H. (1957). "Motion of the Surface of a Uniform Half Space Produced by a Buried Pulse," J. Acous. Soc. Am., Vol. 29, 1233-1238.

Pod"yapol'ski, G. S. (1959). "The Propagation of Elastic Waves in Layered Media-II," Bulletin of the Academy of Sciences of the U.S.S.R., Geophysics Series, Vol. 8, 913-919.

Reid, H. F. (1910). "The Mechanics of the Earthquake: the California Earthquake of April 18, 1906," Report of the State Investigation Committee, Vol. 2, Carnegie Institution of Washington, D.C.

Schwartz, M., Green, S., and Rutledge, W. A. (1960). Vector Analysis with Applications to Geometry and Physics, Harper, New York.

Smirnov, V. I. and Sobolev, S. L. (1933). "On the Application of a New Method of Investigation of the Elastic Vibrations in the Space with Axial Symmetry," Trud. Inst. Seism. Akad. Nauk SSSR, 29.

Smirnov, V. I. (1964). A Course of Higher Mathematics, Vol. III, Part Two, Addison-Wesley, Reading, Mass.

Stauder, S. J. (1962). "The Focal Mechanism of Earthquakes," Advances in Geophysics, Vol. 9, 1-76.

Thompson, J. C. and Robinson, A. R. (1969). "Exact Solutions of Some Dynamic Problems of Indentation and Transient Loadings of an Elastic Half Space," Civil Engineering Studies, SRS 350, University of Illinois, Urbana, Illinois.

Zvolinskii, N. V. (1957). "Reflected and Head Waves Emerging at a Plane Interface of Two Elastic Media-I," Bulletin of the Academy of Sciences of the U.S.S.R., Geophysics Series, Vol. 10, 1-21.

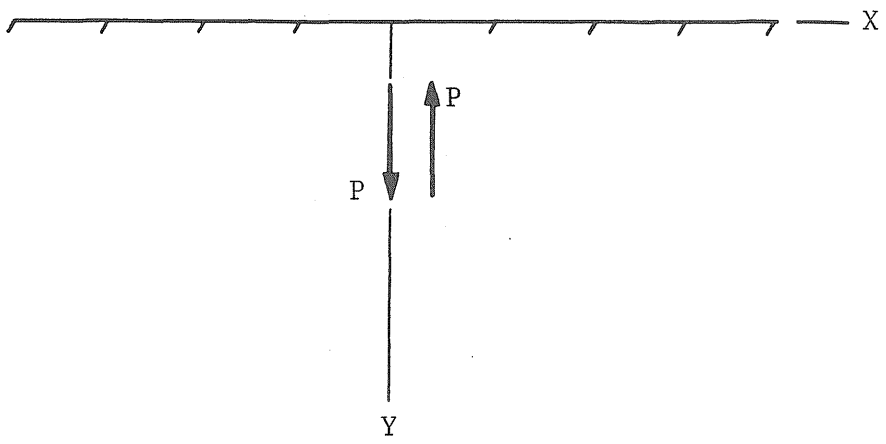

FIGURE 1. CASE Vh; DOUBLE VERTICAL FORCE WITH MOMENT.

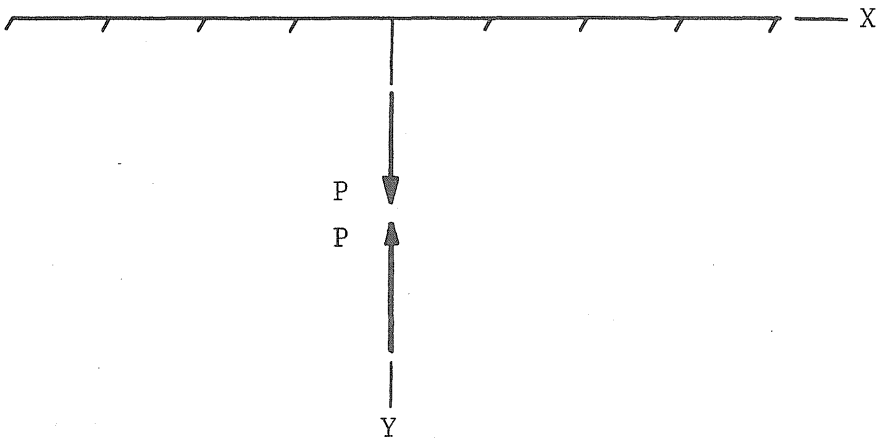

FIGURE 2. CASE Vv; DOUBLE VERTICAL FORCE WITHOUT MOMENT.

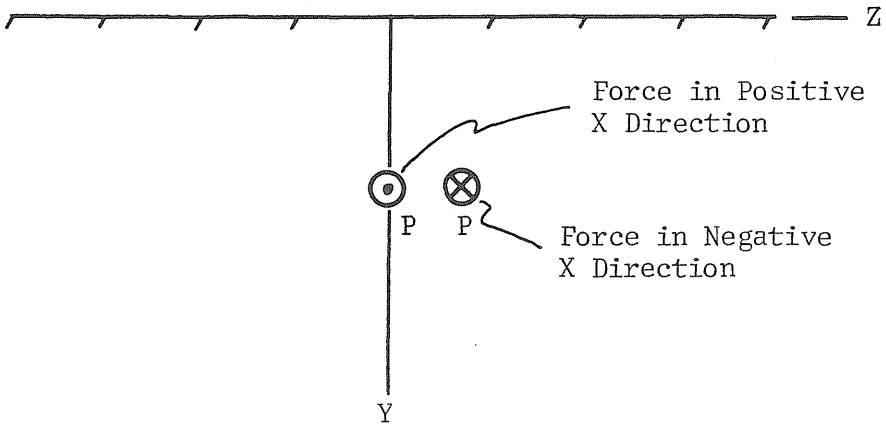

(a) End View.

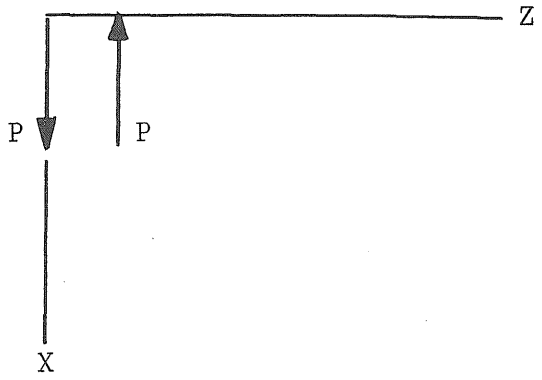

(b) Top View.

FIGURE 3. CASE $H_n h_e$; DOUBLE HORIZONTAL FORCE WITH MOMENT, FORCES IN A HORIZONTAL PLANE.

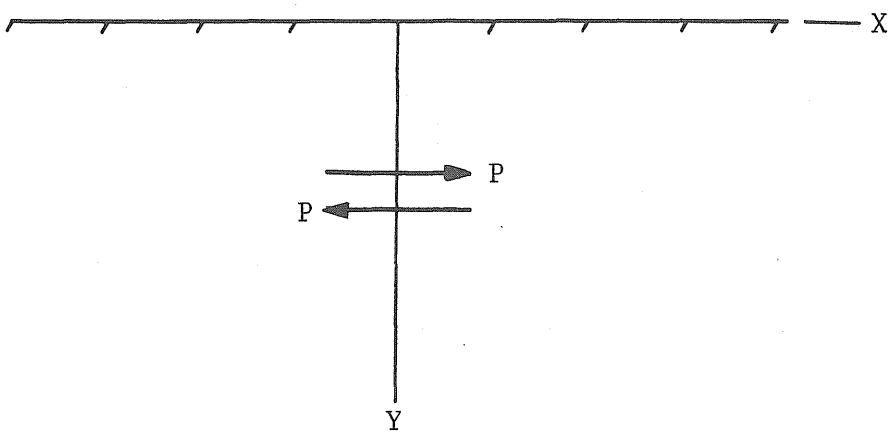

FIGURE 4. CASE Hv; DOUBLE HORIZONTAL FORCE WITH MOMENT, FORCES IN A VERTICAL PLANE.

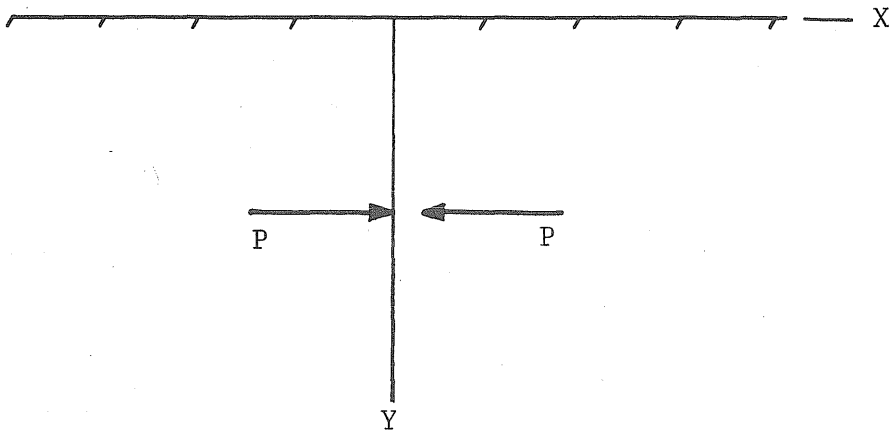

FIGURE 5. CASE $H_e h_e$; DOUBLE HORIZONTAL FORCE WITHOUT MOMENT.

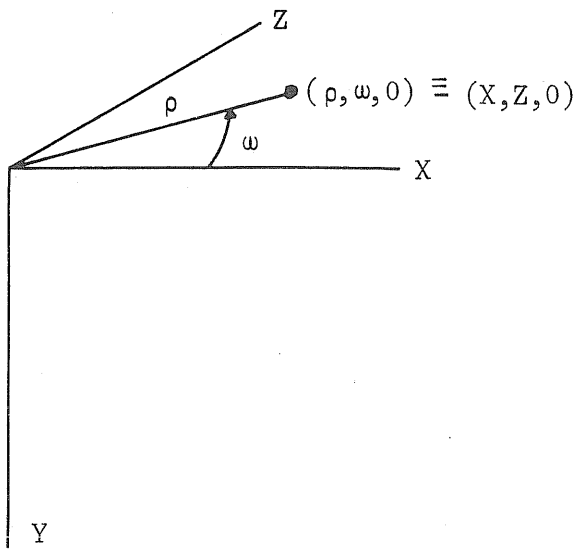

(a) Equivalent (X,Z,Y) and (ρ,ω,Y) global coordinates for description of Y > 0 half space.

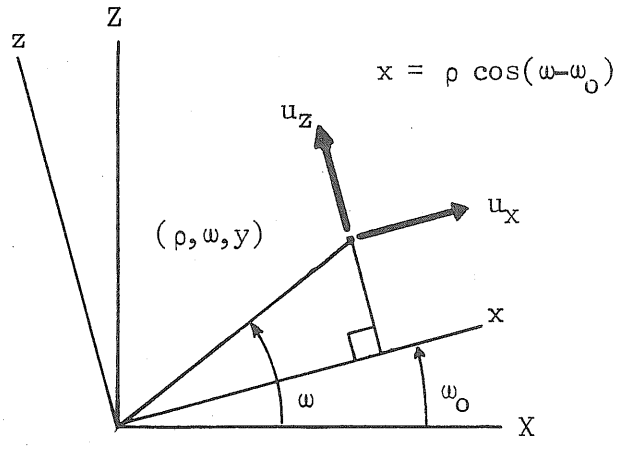

(b) Plan view of axes for plane problems superposed on global axes for three-dimensional description.

FIGURE 6. GEOMETRY OF ROTATIONAL SUPERPOSITION

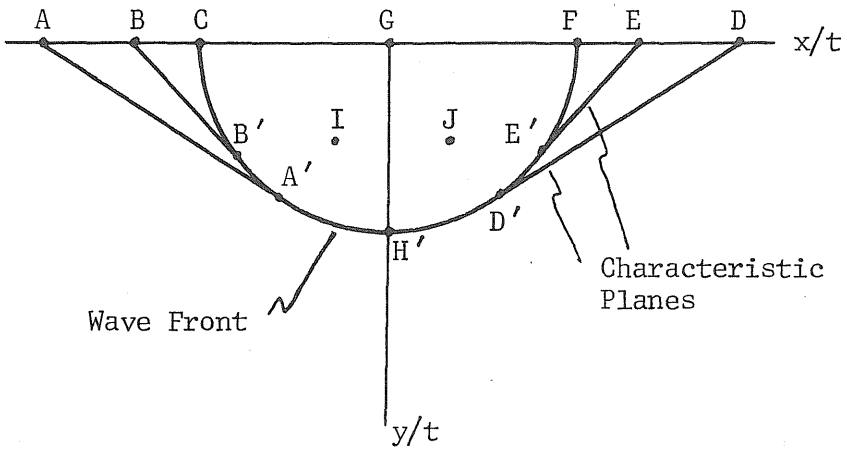

(a) Points in $y \geq 0$ half plane.

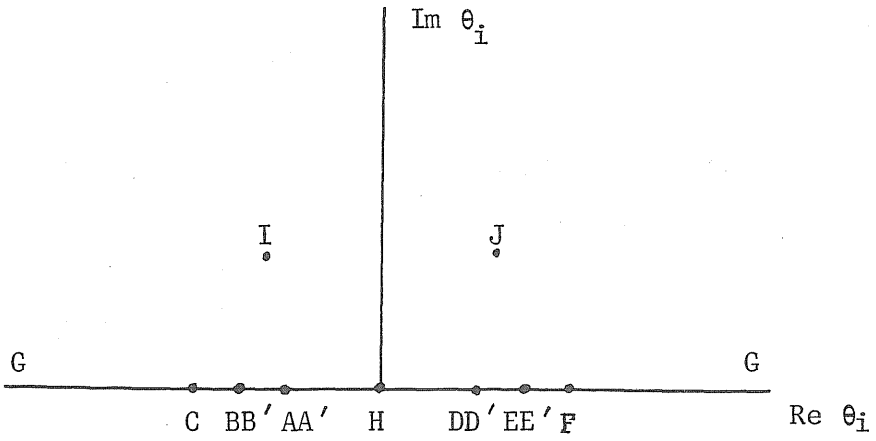

(b) The upper half of the complex θ_i plane.

FIGURE 7. MAPPING OF THE LOWER HALF SPACE INTO THE COMPLEX θ PLANE.

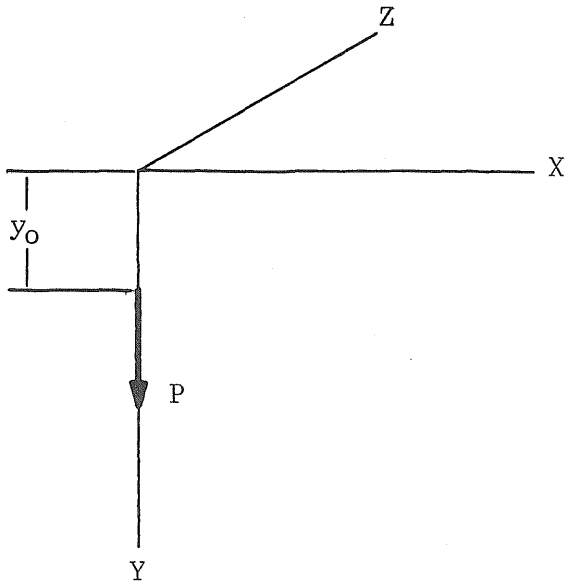

(a) Vertical point force.

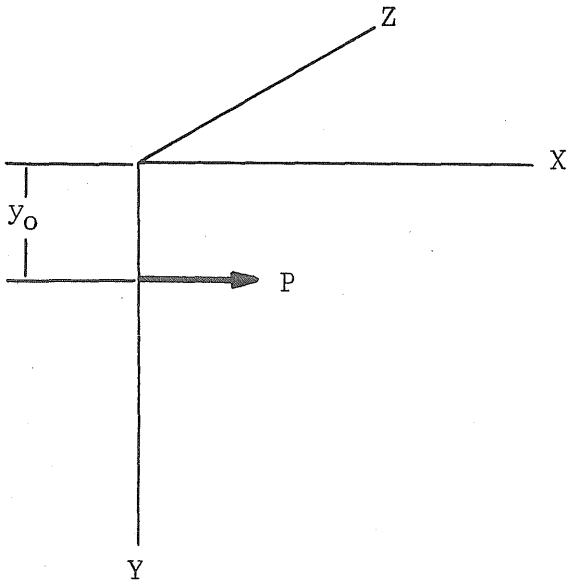

(b) Horizontal point force.

FIGURE 8. DYNAMIC POINT FORCE BENEATH THE SURFACE.

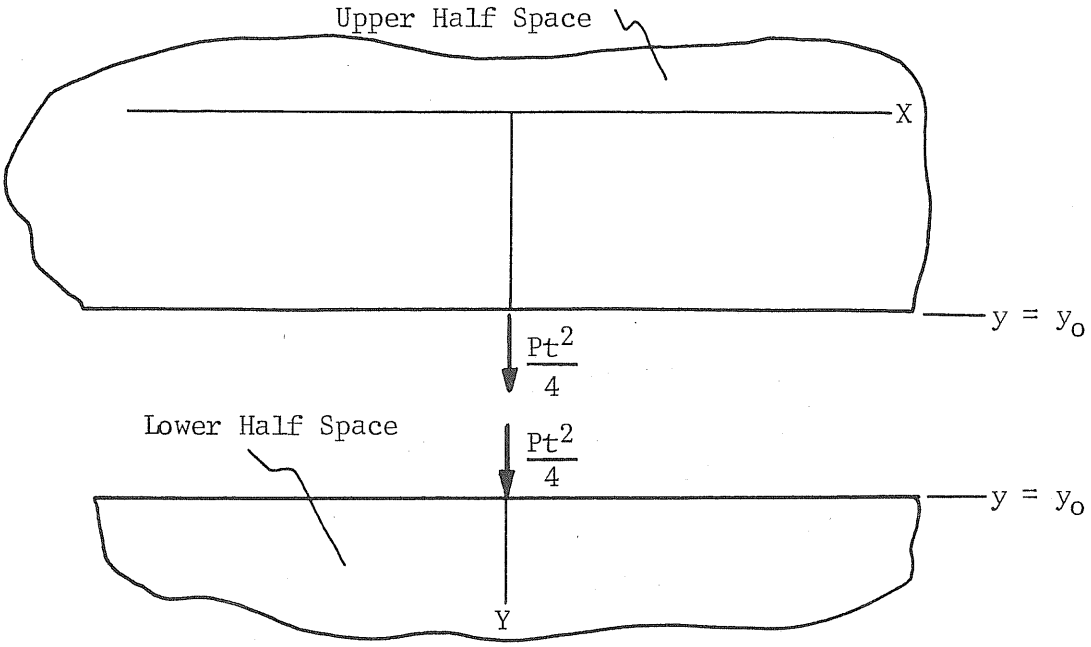

(a) Constituent half spaces.

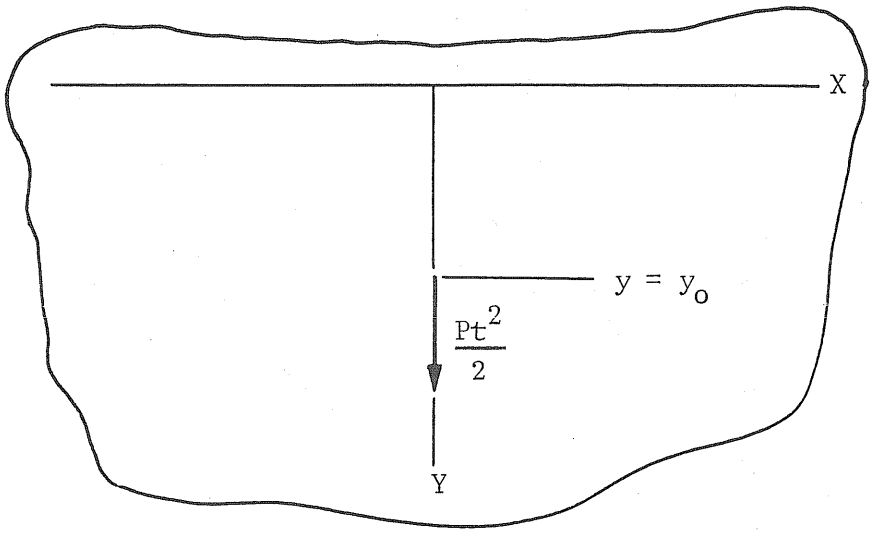

(b) Point load in an infinite medium.

FIGURE 9. REPRESENTATION OF A POINT LOAD IN AN INFINITE MEDIUM BY THE ADDITION OF TWO HALF SPACES.

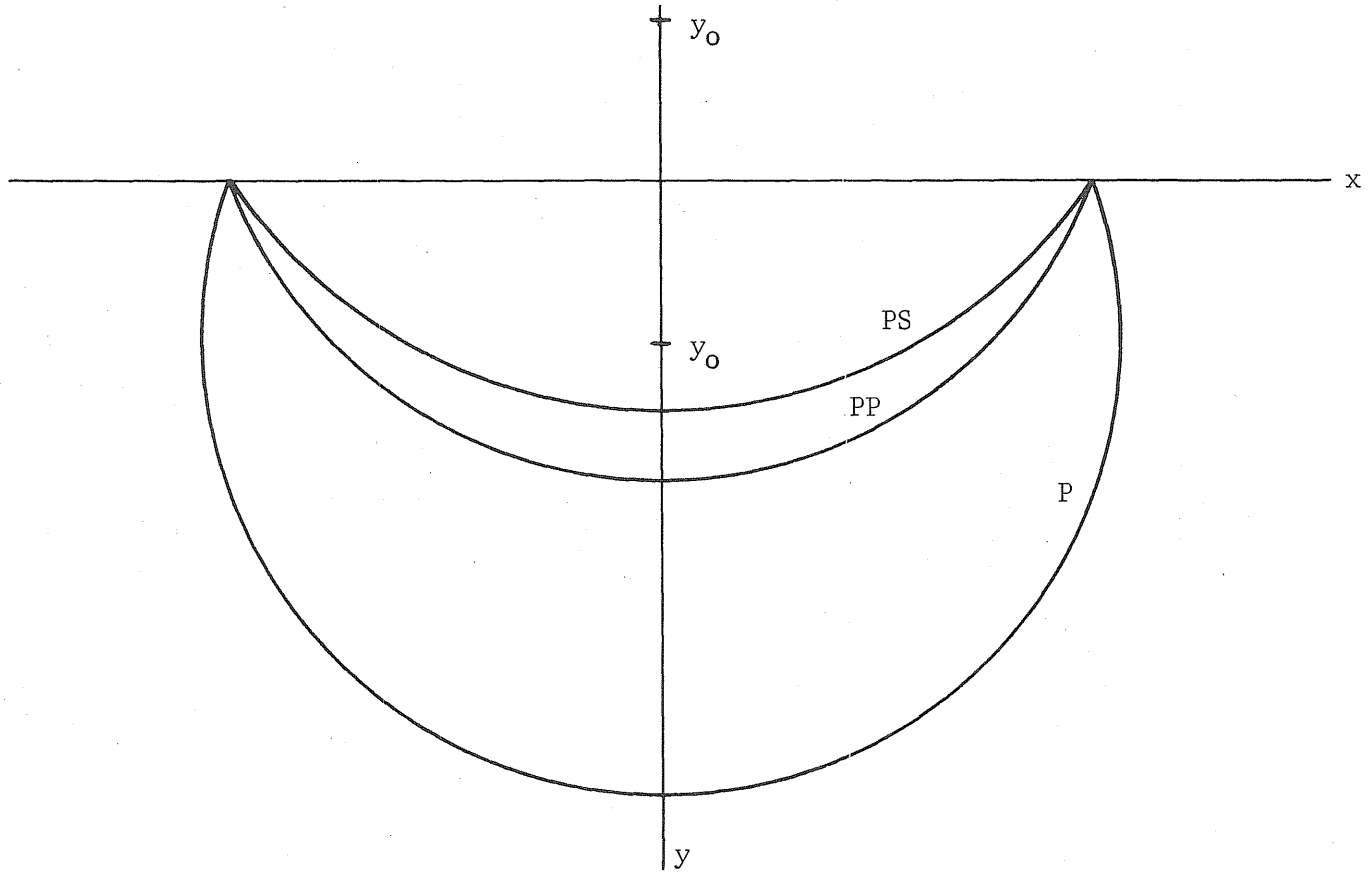

FIGURE 10. TYPICAL WAVE FRONT PATTERN FOR THE P, PP, AND PS WAVES.

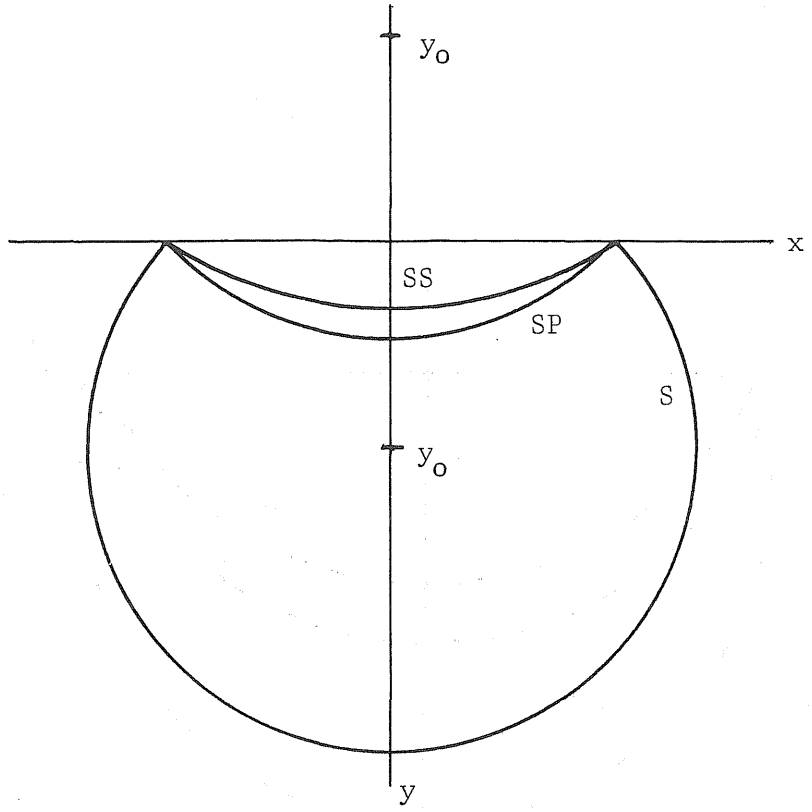

(b) S, SS, and SP wave fronts.

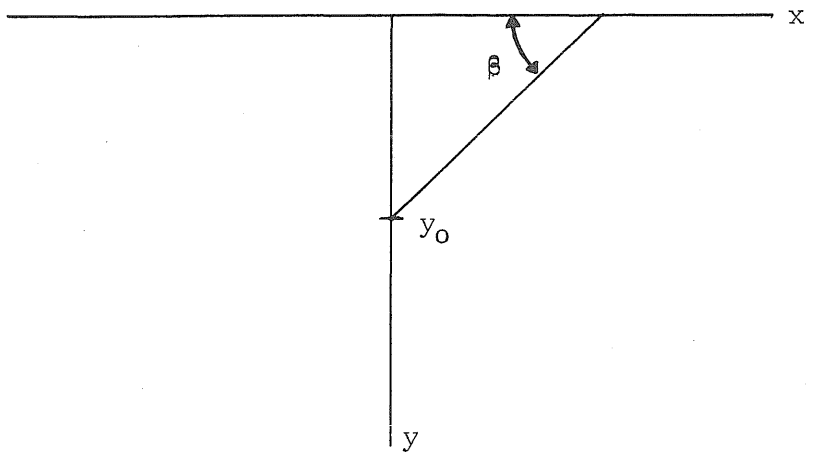

(a) Angle of incidence.

FIGURE 11. TYPICAL WAVE FRONT PATTERN FOR THE S, SS, AND SP WAVES WHEN $\beta \geq \arccos(b/a)$.

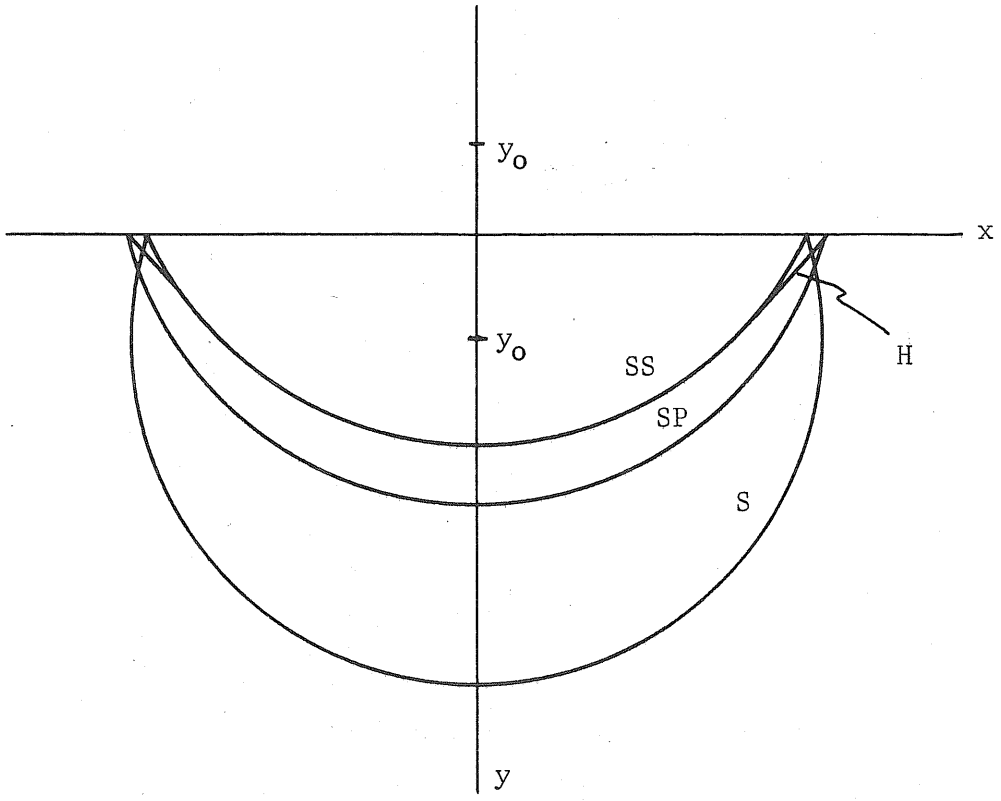

FIGURE 12. TYPICAL WAVE FRONT PATTERN FOR THE S, SS, AND SP WAVES WHEN $\beta \leq \arccos(b/a)$.

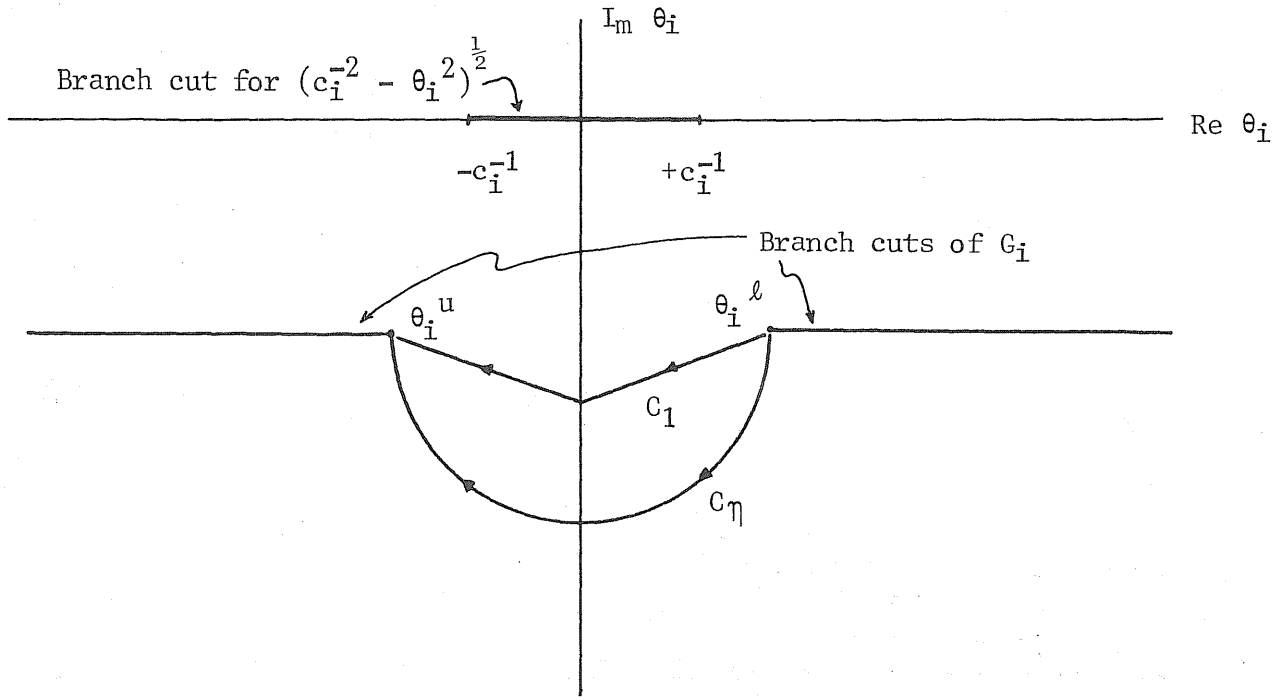

FIGURE 13. ALTERNATIVE CONTOURS OF INTEGRATION IN THE θ_i PLANE.

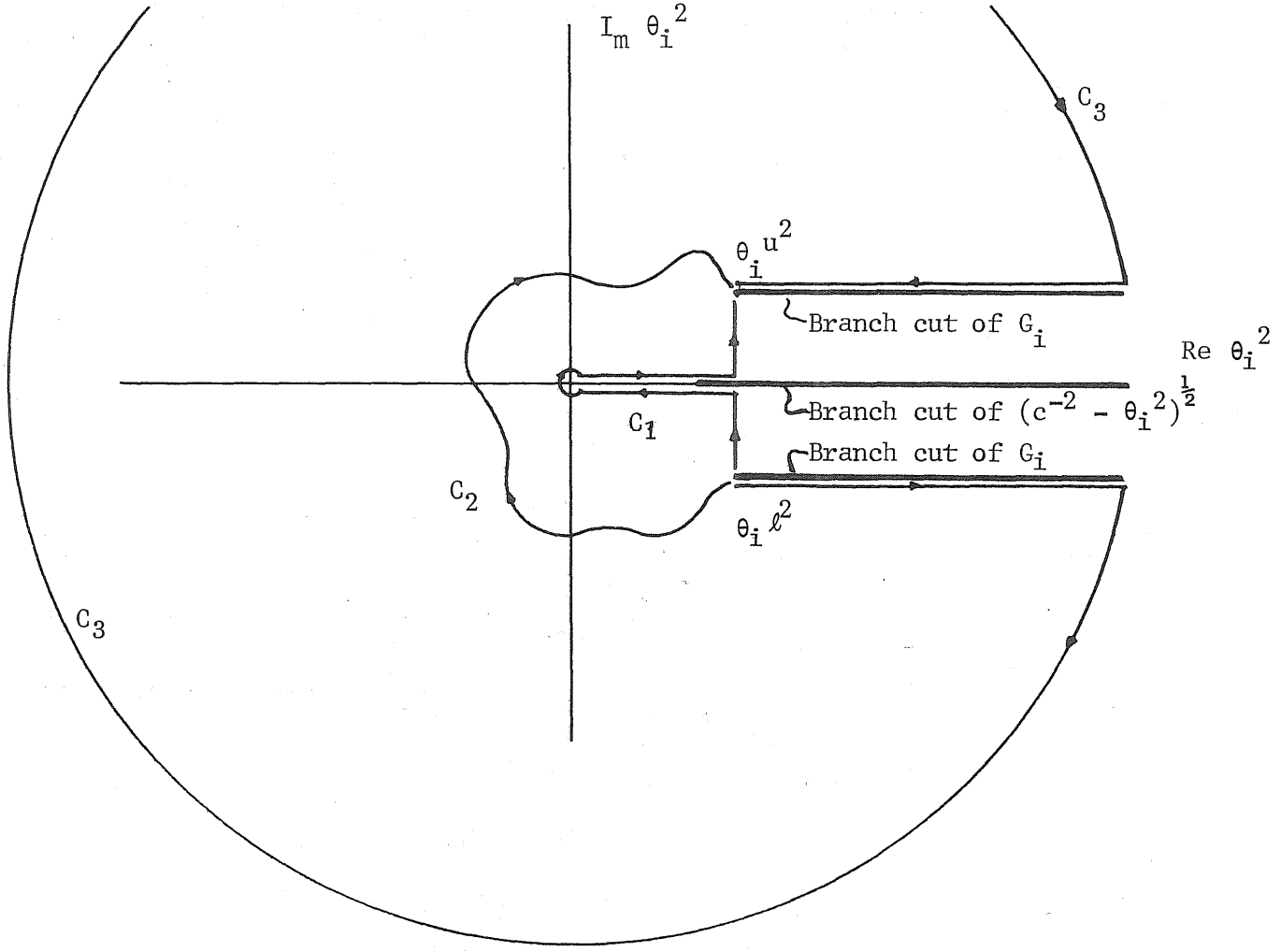

FIGURE 14. ALTERNATIVE CONTOURS OF INTEGRATION IN THE θ_i^2 PLANE.

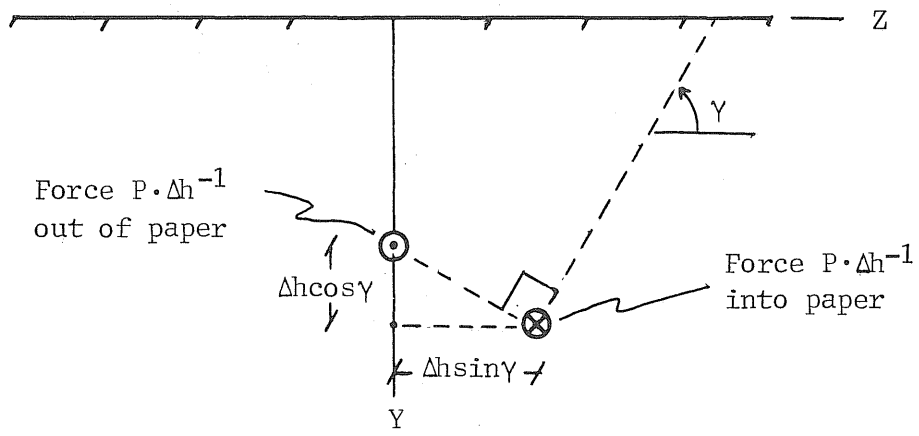

(a) End view of double horizontal force in an inclined plane.

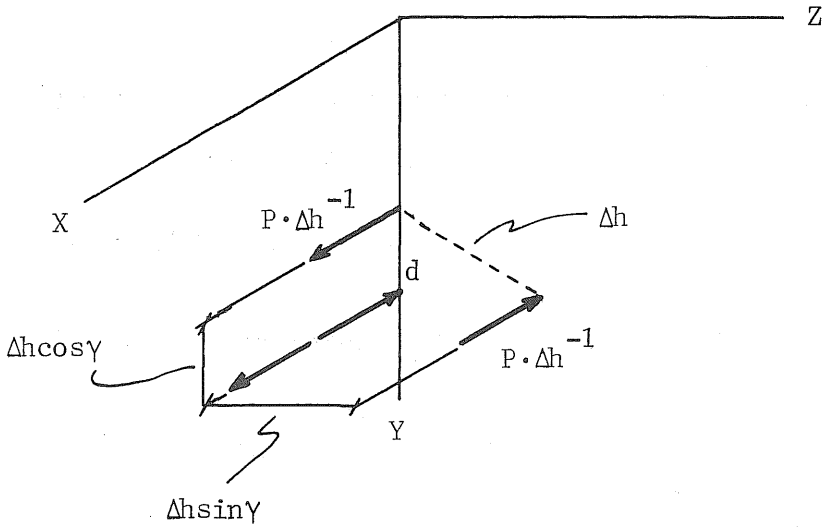

(b) Double horizontal force in an inclined plane as a superposition of double horizontal and double vertical forces.

FIGURE 15. DOUBLE HORIZONTAL FORCE IN AN INCLINED PLANE.

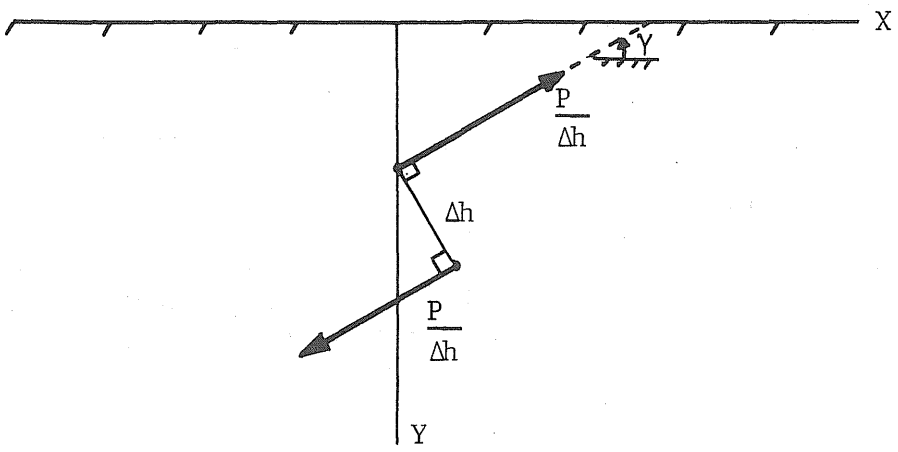

(a) Forces comprising double force.

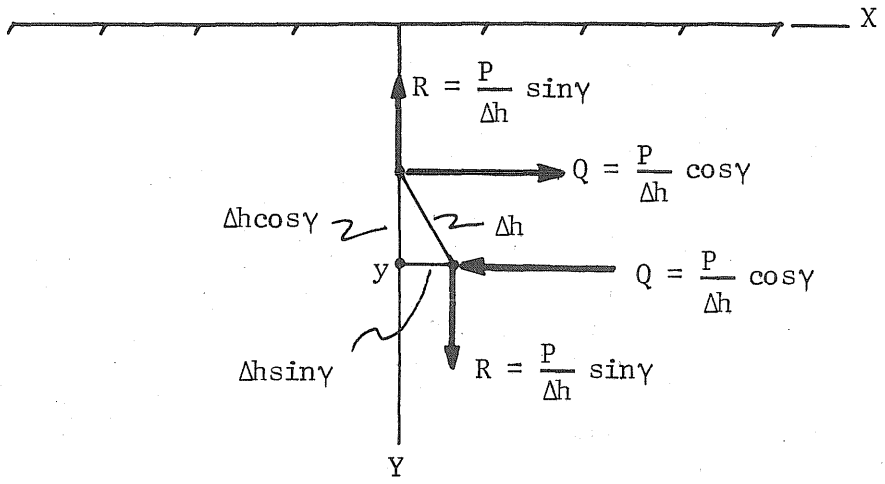

(b) Resolution of double force into horizontal and vertical components.

FIGURE 16. DOUBLE FORCE AT AN ARBITRARY ANGLE IN A VERTICAL PLANE.

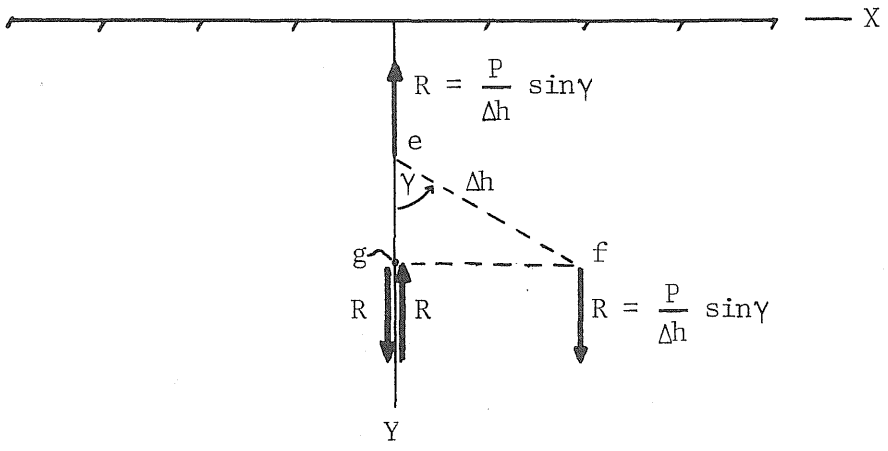

(a) Force system R of Fig. 16b.

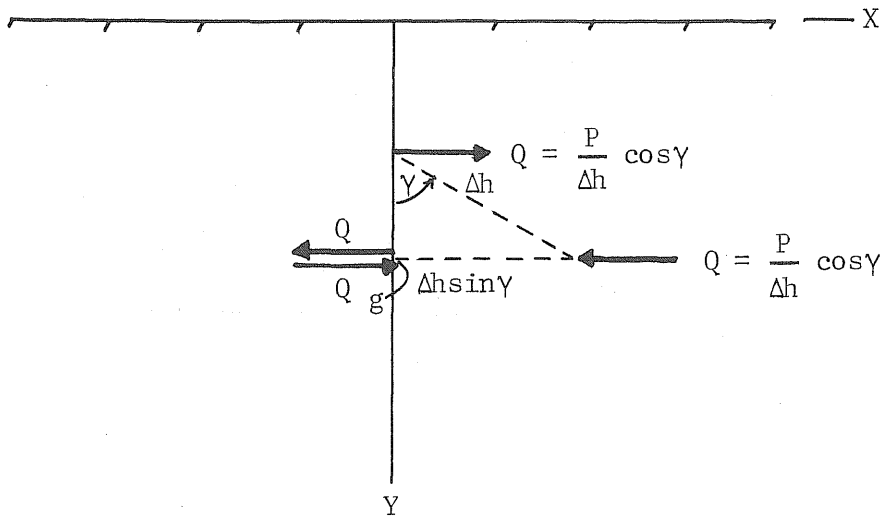

(b) Force system Q of Fig. 16b.

FIGURE 17. SUPERPOSITION OF DOUBLE FORCES TO OBTAIN THE INCLINED DOUBLE FORCE OF FIG. 16a.

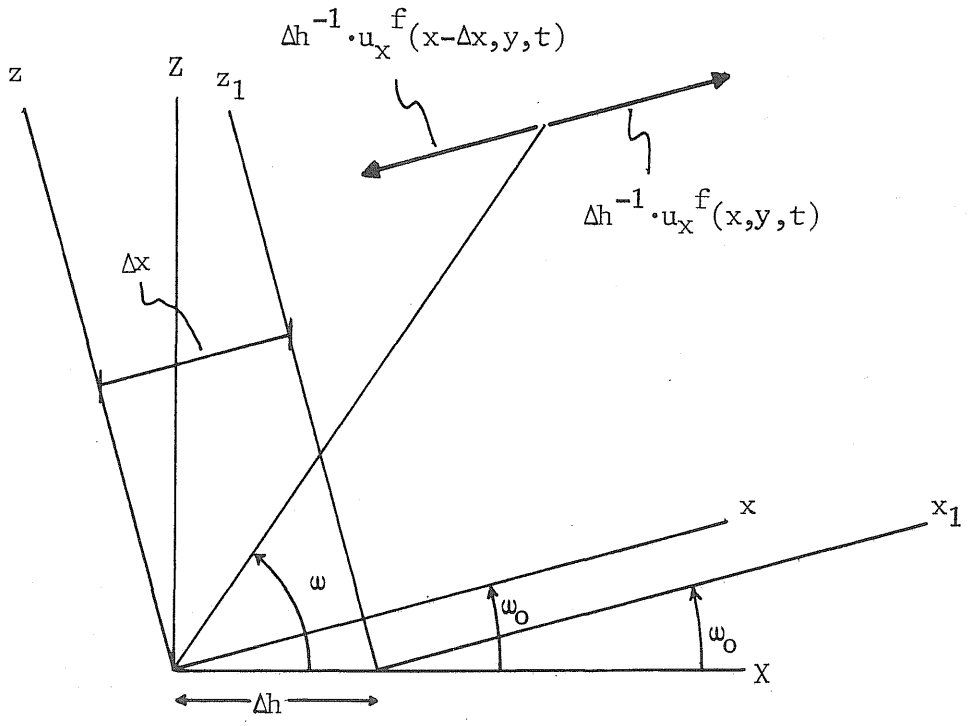

FIGURE 18. SUPERPOSITION OF TYPICAL VECTORS OF THE PLANE FIELDS ASSOCIATED WITH VERTICAL FORCES TO OBTAIN THE PLANE FIELD FOR THE DOUBLE FORCE OF CASE Vh.

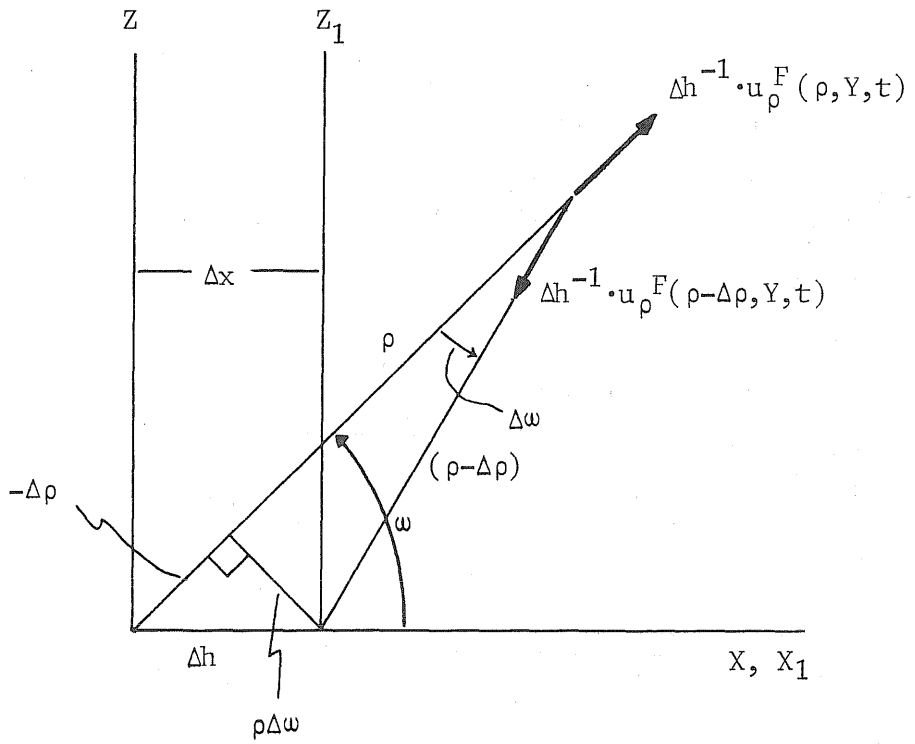

FIGURE 19. SUPERPOSITION OF TYPICAL DISPLACEMENTS FOR VERTICAL FORCES TO OBTAIN THE DOUBLE FORCE OF CASE Vh.

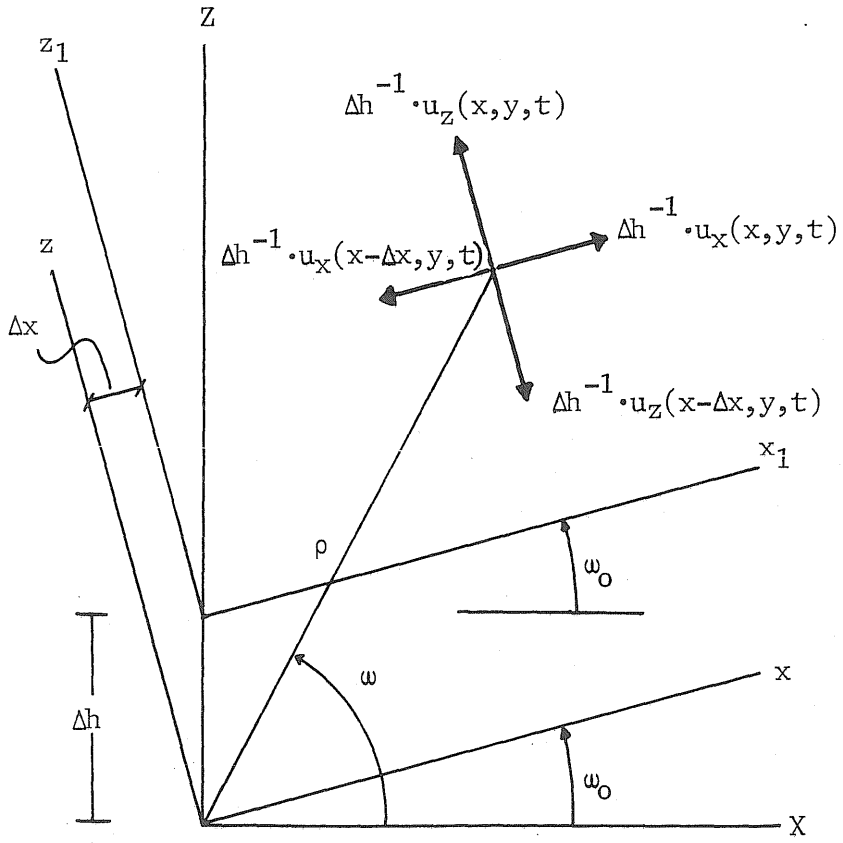

FIGURE 20. SUPERPOSITION OF PLANE FIELDS FOR HORIZONTAL FORCES TO OBTAIN PLANE FIELDS CORRESPONDING TO DOUBLE FORCE CASE $H_n h_e$.

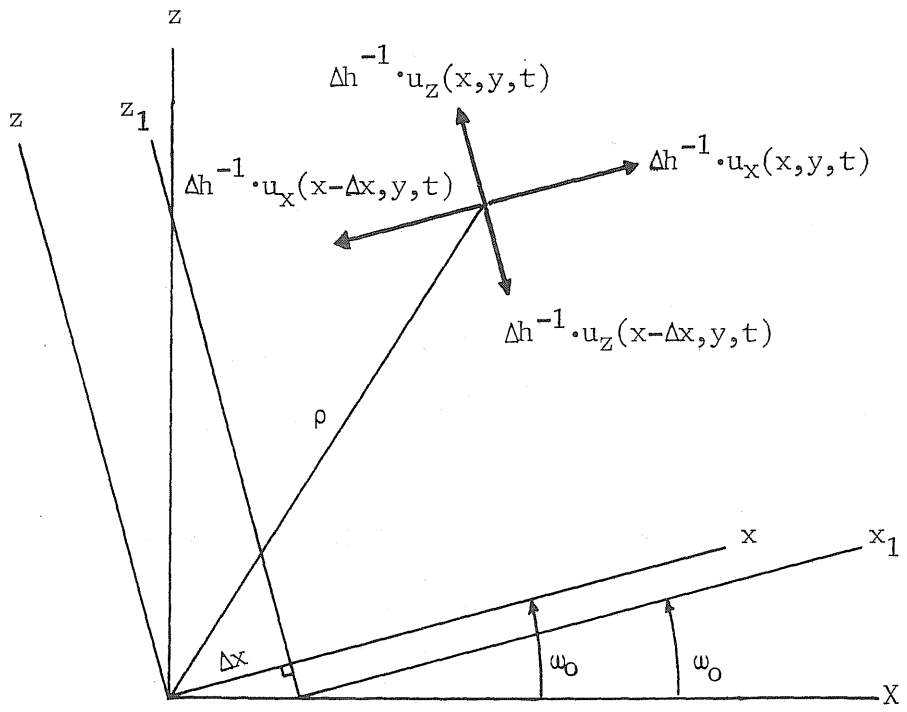

FIGURE 21. SUPERPOSITION OF PLANE FIELDS ASSOCIATED WITH A SINGLE HORIZONTAL FORCE TO OBTAIN DOUBLE FORCE CASE $H_e h_e$.

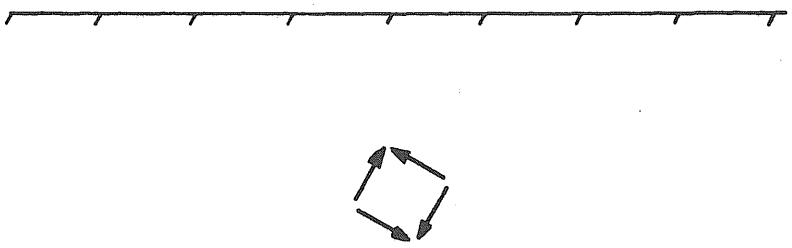

(a) Model of a dip-slip fault dislocation at a point.

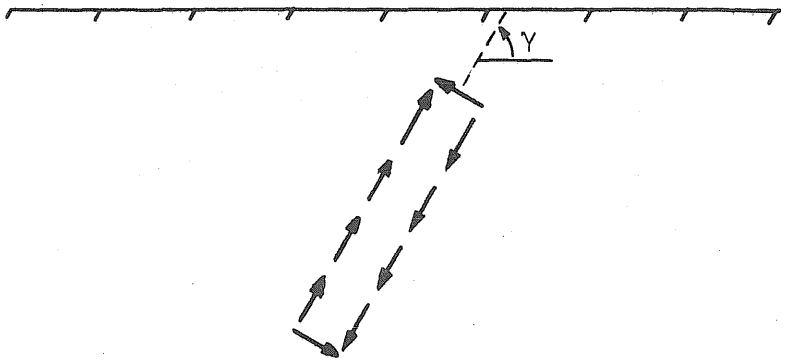

(b) Model of dip-slip fault dislocation of finite length.

FIGURE 22. MODELS FOR DIP-SLIP FAULT DISLOCATION FORMED BY PAIRS OF COUPLES.

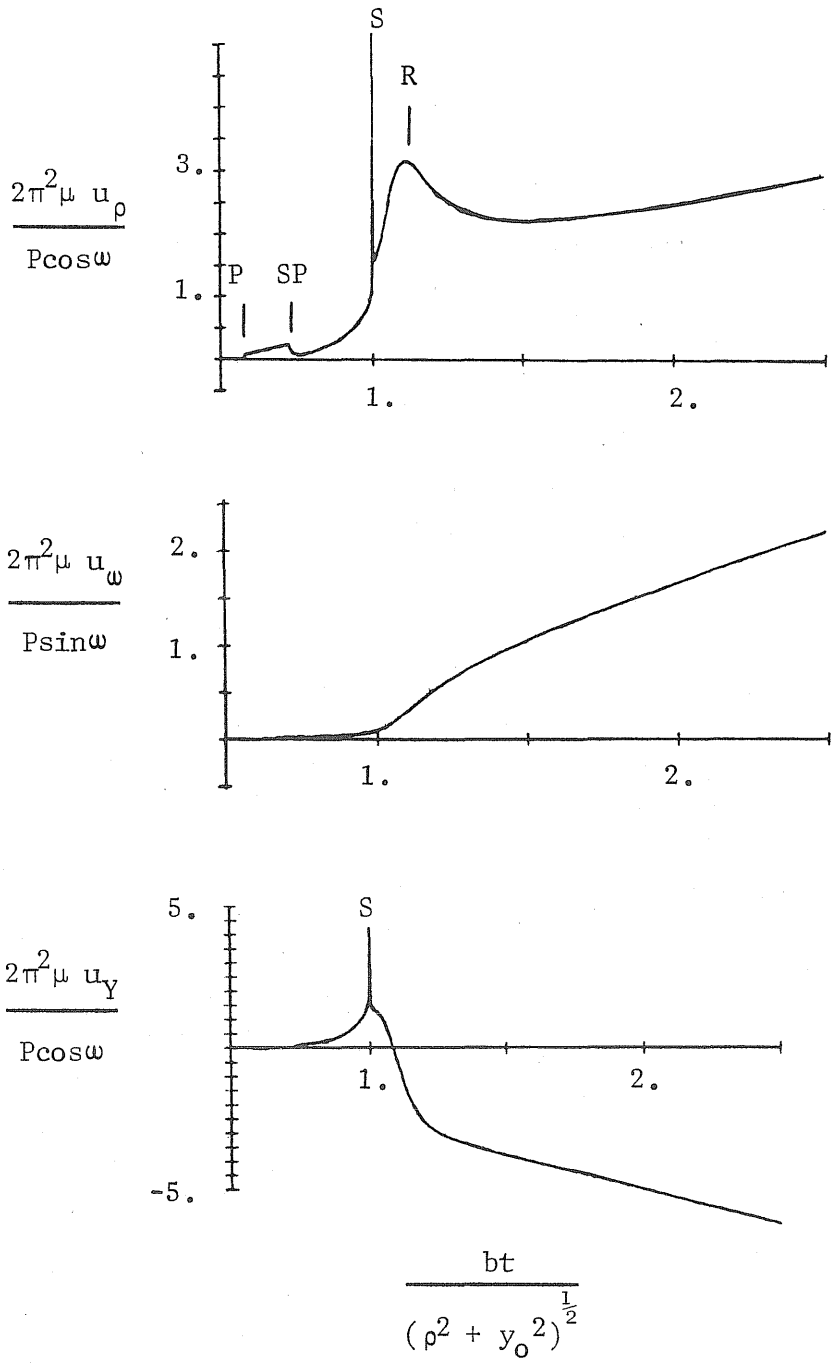

FIGURE 23. SURFACE DISPLACEMENTS FOR CASE Vh WHEN $y_o/\rho = .2$.

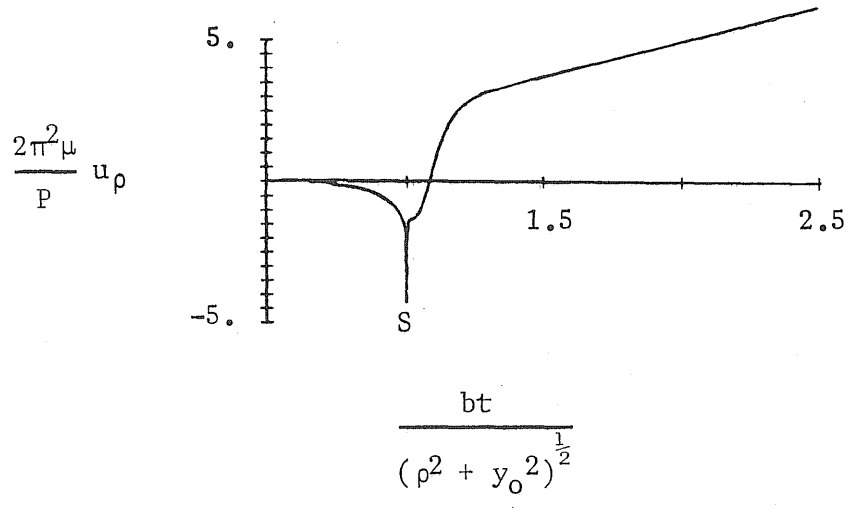

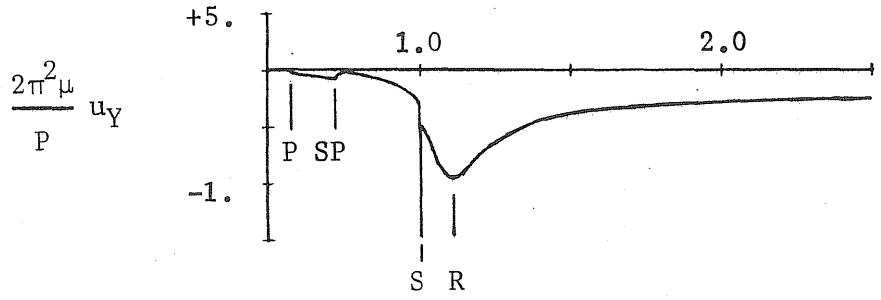

$u_\omega = 0$

FIGURE 24. SURFACE DISPLACEMENTS FOR CASE Vv WHEN $y_o/\rho = .2$.

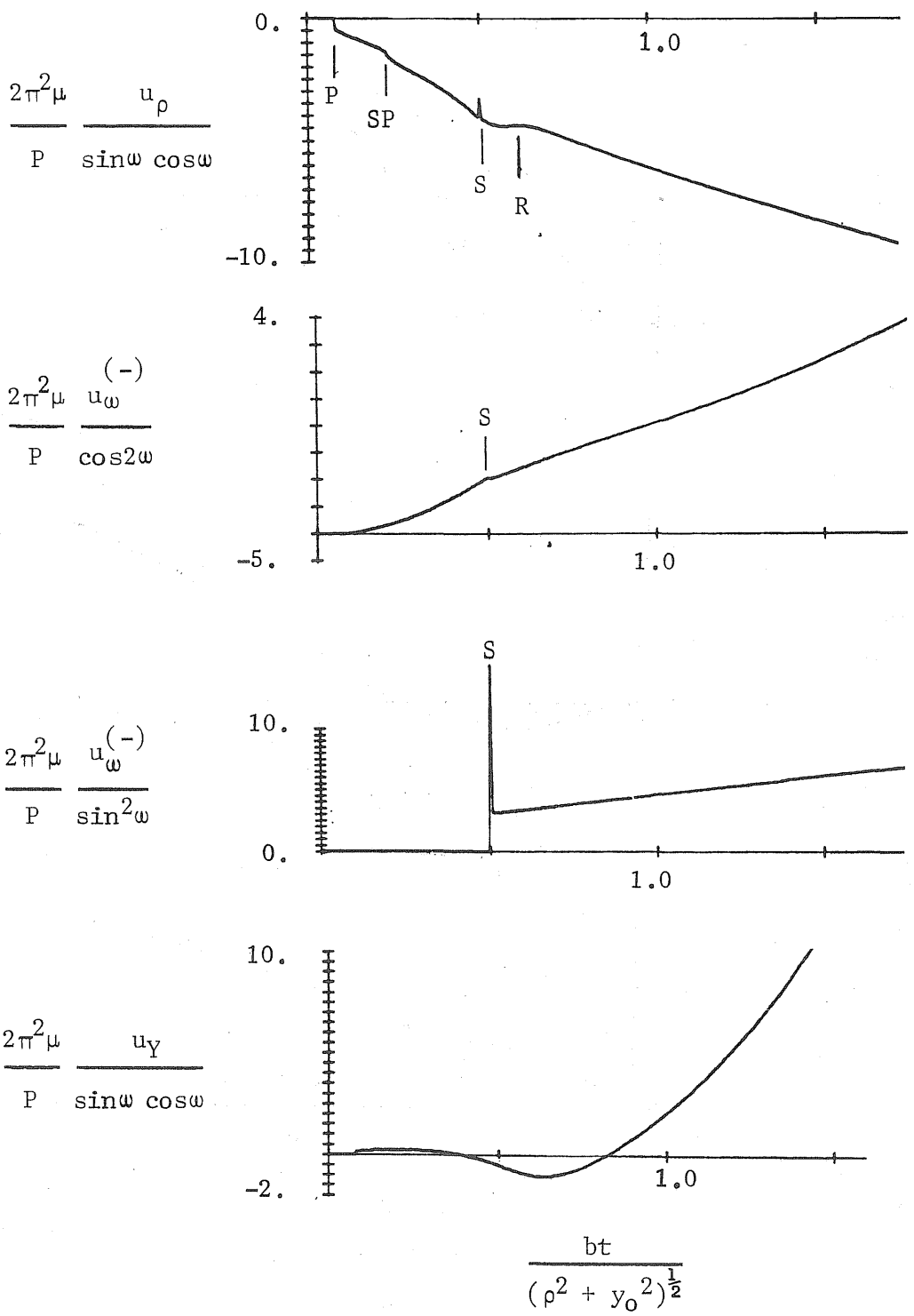

FIGURE 25. SURFACE DISPLACEMENTS FOR CASE $H_n h_e$ WHEN $y_o/\rho = .2$.

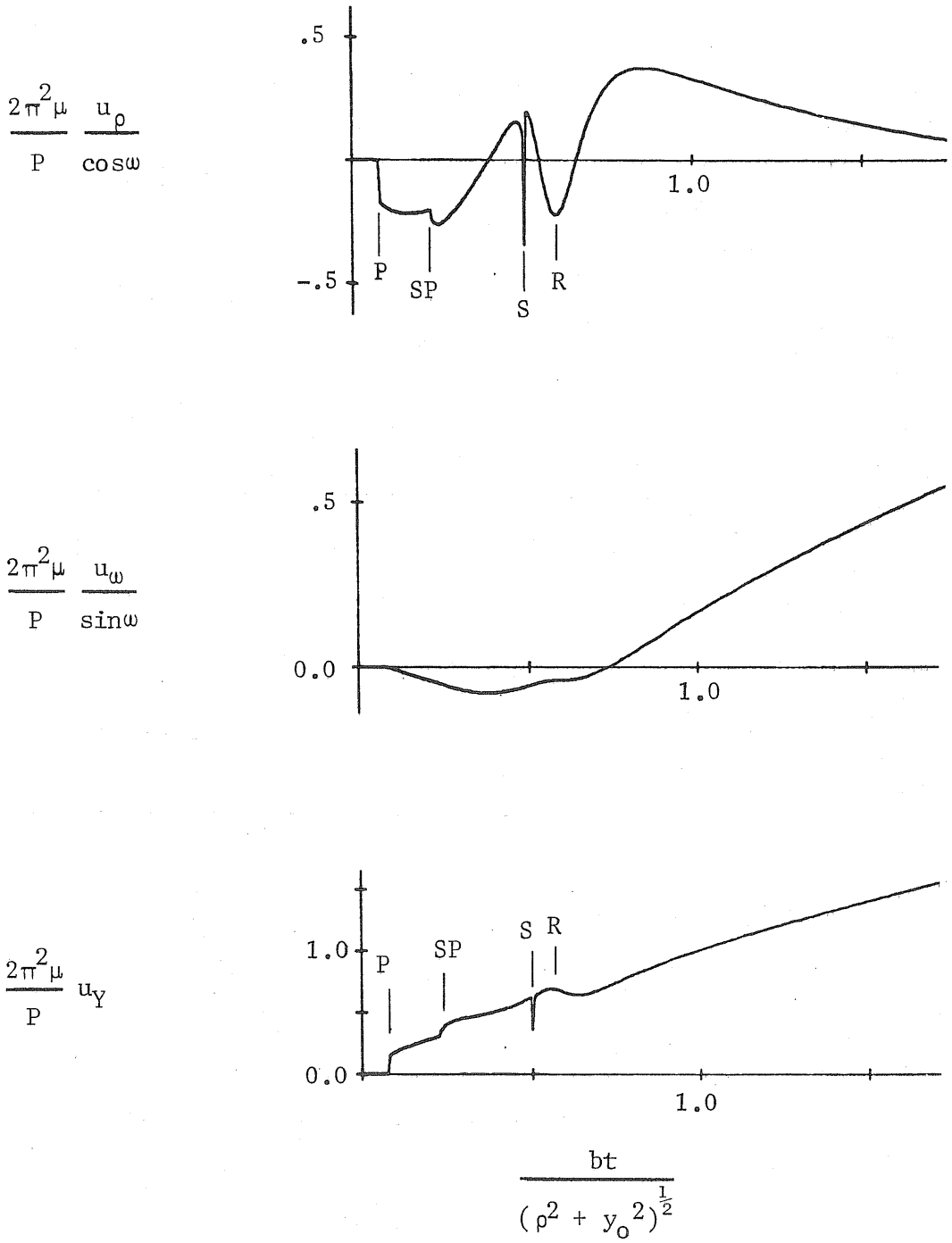

FIGURE 26. SURFACE DISPLACEMENTS FOR CASE Hv WHEN $y_o/\rho = .2$.

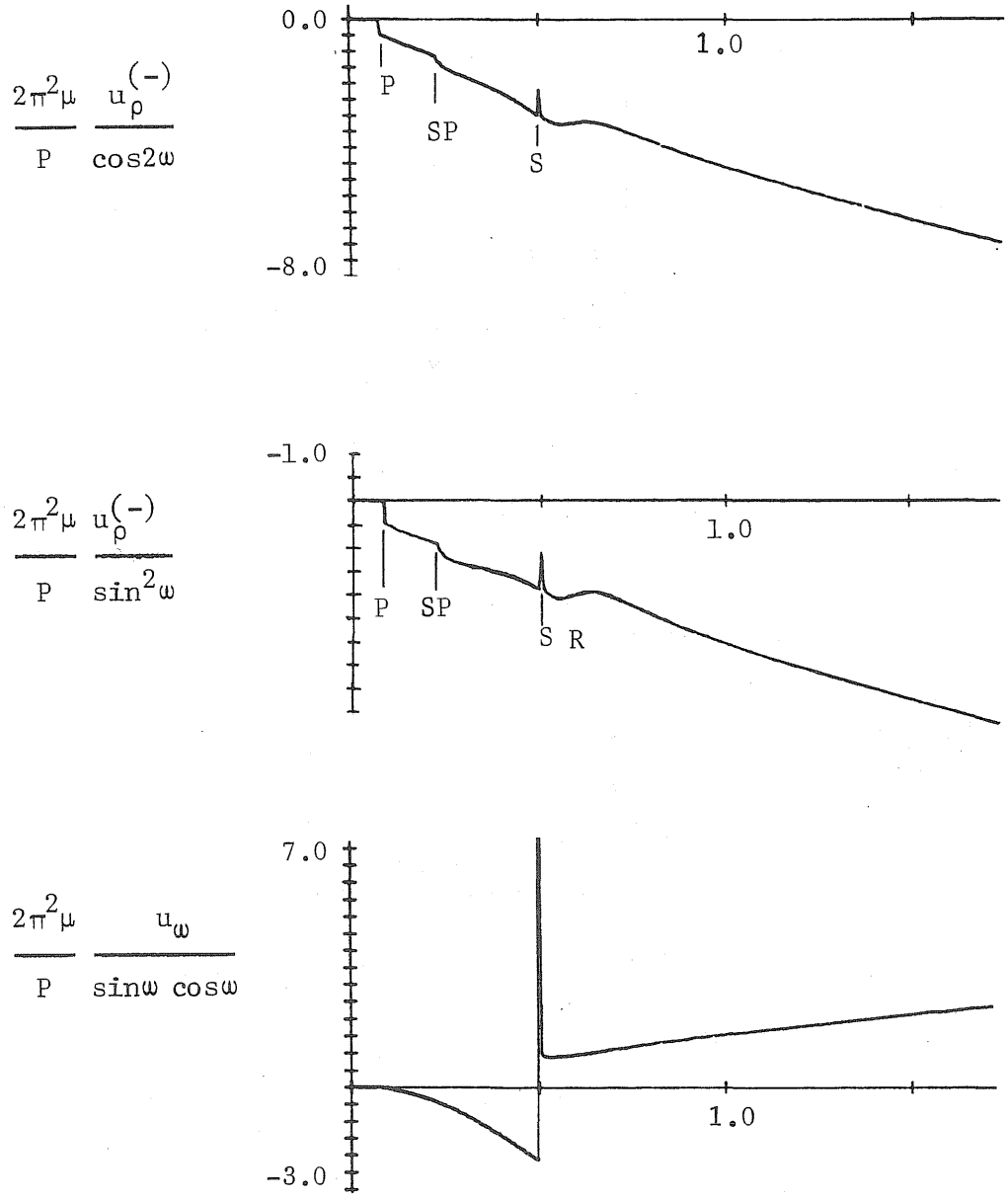

FIGURE 27. SURFACE DISPLACEMENTS u_ρ AND u_ω FOR CASE $H_e h_e$ WHEN $y_o/\rho = .2$.

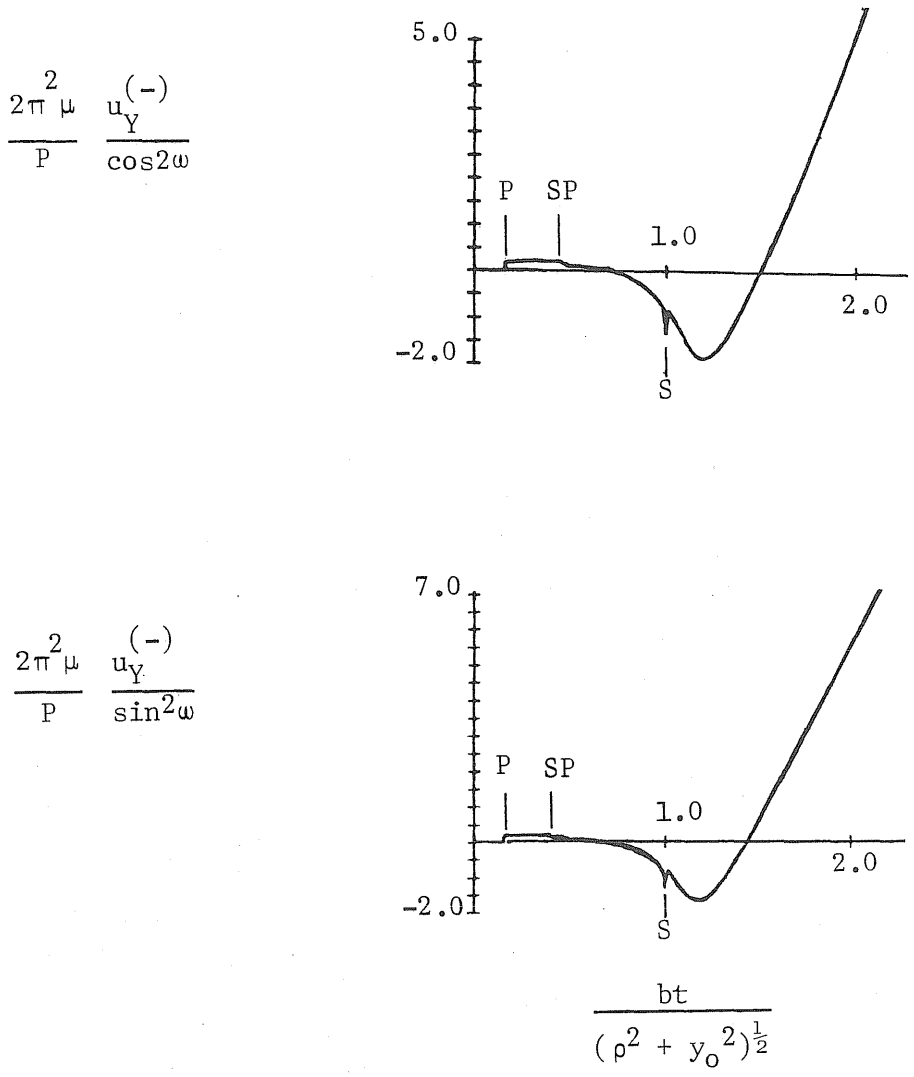

FIGURE 28. SURFACE DISPLACEMENT u_Y FOR CASE $H_e h_e$ WHEN $y_o/\rho = .2$.

APPENDIX. NUMERICAL TECHNIQUE

The numerical analysis conducted in this study is performed in the θ plane. For points on the surface or above $y = y_o$, the endpoints of integration (θ_i^{ℓ} and θ_i^{u}) lie in the lower half θ plane. The path of integration corresponding to a range of η from 0 to π is the path C_η of Fig. 13. By the Cauchy-Goursat theorem (Churchill, 1960), this path may be deformed into one that is more convenient computationally. In this study, the linear path C_1 is used. Note that this path is an admissible contour of integration even though it passes through a region that does not correspond to a physical point in the medium (See the mappings contained in Johnson and Robinson's work, 1972). The path C_1 was chosen instead of a straight line connecting θ_i^{ℓ} and θ_i^{u} in order to avoid any singularities that occur at the origin.

The numerical integration is carried out using Simpson's rule except for five small intervals at the ends of the contour of integration. A special quadrature formula must be used near the endpoints because a square root singularity occurs at the endpoints when the integrands contain the term $\rho\theta_i \cdot \sin\eta$ in the denominator. The form of Eq. (3.29) clearly illustrates this behavior. A special quadrature formula can be derived (Jeffreys and Jeffreys, 1956) by considering the integrand to be of the form

$$\int_{\theta^n}^{\theta^{n+1}} \frac{A + B\theta}{\sqrt{\theta - \theta^{\ell}}}\, d\theta \tag{A.1}$$

over each interval in the region near the endpoints. The resulting formula is

$$\begin{aligned} Q = &\left[2A - \frac{B}{3}\left[2(\theta^n - \theta^{\ell}) + h\right] \right] (\theta^{n+1} - \theta^{\ell})^{\frac{1}{2}} \\ &- \left[2A - \frac{2B}{3}(\theta^n - \theta^{\ell}) \right] (\theta^n - \theta^{\ell})^{\frac{1}{2}} \end{aligned} \tag{A.2}$$

where θ^n and $\theta^{n+1} = (\theta^n - h)$ are the θ values at the start and end of each interval, respectively, and

$$\begin{aligned} A &= F_n \\ B &= \frac{1}{h}(F_n - F_{n+1}) \end{aligned} \tag{A.3}$$

where F_n and F_{n+1} are the values of the integrand (apart from the radical $\sqrt{\theta - \theta^{\ell}}$) at the start and end of each interval.

Particular care must be taken in the evaluation of square roots to insure that the values obtained agree with the definitions used in the earlier derivations. In this study, the radical $\sqrt{c^{-2} - \theta_i^{\,2}}$ is defined as positive when θ is positive imaginary with

a branch cut from $-c^{-1}$ to $+c^{-1}$. Considering $(c^{-1} + \theta_i)$ as a vector of the form $r_1 e^{i\phi_1}$ where the range of ϕ_1 is from $-\pi$ to π and considering $(c^{-1} - \theta_i)$ to be of the form $r_2 e^{i\phi_2}$ where the range of ϕ_2 is from 2π to 4π provide values that are consistent with this definition.

The G_i functions (See Eqs. 3.21) also involve a square root. The branch cuts for these functions are taken outward to infinity from the branch points, $\theta_i{}^{\ell}$ and $\theta_i{}^{u}$, as shown in Fig. 13. The fact that $G_i = \rho\theta_i \sin\eta$ must equal $+\rho\theta_i$ when $\eta = \pi/2$ defines the sign of the square root. Consider that G_i is of the form

$$
\begin{aligned}
G_i = & \left[\left(\rho\theta_i + t + y_o \sqrt{c^{-2} - \theta_i{}^2} \right) \cdot \right. \\
& \left. \left(\rho\theta_i - t - y_o \sqrt{c^{-2} - \theta_i{}^2} \right) \right]^{\frac{1}{2}} \qquad \text{(A.4)} \\
= & \left[\left(r_1 e^{i\phi_1} \right) \cdot \left(r_2 e^{i\phi_2} \right) \right]^{\frac{1}{2}}
\end{aligned}
$$

The first term in Eqs. (A.4) goes to zero at $\theta_i{}^{u}$; the second, at $\theta_i{}^{\ell}$. By considering these terms in polar form shown in Eqs. (A.4) with the same range for ϕ_1 and ϕ_2, as used above, one obtains the proper value and branch cuts for the G_i function. Because the same ranges of ϕ_1 and ϕ_2 are used as before, the same function subprogram used to evaluate $\sqrt{c^{-2} - \theta_i{}^2}$ may be used to evaluate G_i. Note that the

square root singularity is pulled out of the G_i function when the quadrature formula of Eq. (A.2) is used and care must be exercised to ensure that the resulting sign is the same as that obtained by evaluating G_i with the square root included.

Once the square roots are properly defined, carrying out the integration to determine displacements on the surface is a simple matter. The fact that the integration is carried out in the complex plane is computationally useful because, as was pointed out in Sec. 3.2, the imaginary portion of the computed displacements should be zero. Consequently, any errors committed in carrying out the computations will reveal themselves by yielding a nonzero value in the imaginary part of the solution.

PART 1 - GOVERNMENT

Administrative & Liaison Activities

Chief of Naval Research
Department of the Navy
Arlington, Virginia 22217
Attn: Code 439 (2)
Code 468
Code 437

Director
ONR Branch Office
495 Summer Street
Boston, Massachusetts 02210

Director
ONR Branch Office
536 South Clark Street
Chicago, Illinois 60605

Director
Naval Research Laboratory
Attn: Library Code 2029 (ONRL)
Washington, D.C. 20390 (6)

U. S. Naval Research Laboratory
Attn: Technical Information Div.
Washington, D.C. 20390 (6)

Commanding Officer
ONR Branch Office
207 West 24th Street
New York, New York 10011

Director
ONR Branch Office
1030 E. Green Street
Pasadena, California 91101

Defense Documentation Center
Cameron Station
Alexandria, Virginia 22314 (12)

Army

Commanding Officer
U. S. Army Research Off. Durham
Attn: Mr. J. J. Murray
CRD-AA-IP Box CM, Duke Station
Durham, North Carolina 27706

Redstone Scientific Info. Center
Chief, Document Section
U. S. Army Missile Command
Redstone Arsenal, Alabama 35809

Army R & D Center
Fort Belvoir, Virginia 22060

Navy

Commanding Officer and Director
Naval Ship Res & Dev Center
Washington, D. C. 20007
Attn: Code 042 (Tech. Lib. Br.)
Code 700 (Struc. Mech. Lab.)
Code 720
Code 725
Code 727
Code 800 (Appl. Math. Lab.)
Code 901 (Dr. M. Strassberg)
Code 941 (Dr. R. Liebowitz)
Code 945 (Dr. W. S. Cramer)
Code 960 (Mr. E. F. Noonan)
Code 962 (Dr. E. Buchmann)

Naval Research Laboratory
Washington, D. C. 20390
Attn: Code 8400
Code 8410
Code 8430
Code 8440

Director, Aero Mechanics Dept.
Naval Air Development Center
Johnsville
Warminister, Pennsylvania 18974

Undersea Explosion Research Div.
Naval Ship R & D Center
Norfolk Naval Shipyard
Portsmouth, Virginia 23709
Attn: Dr. Schauer Code 780

Nav. Ship R & D Center
Annapolis Division
Annapolis, Maryland 21402
Attn: Code A125 Mr. Y. F. Wang

Navy (Cont'd)

U. S. Naval Weapons Center
China Lake, California 93557
Attn: Code 4062 Mr. W. Werback
Code 4520 Mr. Ken Bischel

Commanding Officer
U. S. Naval Civil Engr. Lab.
Code L31
Port Hueneme, California 93041

Technical Director
U. S. Naval Ordnance Laboratory
White Oak
Silver Spring, Maryland 20910

Technical Director
Naval Undersea R and D Center
San Diego, California 92132

Supervisor of Shipbuilding
U. S. Navy
Newport News, Virginia 23607

Technical Director
Mare Island Naval Shipyard
Vallejo, California 94592

U. S. Navy Underwater Sound Ref. Lab.
Office of Naval Research
P. O. Box 8337
Orlando, Florida 32806

Chief of Naval Operation
Department of the Navy
Washington, D. C. 2-35-
Attn: Code OP-07T

Deep Submergence Systems
Naval Ship Systems Command
Code 39522 Dept. of the Navy
Washington, D. C. 20360
Attn: Chief Scientist

Engineering Dept.
U. S. Naval Academy
Annapolis, Maryland 21402

Naval Air Systems Command
Dept. of the Navy
Washington, D. C. 20360
Attn: NAIR 320 Aero. & Structures
5308 Structures
604 Tech. Library

Naval Facilities Engineering
Command
Dept. of the Navy
Washington, D. C. 20360
Attn: NFAC 03 Res. & Development
04 Engineering & Design
14114 Tech. Library

Naval Ship Systems Command
Dept. of the Navy
Washington, D. C. 20360
Attn: NSHIP 031 Chief Scientists for R & D
03412 Hydromechanics
037 Ship Silencing Div.
2052 Tech. Library

Naval Ship Engineering Center
Prince George Plaza
Hyattsville, Maryland 20782
Attn: NSEC 6100 Ship Sys. Eng. & Des. Dept.
6102C Computer-aided Ship Design
6105 Ship Safety
6110 Ship Concept Design
6120 Hull Division
6120D Hull Division
6128 Surface Ship Struct.
6129 Submarine Struct.

Naval Ordnance Systems Command
Dept. of the Navy
Washington, D. C. 20360
Attn: NORD 03 Res. & Technology
035 Weapons Dynamics
9132 Tech. Library

Air Force

Commander WADD
Wright-Patterson Air Force Base
Dayton, Ohio 45433
Attn: Code WWRMDD
AFFDL (FDDS)
Structures Division
AFLC (MCEEA)

Air Force (Cont'd)

Chief, Applied Mechanics Group
U. S. Air Force Inst. of Tech.
Wright-Patterson Air Force Base
Dayton, Ohio 45433

Chief, Civil Engineering Branch
WLRC, Research Division
Air Force Weapons Laboratory
Kirtland AFB, New Mexico 87117

Air Force Office of Scientific Res.
1400 Wilson Blvd.
Arlington, Virginia 22209
Attn: Mech. Div.

NASA

Structures Research Division
NASA Langley Research Center
Langley Station
Hampton, Virginia 23365
Attn: Mr. R. R. Heldenfels, Chief

National Aeronautic & Space Admin.
Associate Administrator for Advanced
Research & Technology
Washington, D. C. 20546

Scientific & Tech. Info. Facility
NASA Representative (S-AK/DL)
P. O. Box 5700
Bethesda, Maryland 20014

Other Government Activities

Commandant
Chief, Testing & Development Div.
U. S. Coast Guard
1300 E Street, N. W.
Washington, D. C. 20226

Technical Director
Marine Corps Dev. and Educ. Command
Quantico, Virginia 22134

National Science Foundation
Engineering Division
Washington, D. C. 20550

Science & Tech. Division
Library of Congress
Washington, D. C. 20540

Director
STBS
Defense Atomic Support Agency
Washington, D. C. 20350

Commander Field Command
Defense Atomic Support Agency
Sandia Base
Albuquerque, New Mexico 87115

Chief, Defense Atomic Support Agcy.
Blast & Shock Division
The Pentagon
Washington, D. C. 20301

Director Defense Research & Engr.
Technical Library
Room 3C-128
The Pentagon
Washington, D. C. 20301

Chief, Airframe & Equipment Branch
FS-120
Office of Flight Standards
Federal Aviation Agency
Washington, D. C. 20553

Chief, Research and Development
Maritime Administration
Washington, D. C. 20235

Deputy Chief, Office of Ship Constr.
Maritime Administration
Washington, D. C. 20235
Attn: Mr. U. L. Russo

Mr. Milton Shaw, Director
Div. of Reactor Devel. & Technology
Atomic Energy Commission
Germantown, Maryland 20767

Ship Hull Research Committee
National Research Council
National Academy of Sciences
2101 Constitution Avenue
Washington, D. C. 20418
Attn: Mr. A. R. Lytle

PART 2 - CONTRACTORS AND OTHER TECHNICAL COLLABORATORS

Universities

Dr. J. Tinsley Oden
Dept. of Engr. Mechs.
University of Alabama
Huntsville, Alabama 35804

Professor Me. E. Gurtin
Dept. of Mathematics
Carnegie Institute of Technology
Pittsburgh, Pennsylvania 15213

Professor Julius Miklowitz
Division of Engr. & Applied Sciences
California Institute of Technology
Pasadena, California 91109

Dr. Harold Liebowitz, Dean
School of Engr. & Applied Scinece
George Washington University
725 23rd Street
Washington, D. C. 20006

Professor Eli Sternberg
Div. of Engr. & Applied Sciences
California Institute of Technology
Pasadena, California 91109

Professor Paul M. Naghdi
Div. of Applied Mechanics
Etcheverry Hall
University of California
Berkeley, California 94720

Professor W. Nachbar
University of California
Dept. of Aerospace & Mech. Engr.
La Jolla, California 92037

Professor J. Baltrukonis
Mechanics Division
The Catholic Univ. of America
Washington, D. C. 20017

Professor A. J. Durelli
Mechanics Division
The Catholic Univ. of America
Washington, D. C. 20017

Professor R. B. Testa
Department of Civil Engineering
Columbia University
S. W. Mudd Building
New York, New York 10027

Professor H. H. Bleich
Department of Civil Engr.
Columbia University
Amsterdam & 120th Street
New York, New York 10027

Professor R. D. Mindlin
Department of Civil Engr.
Columbia University
S. W. Mudd Building
New York, New York 10027

Professor F. L. DiMaggio
Department of Civil Engr.
Columbia University
616 Mudd Building
New York, New York 10027

Professor A. M. Freudenthal
George Washington University
School of Engineering
and Applied Science
Washington, D. C. 20006

Professor Wm. Prager
Division of Engineering
Brown University
Providence, Rhode Island 02912

Dr. Y. Weitsman
Department of Engineering Sciences
Tel-Aviv University
Ramat-Aviv
Tel-Aviv, Isreal

Professor P. V. Marcal
Brown University
Division of Engineering
Providence, Rhode Island 02912

Professor Norman Jones
Massachusetts Institute of Technology
Department of Naval Architecture
and Marine Engineering
Cambridge, Massachusetts 02139

Dr. S. Dhawan, Director
Indian Institute of Science
Bangalore, India

Dr. Charles E. Hutchinson
School of Engineering
University of Massachusetts
Amherst, Massachusetts 01002

Universities (Cont'd)

Professor Lambert Tall
LeHigh University
Department of Civil Engineering
Bethlehem, Pennsylvania 18015

Dean Bruno A. Boley
Technological Institute
Northwestern University
2145 Sheridan Road
Evanston, Illinois 60201

Prodessor P.G. Hodge
Department of Aerospace Engineering & Mech.
107 Aeronautical Engineering Building
Minneapolis, Minnesota 55455

Dr. D.C. Drucker
Dean of Engineering
University of Illinois
Urbana, Illinois 61801

Professor N. M. Newmark
Dept. of Civil Engineering
University of Illinois
Urbana, Illinois 61801

Professor E. Reissner
University of California, San Diego
Department of Applied Mechanics
La Jolla, California 92037

Professor William A. Nash
Dept. Of Mechs. & Aerospace Engr.
University of Mass
Amherst, Mass. 01002

Library (Cade 0384)
U. S. Naval Postgraduate School
Monterey, California 93940

Professor Arnold Allentuch
Dept. Of Mechanical Engineering
Newark College of Engineering
323 High Street
Newark, New Jersey 07102

Professor E.L. Reiss
Courant Inst. Of Math. Sciences
New York University
4 Washington Place
New York, New York 10003

Dr. George Herrmann
Stanford University
Department of Applied Mechanics
Stanford, Californis 94305

Professor J. D. Achenbach
Technological Institute
Northwestern University
Evanston, Illinois 60201

Director, Ordnance Research Lab.
Pennsylvania State University
P. O. Box 30
State College, Pennsylvania

Professor Eugene J. Skudrzyk
Department of Physics
Ordnance Research Lab.
Penn State Univ. P.O. Box 30
State College, Pennsylvania 16801

Professor J. Kempner
Dept. of Aero. Engr. & Applied Mech.
Polytechnic Institute of Brooklyn
333 Jay Street
Brooklyn, New York 11201

Professor J. Klosner
Polytechnic Institute of Brooklyn
333 Jay Street
Brooklyn, New York 11201

Professor R.A. Schapery
Civil Engineering Department
Texas A and M University
College Station, Texas 77840

Dr. Nicholas J. Hoff
Dept. of Aero. & Astro.
Stanford University
Stanford, California 94305

Professor Max Anliker
Dept. of Aero. and Astro.
Stanford University
Stanford, California 94305

Professor W. D. Pilkey
Department of Aerospace Engineering
University of Virginia
Charlottesville, Virginia 22903

Universities (Cont'd)

Professor Chi-Chang Chao
Division of Engineering Mechanics
Stanford University
Stanford, California 94305

Professor S. B. Dong
University of California
Department of Mechanics
Los Angeles, California 90024

Professor Tsuyoshi Hayashi
Department of Aeronautics
University of Tokyo
Bunkyo-Ku
Tokyo, Japan

Professor J. E. Fitzgerald, Ch.
Dept. of Civil Engineering
University of Utah
Salt Lake City, Utah 84112

Professor R. J. H. Bollard
Chairman, Aeronautical Engr. Dept.
207 Guggenheim Hall
University of Washington
Seattle, Washington 98105

Professor Albert S. Kobayashi
Dept. of Mechanical Engr.
University of Washington
Seattle, Washington 98105

Librarian
Webb Institute of Naval Arch.
Crescent Beach Road, Glen Cove
Long Island, New York 11542

Dr. Daniel Frederick
Dept. of Engr. Mechs.
Virginia Polytechnic Inst.
Blacksburgh, Virginia 24061

Industry and Research Institutes

Dr. Vito Salerno
Applied Technology Assoc., Inc.
29 Church Street
Ramsey, New Jersey 07446

Library Services Department
Report Section, Bldg. 14-14
Argonne National Laboratory
9700 S. Cass Avenue
Argonne, Illinois 60440

Dr. M. C. Junger
Cambridge Acoustical Associates
129 Mount Auburn Street
Cambridge, Massachusetts 02138

Supervisor of Shipbuilding, USN,
and Naval Insp. of Ordnance
Electric Boat Division
General Dynamics Corporation
Groton, Connecticut 06340

Dr. L. H. Chen
Basic Engineering
Electric Boat Division
General Dynamics Corporation
Groton, Connecticut 06340

Dr. Joshua E. Greenspon
J. G. Engr. Research Associates
3831 Menlo Drive
Baltimore, Maryland 21215

Library Newport News Shipbuilding
& Dry Dock Company
Newport News, Virginia 23607

Mr. J. I. Gonzalez
Engr. Mechs. Lab.
Martin Marietta MP-233
P. O. Box 5837
Orlando, Florida 32805

Dr. M. L. Merritt
Division 5412
Sandia Corporation
Sandia Base
Albuquerque, New Mexico 87115

Director Ship Research Institute
Ministry of Transportation
700, Shinkawa
Mitaka
Tokyo, Japan

Dr. H. N. Abramson
Southwest Research Institute
8500 Culebra Road
San Antonio, Texas 78206

Dr. R. C. DeHart
Southwest Research Institute
8500 Culebra Road
San Antonio, Texas 78206

Dr. M. L. Baron
Paul Weidlinger Associates
110 East 59th Street
New York, New York 10022

Industry and Research Institutes (Cont'd)

Mr. William Caywood
Code BBE
Applied Physics Lab.
8621 Georgia Ave.
Silver Springs, Maryland 20034

Mr. J. Hrzina
Bldg. R-1, Room 1104A
TRW Systems
1 Space Park
Dedondo Beach, California 90278

Mr. D. Wilson
Litton Systems, Inc.
AMTD, Dept. 400 El Segundo
9920 West Jefferson Blvd.
Culver City, California 90230

Mr. P. C. Durup
Aeromechanics Department, 74-43
Lockheed-California Co.
Burbank, California 91503

Dr. Kevin J. Forsberg, Head
Solid Mechanics
Orgn. 52-20, Bldg. 205
Lockheed Palo Alto Research Lab.
Palo Alto, California 94302

Dr. E. M. Q. Roren
Head, Research Department
Det Norske Veritas
Post Box 6060
Oslo, Norway

Westinghouse Electric Corporation
Bettis Atomic Power Laboratory
P. O. Box 79
West Mifflin, Pennsylvania 15122

Dr. Andrews F. Conn
Hydronautics, Incorporated
Pindell School Road, Howard County
Laurel, Maryland 20810

Unclassified
Security Classification

DOCUMENT CONTROL DATA - R & D

(Security classification of title, body of abstract and indexing annotation must be entered when the overall report is classified)

1. ORIGINATING ACTIVITY (Corporate author)	2a. REPORT SECURITY CLASSIFICATION
University of Illinois at Champaign-Urbana, Ill. Department of Civil Engineering	Unclassified
	2b. GROUP

3. REPORT TITLE

WAVE PROPAGATION IN AN ELASTIC HALF SPACE DUE TO COUPLES APPLIED AT A POINT BENEATH THE SURFACE

4. DESCRIPTIVE NOTES (Type of report and inclusive dates)

Report

5. AUTHOR(S) (First name, middle initial, last name)

Thomas E. Farewell
Arthur R. Robinson

6. REPORT DATE	7a. TOTAL NO. OF PAGES	7b. NO. OF REFS
	178	25

8a. CONTRACT OR GRANT NO.	9a. ORIGINATOR'S REPORT NUMBER(S)
DO161102B33G (U.S. Army Research Office-Durham) b. PROJECT NO. D-52 c. Contract No.: N00014-67-A-0305-0010 (Office of Naval Research) d. Project No.: NR 064-183	Structural Research Series No. 411
	9b. OTHER REPORT NO(S) (Any other numbers that may be assigned this report) None

10. DISTRIBUTION STATEMENT

Qualified requestors may obtain copies of this report from DDC

11. SUPPLEMENTARY NOTES	12. SPONSORING MILITARY ACTIVITY
	Army Research Office-Durham, Dept. of the Army; Office of Naval Research, Navy Dept.

13. ABSTRACT

This study presents a useful technique for determining the disturbances that result from application of dynamic couples at a point beneath the surface of an elastic half space. This problem is of distinct engineering importance because it provides a basis for earthquake modeling. The disturbances from couple sources simulate the elastic motion following a fault dislocation and occurring in the presence of an initial strain state. This study does not defend any particular model but provides an efficient approach for determining the disturbances for any model by superposition of five fundamental "double force" cases.

The method of rotational superposition presents the solution to the fundamental double force cases as a superposition of more easily solved two-dimensional problems. The method of self similar potentials provides the solution to the two-dimensional problems by a simple modification of the potential functions for the single force case when the single force problem is formulated using the same methods. The time variation of the moment produced by the double force emerges in a natural fashion as a linear function in time. As a necessary intermediate step, the problem of a subsurface vertical force in a half space is solved anew using the above methods.

A simple quadrature in the complex plane provides the displacements on the surface of the half space for the fundamental cases. The form of the solution is quite suitable for obtaining other source models by superposition. Guidelines for obtaining other source models and other time variations from the linear time variation are presented.

DD FORM 1 NOV 65 1473 (PAGE 1)
S/N 0101-807-6811

Unclassified
Security Classification

A-31408

14. KEY WORDS	LINK A		LINK B		LINK C	
	ROLE	WT	ROLE	WT	ROLE	WT
Elastic Wave Propagation						
Earthquake Focal Mechanisms						